PVPylation of Catalase

By André Michler

Thesis presented in partial fulfilment of the requirements for the degree of Master of Science (Polymer Science)

Supervisor: Prof Bert Klumperman

Co-supervisor: Dr Reuben Pfukwa

University of Stellenbosch

Department of Chemistry and Polymer Science

March 2017

Declaration

I, hereby declare by submitting this thesis that the work contained is my own original work unless explicitly stated otherwise and that I have not previously submitted any part of this for the reason of obtaining a qualification.

…...……
Andre Michler

March
2017

Abstract

Hair greying has been attributed to the loss of pigment-forming melanocytes from the hair follicle. Melanocytes are lost due to a high concentration of hydrogen peroxide, a reactive oxidative species found in the hair follicle, reacting with the melanocytes. Hydrogen peroxide is formed through the melanogenesis process, where melanocytes are formed, which takes place in the growth phase of the hair. Repair mechanisms and enzymes exist to combat this problem, the results of these natural processes are insufficient. One of the enzymes present on hair is catalase. This enzyme catalyzes the decomposition of hydrogen peroxide into water and oxygen.

Bioconjugation is a method of attaching polymers as carriers to active molecules for therapeutics and nanomedicine. In this method a polymer is conjugated to an enzyme, protein or biological active molecule with a specific end function. It has been shown that bioconjugation increases the half-life and stability of biological active molecules during their usage.

In this thesis we are conjugating poly(*N*-vinylpyrrolidone) (PVP) to catalase to determine whether the PVP has an effect on the enzymatic activity and structure of catalase.

PVP is a polymer synthesized through the polymerization of *N*-vinylpyrrolidone (NVP). The polymerizations described in this thesis are conducted through Reversible Addition Fragmentation chain Transfer (RAFT) mediated polymerization. In this polymerization a chain transfer agent (CTA) is used. This CTA is used due to its ease of use and control it has over the polymerization and the end functional groups on the CTA that can be used for post polymerization reactions. In this thesis we are functionalizing the one end group to a desired aldehyde functionalized end group, where this end group will be used in the conjugation with catalase. This conjugation to catalase will take place on the lysine amino acid groups present on catalase.

RAFT-mediated polymerization was used successfully to polymerize four different molecular weight polymers, each with the desired end group. This end group was then successfully converted to the aldehyde end group needed for the conjugation reaction. Conjugation of PVP through the aldehyde end group was successful and an increase in the molecular weight of the enzyme is seen in SDS-PAGE. This is followed by enzymatic assay analyses, where it was found that conjugation of PVP to catalase does not have a negative effect on the catalytic activity of the enzyme. It was further found that there is actually an increase in the enzymatic activity of catalase if a small amount of polymer is conjugated to catalase. A change in the structure of catalase after conjugation was found. It was also determined that conjugation of a constant number of PVP chains with different molecular weight (below 40 x 10^3 g/mol), does not have a significant effect on the enzymatic activity of the catalase-PVP conjugate.

Abstract

Thus the conjugation of catalase was successful and catalase can be used in the presence of PVP for the decomposition of hydrogen peroxide.

Opsomming

Haarvergrysing word toegeskryf aan die verlies van die pigmentvormende melanosiete in die haarfollikel. Melanosiete gaan verlore as gevolg van 'n hoë konsentrasie waterstofperoksied, 'n reaktiewe oksideringspesie wat gevind word in die haarfollikel, wat reageer met die melanosiete. Waterstofperoksied word gevorm deur 'n proses wat melanogenesis genoem word, waar melanosiete ook gevorm word, wat plaasvind in die groeifase van die haar. Herstelmeganismes en ensieme bestaan om hierdie probleem te beveg, maar die resultate na 'n tyd is nie bevredegind nie. Katalase is 'n ensiem wat teenwoordig is in hare. Dit verhoog die tempo van waterstofperoksied ontbinding na water en suurstof.

Bio-konjugasie is 'n metode waar polimere gebruik word as toevoermiddels vir terapie en nanogeneeskunde. In die metode word 'n polimeer gekonjugeer aan 'n ensiem, proteïen of biologiese aktiewe molekule met 'n spesifiek eindfunksie. Daar is bewys dat bio-konjugasie die halfleeftyd en stabiliteit van hierdie biologiese aktiewe molekules tydens gebruik verhoog.

In hierdie tesis word die konjugasie van 'n eksterne katalase tot polyvinylpyrrolidone (PVP) gedoen, om te bepaal of die PVP 'n effek het op die ensiematiese aktiwiteit en struktuur van katalase.

PVP is 'n polimeer wat gevorm word met die polimerisasie reaksie van *N*-vinylpyrrolidone (NVP). Dié polimerisasie reaksie in hierdie studie is gedoen deur omkeerbare addisie fragmentasie kettingoordrag (RAFT) bemiddelde polimerisasie. In hierdie polimerisasie word 'n kettingoordragmiddel (CTA) gebruik. Hierdie CTA word eerstens gebruik as gevolg van die gemak van gebruik en beheer wat dit gee oor die polimerisasie. Tweedens kan die eindfunksionele groepe op hierdie CTA gebruik word vir post-polimerisasie reaksies. In hierdie tesis word een van hierdie eindgroepe verander na 'n gewenste aldehied eindgroep, waar hierdie eindgroep gebruik gaan word in die konjugasie met katalase.

RAFT-bemiddelde polimerisasie is suksesvol gebruik om vier verskillende molekulêre gewigspolimere te sintetiseer, elk met die gekose eindgroep. Hierdie eindgroep word dan suksesvol omgeskakel na 'n aldehied eindgroep wat benodig word vir die konjugasie reaksie. Konjugasie van PVP deur hierdie aldehied eindgroep was suksesvol en 'n verhoging in die molekulêre gewig van die ensiemkonjugaat word gesien. Hierdie is gevolg deur ensiematiese aktiwiteitsanalise, waar dit bevind is dat die konjugasie van PVP tot katalase nie 'n negatiewe effek op die ontbindingsproses van waterstofperoksied het nie. Daar is verder bevind dat daar eintlik 'n verhoging in die ensiematiese aktiwiteit van katalase is as 'n klein hoeveelheid van die polimeer tot katalase gekonjugeer is. 'n Verskil in die struktuur van katalase word gevind wat verwys na 'n verandering ná konjugasie. Daar is

ook bevind dat met die konjugasie van verskillende molekulêre gewigspolimere onder 40 x 10^3 g/mol, nie 'n groot effek op die ensiematiese aktiwiteit in vergelyking tot mekaar het nie.

Dus was die konjugasie van katalase suksesvol en katalase kan gebruik word in die teenwoordigheid van PVP met die ontbinding van waterstofperoksied.

Acknowledgements

I would like to thank my supervisor Prof Bert Klumperman for the opportunity to be part of his research group. I would also like to thank him for the project, guidance, input and support during this project.

I would also like to thank my co-supervisor Dr Rueben Pfukwa for the help, guidance, support and input during my research in this group.

I would also like to thank Anna Kargaard for all the advice, help, guidance and editing during this project. Not just somebody who I can turn to in time of need, but a great friend as well. Thank you for the numerous coffees and patience.

Inge Weideman and Stefan Wagenaar for all the help, guidance and fun we had along the way. I am very grateful to have had you as my research partners during this time.

I would like to thank the following staff at the department of Chemistry and Polymer science for their help during this project: Dr Maggie Brand, Mr Deon Koen, Mrs Aneli Fourie, Mrs Erinda Cooper and Mr Jim Motshweni. A big thank you goes to Mr Kelvin Maart, for all the help and support and a smile to go with it. I would also like to thank every individual within the Klumperman Research Group for the help and guidance during this time.

I would like to thank Mrs Elsa Malherbe and Mr Jaco Brand for their help and fast service with a smile with the NMR and CD analysis. I would also like to thank Timo Tait and Megan Cartwright for their help with the SDS-PAGE analysis and advice.

I would like to thank the National Research Fund and Stellenbosch University for the funding during this research.

A thank you goes to each and every friend (too many to mention by name) within and beyond the polymer faculty, for your help, guidance and advice. Putting up with complaints and being there for the celebrations.

A special thank you goes to the most important people in my life, my family. Thank you for the help, guidance, time and effort. I do not know how I would have done it without you. I will always be grateful for the opportunity and help you have given me.

Lastly and certainly not the least, to the love of my life: Da'Niel Smit. Thank you firstly for the editing and help with the project, but mostly for the time together and an ear that could listen. Thank you mostly of all for all the encouragement, motivation and sanity that you have brought into my life during this busy time.

Table of Contents

Table of contents

Table of contents

List of acronyms

AIBN	2,2'-Azo bis(isobutyronitrile)
ATRP	Atom-transfer radical polymerization
$CDCl_3$	Deuterated chloroform
DMSO-d_6	Deuterated dimethyl sulfoxide
CD	Circular Dichroism
CTA	Chain transfer agent
DMSO	Dimethyl sulfoxide
DMAc	*N*,*N*-Dimethylacetamide
DP	Degree of polymerization
MePEG	Monomethoxypoly(ethylene glycol)
NMR	Nuclear magnetic resonance
NMP	Nitroxide-mediated polymerization
NVP	*N*-vinylpyrrolidone
PAA	Poly(acrylic acid)
PBS	Phosphate buffer saline
PEG	Poly(ethylene glycol)
PMMA	Poly(methyl methacrylate)
PVP	Poly(*N*-vinylpyrrolidone)
P(S-DVB)	Poly (styrene-*co*-divinylbenzene)
P(S-*b*-GMA)	Poly(styrene-*b*-glycidylmethacrylate)
RAFT	Reversible addition fragmentation chain transfer
RDRP	Reversible deactivation radical polymerization
ROS	Reactive oxygen specie
SDS	Sodium dodecyl sulphate
SDS-PAGE	Sodium dodecyl sulphate - polyacrylamide gel electrophoresis
SEC	Size-exclusion chromatography
TEDETA	Tetraethyldiethylene triamine
TLC	Thin layer chromatography
TNBSA	2,4,6-Trinitrobenzene sulfonic acid
UV-vis	Ultraviolet-visible

List of Symbols

A	Absorbance
c	Concentration (mol L^{-1})
$Đ$	Dispersity
θ	Molar ellipticity (deg cm^2 $dmol^{-1}$)
ε	Molar extinction coefficient (L mol^{-1} cm^{-1})
l	Length (cm)
M_n	Number-average molecular weight
R	R group on CTA
Z	Z group on CTA

List of Figures

List of Schemes

List of Tables

Chapter 1: Introduction, Aim and Objectives

1.1 Introduction

Hair greying and loss of hair colour due to the loss of pigment, is one of the visual signs of ageing in humans. This leads to a source of embarrassment, especially where premature greying of the hair takes place. Although dyeing of hair is an option, it is not a solution. This removes the embarrassment of grey hair, through externally placing colour on the hair. This however, does not resolve the problem of loss inside the hair. Hair greying has been attributed to the negative effect of oxidative stress on the pigmentary system.[1,2] The oxidative stress is caused by the formation of hydrogen peroxide, formed in the process of hair colour production. Hydrogen peroxide forms a radical which removes the colour pigments from the hair follicles.[1–3] This reactive species also attacks other molecules such as methionine sulfoxide, which aids the repair of the hair[4]. Humans have an enzyme, catalase, present specifically for catalysing the breakdown of hydrogen peroxide into water and oxygen, however, with time, these enzymes lose the activity towards hydrogen peroxide, due to structural damage of the enzyme.[4] In theory, adding more catalase, from an external source, would decrease the concentration of the hydrogen peroxide, leading to the return of colour to the hair. Stabilization of this catalase however, is needed. Stabilization ensures usability in conditions which will denature the enzyme. In this research, this stabilization of the catalase will be done through the conjugation with a polymer, specifically poly(*N*-vinylpyrrolidone) (PVP).

A field in which polymers are used frequently, is that of nanomedicine and therapeutics.[5,6] In this field, polymers that are biocompatible, are attached to a bioactive molecule, such as an enzyme. The purpose of these polymers is to stabilize these molecules and in turn combat illness.[7] Polymers thus act as drug carriers for specific treatments due to the advantageous properties they impart on drug delivery systems,[8,9] which include an increased half-life, protection against degradation, site-specific targeting. All of these beneficial properties contribute to lowering antigenic activity of the drugs.[8,10–14] This is done with reduced side effects, when compared to small molecules used for the same purpose of combating the illness.[10,11,15]

PVP was chosen as the polymer to which catalase will be conjugated, due to PVP's properties including its amphiphilic nature,[16] and biocompatibility.[17,18] It is seen as a promising polymer for polymer drug conjugates. In addition, PVP was chosen for this conjugation due to its use in cosmetic related products[19], ensuring possible compatibility with existing cosmetic product formulations.

1.2 Aims

The aims of this project are as follows: The first aim is the RAFT-mediated polymerization of *N*-vinylpyrrolidone (NVP), through the use of an appropriate chain transfer agent (CTA). The second aim is the end-functionalization of this polymer to introduce an end group on the polymer that can be used for the subsequent conjugation reaction. The third aim is the attachment, through conjugation, of PVP to catalase. The fourth aim is the determination of enzymatic activity of the conjugated catalase in comparison to unconjugated catalase. This is done to determine to what extent the conjugated catalase has retained its catalytic activity.

1.3 Objective

The motivation for this study is the reversal of hair greying through the stabilization of an enzyme capable of removing excess hydrogen peroxide. This stabilization is based on the conjugation of biocompatible polymers to bioactive molecules. This study will investigate if it is possible to conjugate PVP to the enzyme catalase. If this is possible, the catalytic activity of this conjugated catalase will be determined. This is done to confirm that the conjugated catalase retains its ability to catalyze hydrogen peroxide decomposition. The details of this study are briefly discussed in the following section.

1.4 Layout of thesis

This thesis consists of 6 chapters, as briefly described below.

1.4.1 Chapter 1: Introduction, Aim and Objectives

Chapter 1 gives a brief introduction into the problem of hair greying and the use of polymers for therapeutics. It also contains the aim and objectives of this thesis and information regarding the other chapters to follow.

1.4.2 Chapter 2: Theoretical background

The literature study discusses and gives background information pertaining to the main themes that were pursued in this study. The main themes of this study are the origin and problem of hair greying, catalase, used in the decomposition of hydrogen peroxide, and bioconjugation of catalase. Background will also be given into RAFT-mediated polymerization and PVP.

1.4.3 Chapter 3: Synthesis

In Chapter 3, the synthesis of the CTA capable of mediating the polymerization of NVP is described. This is followed by the RAFT-mediated polymerization of NVP with this CTA. In this study different molecular weight polymers are synthesized, which will be used in subsequent chapters for end functionalization and bioconjugation.

1.4.4 Chapter 4: End Functionalization

In Chapter 4, the end functionalization of the PVP synthesized in Chapter 3 is described. The end functionalization on the ω xanthate end group is performed to achieve an aldehyde on this ω end group. This aldehyde ω end group will be used for subsequent bioconjugation.

1.4.5 Chapter 5: Bioconjugation

The bioconjugation of PVP to catalase is described in Chapter 5. For this bioconjugation the polymer is conjugated through the aldehyde ω end group, as functionalized in Chapter 4. The conjugation was performed to target different fractions of the 112 lysine residues present on the tetrameric structure of catalase. Analysis was performed on these conjugates to determine what effect the conjugation has on the catalase activity and structure.

1.4.6 Chapter 6: Conclusions and future work

Chapter 6 concludes this study, describing achievements reached within this study and additional suggestions for future work on PVP-catalase conjugations.

1.5 References

(1) Trüeb, R. M. *J. Cosmet. Dermatol.* **2005**, *4*, 60–72.

(2) Seiberg, M. *Int. J. Cosmet. Sci.* **2013**, *35*, 532–538.

(3) Nanninga, P. B.; Ghanem, G. E.; Lejeune, F. J.; Bos, J. D.; Westerhof, W. *Pigment Cell Res* **1991**, *4*, 193–198.

(4) Wood, J. M.; Decker, H.; Hartmann, H.; Chavan, B.; Rokos, H.; Spencer, J. D.; Hasse, S.; Thornton, M. J.; Shalbaf, M.; Paus, R.; Schallreuter, K. U. *FASEB J.* **2009**, *23*, 2065–2075.

(5) Nicolas, J.; Mantovani, G.; Haddleton, D. M. *Macromol. Rapid Commun.* **2007**, *28*, 1083–1111.

(6) Vilar, G.; Tulla-Puche, J.; Albericio, F. *Curr. Drug Deliv.* **2012**, *9*, 367–394.

(7) Duncan, R. *Nat. Rev. Drug Discov.* **2003**, *2*, 347–360.

(8) Polyak, D.; Eldar-Boock, A.; Baabur-Cohen, H.; Satchi-Fainaro, R. *Polym. Adv. Technol.* **2013**, *24*, 777–790.

(9) Ulbrich, K.; Pechar, M.; Strohalm, J.; Subr, V. *Macromol. Symp.* **1997**, *585*, 577–585.

(10) Park, E. Y.; Ishikiriyama, M.; Nishina, T.; Kato, T.; Yagi, H.; Kato, K.; Ueda, H. *J. Biotechnol.* **2009**, *139*, 108–114.

(11) Leader, B.; Baca, Q. J.; Golan, D. E. *Nat. Rev. Drug Discov.* **2008**, *7*, 21–39.

(12) Kaneda, Y.; Yamamoto, Y.; Kamada, H.; Tsunoda, S.; Tsutsumi, Y.; Hirano, T.; Mayumi, T. *Cancer Res.* **1998**, *58*, 290–295.

(13) Tsutsumi, Y.; Kihira, T.; Tsunoda, S.; Kamada, H.; Nakagawa, S.; Kaneda, Y.; Kanamori, T.; Mayumi, T. *J. Pharmacol. Exp. Ther.* **1996**, *278*, 1006–1011.

(14) Tsutsumi, Y.; Tsunoda, S.; Kamada, H.; Kihira, T.; Kaneda, Y.; Ohsugi, Y.; Mayumi, T. *Thromb. Haemost.* **1997**, *77*, 168–173.

(15) Hamid Akash, M. S.; Rehman, K.; Chen, S. *Polym. Rev.* **2015**, *55*, 371–406.

(16) Kirsh, Y. E.; Chichester, U. K. *Water Soluble Poly-N-Vinylamides: Synthesis and Physicochemical Properties; Wiley*: Chichester, 1998; pp 129–215..

(17) Higa, O. Z.; Rogero, S, O.; Machado, L, D, B.; Mathor, M, B.; Lugão, A, B. *Radiat. Phys. Chem.* **1999**, *55*, 705–707.

(18) Bindu, N. *Int. J. Toxicol.* **1998**, *17*, 95–130.

(19) Shelanski, H. A.; Shelanski, M. V.; Cantor, A. *J. Cosmet. Sci.* **1954**, *5*, 129–132.

Chapter 2: Theoretical background

2.1 Greying of Hair

According to Keogh *et al.*, half of people are 50% grey by the age of 50.[1] In the cases where greying occurs prematurely, it can lead to self-esteem problems as people usually attribute greyness to old age.[2] Studies have deduced that the loss of hair colour is due to oxidative stress, especially by hydrogen peroxide, acting on the hair and its enzymes.[3,4] In their study using FT Raman spectroscopy, Wood *et al*. found that millimolar quantities of hydrogen peroxide (H_2O_2) are present in white and grey hair, but not in normal colour hair (Figure 2.1).[5] They concluded that elimination of hydrogen peroxide from the hair follicle could combat hair greying.

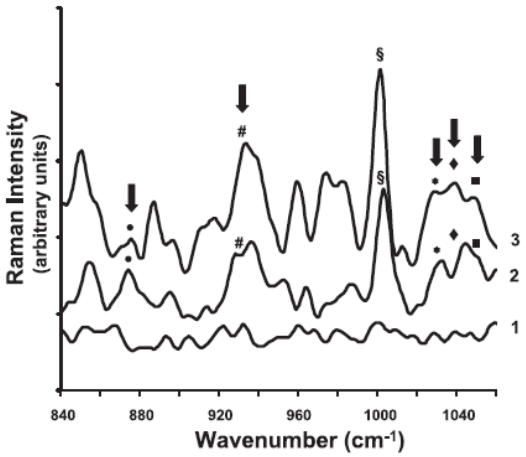

Figure 2.1: FT-Raman spectroscopy identifies *in vivo* millimolar amounts of H_2O_2 and its oxidation products in grey and white hair shafts. Peaks are assigned accordingly: ●, H_2O_2 at 875 cm^{-1}; §, phenylalanine at 1004 cm^{-1}; *, methionine sulfoxide (Met-S=O) at 1030 cm^{-1}; #, 5-OH-tryptophan (5-OH Trp) at 930 cm^{-1}; ■ N-formyl kynurenine/kynurenine at 1050 cm^{-1}; ♦ , cysteic acid at 1040 cm^{-1}). Spectrum 1, brown hair; spectrum 2, grey hair; spectrum 3, white hair.[5] (Reproduced from Senile hair graying: H_2O_2-mediated oxidative stress affects human hair color by blunting methionine sulfoxide repair by J. M. Wood, 2009, The FASEB journal, 23, 2068. .Reproduced with permission)

In Figure 2.1, hydrogen peroxide and products, found in hair after reaction with hydrogen peroxide are seen in grey and white hair spectrum (2 and 3 respectively). These are seen between 840 cm^{-1} and 1060 cm^{-1} in the FT-Raman spectrum. The peak at 875 cm^{-1} corresponds to that O-O stretch of hydrogen peroxide. The oxidation of L-tryptophan, 5-OH Trp is seen at 930 cm^{-1}. The phenylalanine peak is seen at 1004 cm^{-1}. At 1030 cm^{-1} the Met-S=O stretch is seen, this is the product from methionine sulfoxide reductase. Cysteic acid, the product from cysteine is seen at 1040 cm^{-1}. *N*-formyl kynurenine/kynurenine is seen at 1050 cm^{-1}.[5]

The cycle of hair growth consists of three phases, the anagen phase, catagen phase and the telogen phase. In the anagen phase, growth of the hair takes place. During this phase, the pigment is formed by melanocytes in the hair follicle. This pigment is responsible for the colour of the hair. Melanocytes reside in the bulb of the hair, where the pigment is incorporated. After the anagen phase, the hair goes into a resting or catagen phase where no growth or colouring takes place.[5–7] During the anagen phase these melanocytes are formed through a process called melanogenesis, which uses an enzyme called tyrosinase. As with all enzymes, tyrosinase increases the rate at which a biochemical reaction takes place and in this case it is the melanogensis process. During the melanogenesis process, where melanocytes are formed, hydrogen peroxide is also formed. If this hydrogen peroxide concentration is high, due to less removal of this reactive oxygen species, the tyrosinase activity is negatively affected and the enzyme may even be deactivated. Hydrogen peroxide as a reactive oxygen species also has negative effects on other enzymes, peptides and proteins[5]. Due to the increase in hydrogen peroxide concentration, methionine sulfoxide reductases A and B, repair mechanisms for free and bound methionine sulfoxide, as well as catalase, a hydrogen peroxide reducing enzyme, are damaged. Thus, the production of hydrogen peroxide from melanogenesis has a negative impact on melanocytes and as a result no pigment is formed. Furthermore, it has a negative impact on hair repair mechanisms.[5] Removing hydrogen peroxide from the hair should have a positive effect on melanocytes, pigments, enzymes present and repair mechanisms.

2.2 Catalase

The primary function of an enzyme is the lowering of the activation energy of metabolic pathways. This lowering of activation energy for chemical reactions, takes place under physiological conditions.[8] These enzymes have 2 fundamental properties: they increase the rate at which the biochemical reactions take place without being altered themselves, and secondly without changing the equilibrium between the products and reactants. In the absence of an enzyme, a chemical reaction has a substrate (S) which is converted to the product (P) due to a chemical reaction. This follows the normal law of thermodynamics (Equation 2. 1).

$$S \rightleftharpoons P \qquad (2.\ 1)$$

For this reaction to take place with an enzyme (E), an intermediate product is formed (SE) (Equation 2.2). The substrate complexes with the active site of the enzyme, forming the intermediate product, where after the product formation takes place. After the the product is removed and a new substrate complexes with the active site. This lowers the activation energy and increases the rate of product formation.

$$S + E \rightleftharpoons SE \rightleftharpoons E+P \qquad (2.\ 2)$$

Catalase (hydrogen-peroxide oxidoreductase) is such an enzyme, catalysing the decomposition of a reactive oxygen species (ROS), hydrogen peroxide.[9,10] Through catalase, hydrogen peroxide is catalytically decomposed into water (H_2O) and oxygen (O_2)[9,11] (Equation 2.3) and in so doing, it controls the concentration of this ROS.[12,13] This enzymes is found in various animals,[14–16] fungi,[17,18] bacteria[17,19,20] and plants.[21,22]

$$2\,H_2O_2 \xrightarrow{\text{Catalase}} 2\,H_2O + O_2 \qquad (2.3)$$

Catalase consists of 4 subunits joined to form a tetramer. Each of these subunit units consist of 506 amino acid residues. Each subunit also consists of an iron heme (Fe (III)) complex, which is the active site of catalase, buried within the subunit. This iron heme complex is accessible by a hydrophobic channel ensuring nothing else enters to the active site but hydrogen peroxide.[23] These iron hemes, contained within a porphyrin group (Por), complex to the hydrogen peroxide as stated in Equation 2.4.[16,23–26]

From literature it is found that there is a 2 stage process that takes place inside the catalase itself, when hydrogen peroxide is decomposed. This occurs in the following manner: [26–28]:

$$\text{Enzyme (Por - } Fe^{III}) + H_2O_2 \longrightarrow \text{Enzyme (}Por^{+} - Fe^{IV}{=}O) + H_2O \qquad (2.4)$$

$$\text{Enzyme (}Por^{+} - Fe^{IV}{=}O) + H_2O_2 + e^{-} + H^{+} \longrightarrow \text{Enzyme (Por - } Fe^{III}) + H_2O + O_2 \qquad (2.5)$$

In the first stage (Equation 2.4), the porphyrin group and Fe (III)) are oxidised, from oxygen state III to IV for the iron heme, due to the hydrogen peroxide. An oxyferryl group is formed in this oxidation step, where the first water molecule is formed. The second stage, (Equation 2.5), is the reduction back to the starting, unaltered, enzyme. For this step, another hydrogen peroxide specie is needed. This provides enough electrons that are used to reduce the porphyrin group back to its original state and iron back to an oxidation state of III. Due to this reduction, the second water molecule and one oxygen molecule are formed. However, side reactions can take place from the oxidised state (Equation 2.4). Equations 2.6 and 2.7 describe these side reactions.

$$\text{Enzyme (}Por^{+} - Fe^{IV}{=}O) + e^{-} + H^{+} \longrightarrow \text{Enzyme (Por - } Fe^{IV}{-}OH^{+}) \qquad (2.6)$$

$$\text{Enzyme (}Por^{+} - Fe^{IV}{=}O) + e^{-} \longrightarrow \text{Enzyme (Por - } Fe^{IV}{=}O) \qquad (2.7)$$

The oxyferryl formed in Equation 2.4 can undergo electron reduction, with (Equation 2.6) or without (Equation 2.7) a proton, which forms an inactive enzyme unable to catalyse the decomposition of hydrogen peroxide.[26–28]

The decomposition of hydrogen peroxide depends on the concentration of the catalase and is independent of the hydrogen peroxide concentration and is a spontaneous process.[29] The optimal pH for catalase is approximately 7.0.[30] It has been found that catalase can be divided into groups, monofunctional heme-containing catalases (primarily decomposes hydrogen peroxide), bifunctional catalase-peroxidases (catalytic activity and preoxidatic activity) [26,31–33] and non-heme containing catalases (manganese as active complex site).[26,34–36] Studies have been conducted to determine the crystal structure of catalase within various organisms, including in *Penicillium vitale*,[37,38] beef liver catalase[24,25] and human erythrocytes.[39,40]

2.3 Bioconjugation of polymer to enzymes

Amino acids are defined as organic molecules containing an amino group ($–NH_2$), a carboxyl group (–COOH), a hydrogen (–H) and a functional organic R group, all attached to a central carbon (Figure 2.2).[41] Different amino acids are characterized by their R group substituent.[41] These R groups range from a hydrogen atom, to a methyl group, phenyl group or a variety of functional group-containing alkyl substituents (hydroxyl, amine, thiol, etc).[41] There are 20 different natural amino acids that can be placed into 5 groups namely: non-polar-, polar uncharged-, charged-, aromatic- and specially-functioned amino acids[41]. Non-polar groups are amino acids containing only methylene ($–CH_2$) and methyl ($–CH_3$) groups. Polar uncharged amino acids contain R groups with oxygen (or only hydrogen). Charged amino acids have R groups that are acids or bases. Aromatic amino acids as the name state contain an aromatic group. Proteins are macromolecules containing a unique sequence of these 20 amino acids covalently bonded, through peptide bonds, to form long polymer chains called a polypetide.[42] This unique amino acid sequence, forming the protein, has an effect on the function, shape and reactivity of the protein.[42]

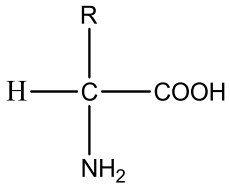

Figure 2.2: General structure of an amino acid

Due to the function, shape and reactivity of proteins, they have important capacities within the body, including transportation of molecules,[43–49] catalysis of biochemical reactions through enzymes,[15] contractile proteins used for the movement of muscles[50,51] and proteins aiding in structural integrity[52]. These are just a few examples of proteins used in bodily functions. Proteins have also been used to combat diseases through therapeutics. One such example is the use of insulin, which was first purified from bovine pancreas and then used on patients with diabetes mellitus type 1, due to the structure, function and in turn the amino acid sequence of the protein. Insulin is now produced through the

isolation of human insulin and through production in *Escherichia coli*, which is used to express human insulin through recombinant DNA.[53–55]

In order to capitalize on these favourable properties of proteins and use them in therapeutics, one has to overcome challenges associated with stabilizing them, and increasing their resistance to proteases. One approach is to conjugate them to polymers. This stabilization is required because of proteins' rapid clearance from circulation[56] and undesired side effects.[57–59] This can be achieved via covalent bonds as well as through electrostatic interactions. Through these polymer-protein conjugations, with the aim of drug delivery systems for medical purposes, protein therapeutics were born.[60] Protein therapeutics has an advantage over small molecule drugs.[61,62] Due to their size and specific functionality, protein therapeutics are more selective and specificity is improved.[62]

In essence these polymer conjugates improve the protein's resistance to proteases and degradation increasing the circulation, half-life and distribution of the protein. Enhancing the effects of the protein, to the needed tissue, and reduce side effects.[63–65]

Many studies have been performed where poly(ethylene glycol) (PEG) is conjugated to proteins.[66–69] The first enzymes to which PEG was conjugated were catalase and albumin.[66,70] The conjugation to PEG is performed through a covalent linker (alkylation[66,71,72] or acylation[73–75]) or, more importantly for this study through aldehyde conjugation. Through the end-functionalization of the monomethoxy-poly(ethylene glycol)'s (MePEG) hydroxyl group functionalization to an aldehyde,[76] and subsequent conjugation to the *N* terminus or/and lysine residues (Figure 2.3).[77] During this reaction, a Schiff base is formed,[77] whereby the imine is reduced using sodium cyanoborohydride.[78]

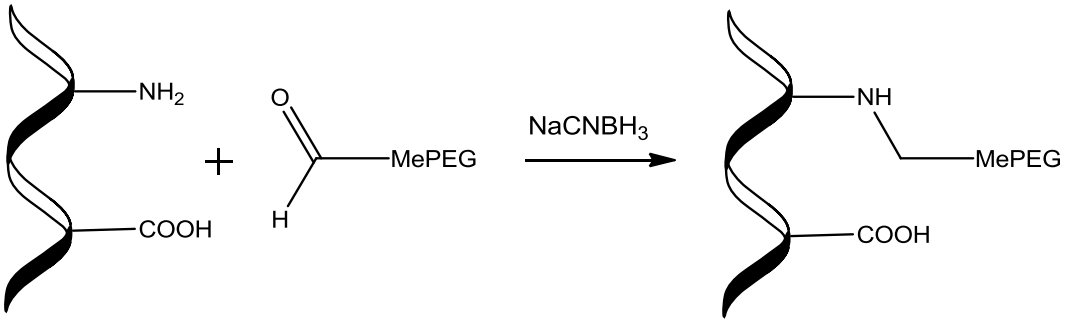

Figure 2.3: MePEG conjugation to amine groups

2.4 Conjugation to catalase

Nishikawa *et al.*[79–81] studied the effect of conjugated PEG-catalase on different tumour related complications in mice. They used conjugated PEG-catalase in the suppression of pulmonary metastasis[82,83] and hepatic metastases of colon carcinoma cells.[80] Conjugated PEG-catalase was also used to prevent further metastatic tumour growth after the removal of the tumour from mice.[82] In another study Shi *et al.*[83] studied the effect that PEG-human catalase has on H1N1 influenza-induced

pneumonia in mice, and found that this conjugation increased the circulation time of the catalase and improved the therapeutic efficiency.

PEG is not the only structural support system to which catalase has been conjugated; Bayramoglu *et al.*[84] grafted poly(styrene-*b*-glycidylmethacrylate) (P(S-*b*-GMA)) brushes onto poly (styrene-*co*-divinylbenzene) (P(S-DVB)) beads. The P(S-*b*-GMA) was functionalised with tetraethyldiethylene triamine (TEDETA) ligands to which the catalase was reversibly immobilized, forming a P(S-DVB)-*g*-P(S-*b*-GMA)-TEDETA-catalase compound. It was found that this immobilization increased the optimum temperature and pH at which the catalase is operational. This support system could be used five times before the loss of enzyme activity or adsorption capacity. Riccardi *et al.* [85] used poly(acrylic acid) (PAA) activated through the attachment of 1-ethyl-3-(3-(dimethylamino)propyl)-carbodiimide, to the carboxylic acid groups, as their structural support system for catalase. PAA was activated by attaching 1-ethyl-3-(3-(dimethylamino) propyl)-carbodiimide to the carboxylic acid groups. The amine groups on catalase were conjugated to the carboxylic acid groups on the PAA by displacement of the carbodiimide activator. Catalase has also been attached to glass beads with controlled pore size.[86] The catalase was attached to a glutaraldehyde-3-aminopropyltriethoxysilane (3-APTES) substrate, which was attached to the glass beads. Its use in batch and plug-flow type reactors as a biocatalyst for hydrogen peroxide in the reactors, was studied.[86] Catalase has also been encapsulated in liposomes[87–89] and nano vesicles of a non-ionic sugar ester composition.[90] It has also been attached to bentonite and sepiolite[91] to increase the operational properties of catalase.

For the present study, poly(*N*-vinylpyrrilidone) (PVP) is chosen as a conjugation polymer. PVP has also been used as a drug delivery system for some applications,[92–94] due to its increased half-life and distribution when compared to PEG.[95–98] PVP is also chosen due to its low toxicity and antigenicity.[99,100]

2.5 Poly(*N*-vinylpyrrolidone)

PVP is the polymer formed by polymerizing *N*-vinylpyrrilidone (NVP) monomer (Scheme 2.1).[101] A wide range of applications of PVP, in the biomedical field, has been found, due to PVP's low toxicity,[102–104] good biocompatibility[105,106] and its solubility in water[107]. These applications include biomedical drug delivery,[96,108,109] wound dressings,[110,111] disinfectants[112,113] and pharmaceutical tablets[114,115] among others. During World War II it was used as a blood plasma expander due to it being non-toxic, water soluble and its ability to change the isotonicity of aqueous solutions.[100] The free radical polymerization of PVP can be achieved through solution polymerization[116,117] or bulk polymerization[118–121].

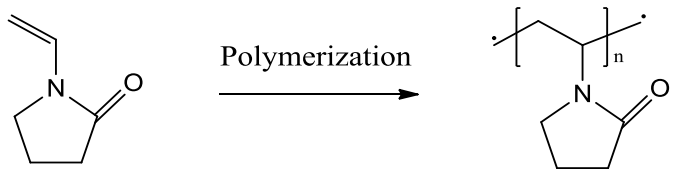

Scheme 2.1: General scheme of NVP polymerization.

NVP is synthesised using acetylene chemistry discovered by Walter Reppe[122]. Its subsequent polymer consists of a cyclic amide (lactam) group attached to a polymethylene backbone. Due to this the molecule can form hydrogen bonds and has an amphiphilic nature, making it soluble in water and some organic liquids,[107] including methanol, chloroform and dichloromethane.[123] When PVP is dry, it is a hygroscopic powder that can absorb up to 40% of its weight in water[122,124].

NVP was first polymerized in 1939 by Fikentscher and Herrle. This was done in water using hydrogen peroxide and ammonia.[118,125] In 2005 Wan *et al.*[126] published a paper where NVP was polymerized using a xanthate chain transfer agent (CTA) (Figure 2.4), which is fundamentally via the reversible addition–fragmentation chain transfer polymerization (RAFT) process. Through this CTA a polymer was obtained with control over the molecular weight and a relative low dispersity ($Đ$ = 1.35). Fluoroalcohol was used in this study as control for the tacticity of the polymer.[126] This was the first successful polymerization of NVP using a reversible deactivation radical polymerization (RDRP) process.

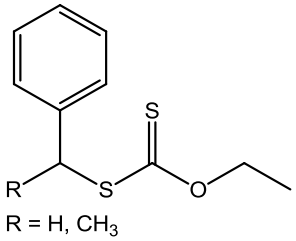

Figure 2.4: CTA for the polymerization of NVP as used by Wan *et al.*[126]

This type of polymerization, using a CTA, is shown in Scheme 2.2. In their study Moad *et al.*[127] presented guidelines for the CTA to be used in the polymerization of NVP, *vide infra* RAFT section.

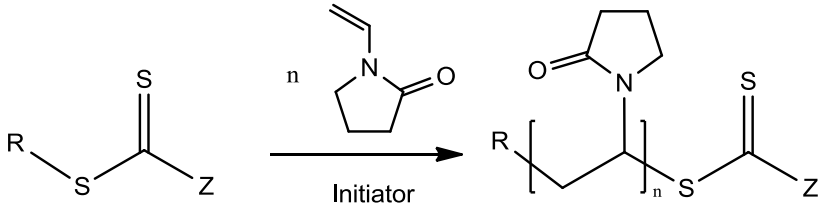

Scheme 2.2: CTA polymerization of NVP

This method of polymerization through the use of a CTA has another useful advantage. On both end groups present on the CTA and subsequently on the polymer, end-functionalization can be used to acquire a desirable functional group for the use of other applications such as bioconjugation, as described earlier.

2.6 Reversible addition–fragmentation chain transfer polymerization

Reversible deactivation radical polymerization (RDRP) is a chain growth process, of monomers to polymers, through the propagation of radicals.[128,129] The biggest attribute of this type of polymerization is that all of the chains formed, grow simultaneously, ensuring equal growth probability.[130] This leads to a polymer where all of the chains are more or less of equal length and thus possess a low dispersity (*Đ*).[129,131] Ideally, all of the chains are initiated in the beginning and grow at the same rate, without termination taking place. During initiation a radical is formed which adds to a monomer, exchanging the radical to this newly added monomer, monomers are added in a similar fashion to form a chain (Scheme 2.3 and Scheme 2.4).[130,132] Chain carriers are used in this radical polymerization method to ensure the process of polymerization is controlled.[133] Due to these chain carriers different techniques of reversible radical polymerization are possible.

In Scheme 2.3 and Scheme 2.4 the concept of reversible radical polymerization is illustrated. In Scheme 2.3 initiation as well as the reversible chain transfer is shown. After initiation the primary radical ($I^{\bullet}$) is formed, with the addition of monomer the chain ($P_n^{\bullet}$) will grow until it is made reversibly dormant ($P_n - X$) which gives another chain the chance to polymerize ($P_m^{\bullet}$). Scheme 2.4 represents the initiation ($I^{\bullet}$) and reversible deactivation of a chain to ensure dormant species are formed.

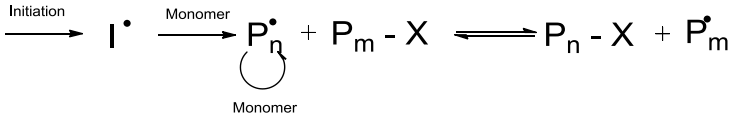

Scheme 2.3: Initiation and reversible chain transfer.[130]

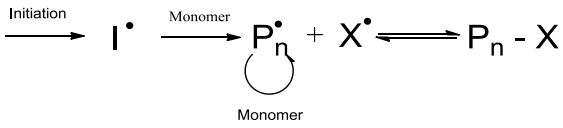

Scheme 2.4: Initiation and reversible deactivation.[130]

Due to the equilibria, depicted in Scheme 2.3 and Scheme 2.4, between the active and dormant species, the chains have an equal chance of growing, although intermittently. Due to this, the molecular weight increases linearly with increasing monomer conversion, and dispersity will be low.

Three techniques are widely used for reversible radical polymerizations. These are reversible addition–fragmentation chain transfer (RAFT) mediated polymerization, atom-transfer radical polymerization (ATRP) and nitroxide-mediated polymerization (NMP).

RAFT polymerization is used due to the various benefits it has on the polymers produced. These benefits include the control it achieves over the molecular weight (M_n), dispersity[129] and the synthesis of advanced architectures.[131] Also a wide range of monomers can be polymerized in comparison to other methods,[129] and it is amenable to copolymerizations of different monomers[134] RAFT polymerization can be performed via four methods, namely suspension, emulsion, bulk and solution.[129] To ensure control is established during RAFT polymerization, chain transfer agents (CTA) is used.[129,131,134] Scheme 2.5 represents the RAFT mediated polymerization mechanism using a CTA.

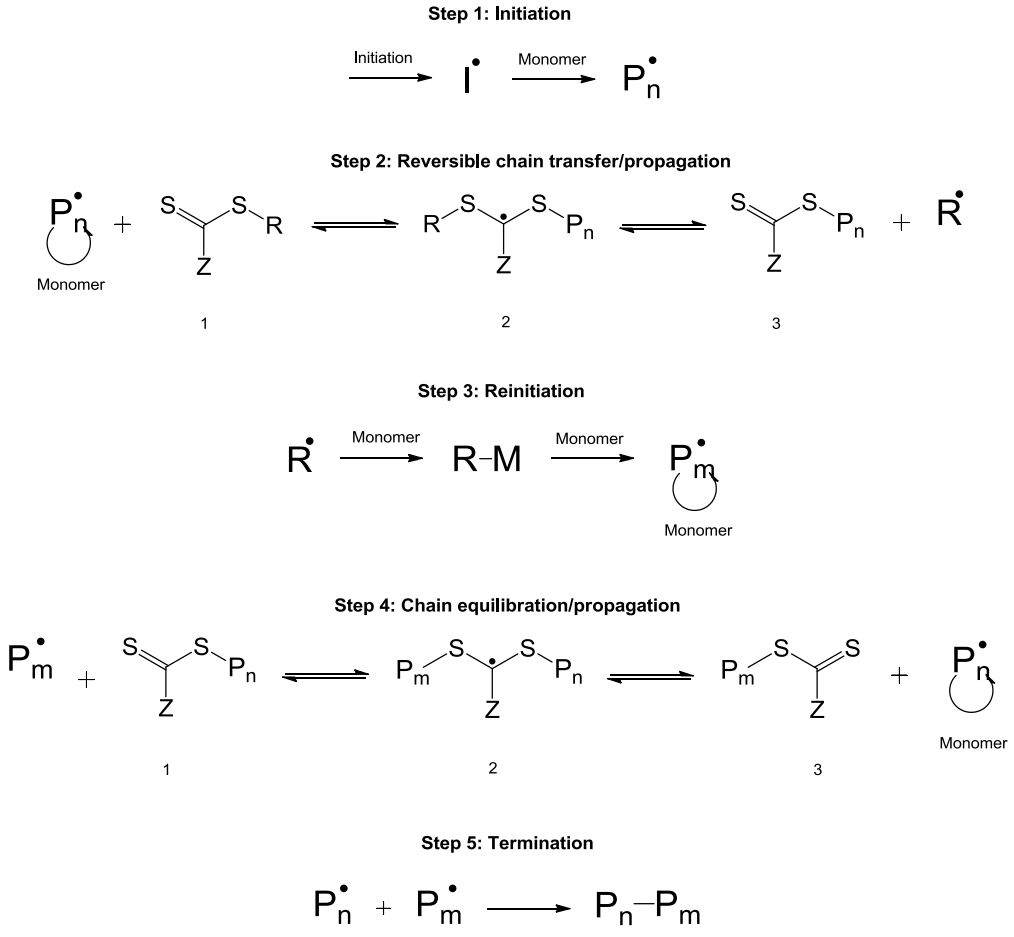

Scheme 2.5: Mechanism of the RAFT-mediated polymerization.[130]

Step 1 of this mechanism is the initiation of the reaction through an initiator. An external source of energy, such as heat or light is required, which decomposes the initiator into forming the first (primary) radicals ($I^{\bullet}$). The propagating species ($P_n^{\bullet}$) are formed when this radical reacts with monomer, as seen in step 1. During step 2 this propagating species adds to the CTA (1), forming the so-called intermediate radical (2). This forces a radical ($R^{\bullet}$) formation from the CTA (3). This radical

reinitiates to form another chain ($P_m^{\bullet}$) as seen in step 3. The new propagating species ($P_m^{\bullet}$) will grow in the presence of monomer. In step 4 this chain $P_m^{\bullet}$ transfers to the CTA (1). The radical is placed on the CTA (3). The radical forces the dormant chain ($P_n^{\bullet}$) to release from the CTA with a radical (3). Growth can take place on this new propagating species ($P_n^{\bullet}$) in the presence of monomer. During this step 4 chain growth will take place on all of the chains formed due to continuous initiation and termination. Step 5 is the termination of the chains.

The CTAs ensure the different polymer chains grow a few repeat units at a time, instead of instantaneous full chain growth thus, ensuring the control of molecular weight and dispersity.

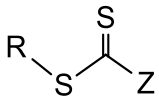

Figure 2.5: Structural design of a CTA[129,131,135]

A CTA compound consists of a free radical leaving group or R group, an activating/stabilizing group or Z group and a thiocarbonyl thio group (S=C-S) as shown in Figure 2.5. The choice of R and Z groups depends on the monomer being used for the polymerization and should be used in conjunction with each other in controlling the polymerization,[136,137] due to the effect it has on the fragmentation and addition during polymerization and, thus, how effective the CTA will be.[138,139]

The Z group, on the CTA, influences the reactivity of the thiocarbonyl double bond towards the radical polymer chain, stabilizing the intermediate radical and as a consequence, having an effect on the rates of addition and fragmentation.[139] The choice of Z group used, on the CTA, depends on this activation/stabilization it has towards the monomer, in the polymerization process. Trithiocarbonates (alkylthio) and dithioesters (aryl or alkyl) Z groups, stabilize the more activated monomers (styrene, methacrylates, acrylates, acrylonitrile and acrylamide).[140] Whereas for the less activated monomers (vinyl acetate, *N*-vinylcarbazole and *N*-vinylpyrrolidone), xanthates (alkoxy) and *N*,*N*-dialkyl- or *N*-alkyl-*N*-aryl dithiocarbamates (*N*,*N*-dialkylamino or *N*-alkyl-*N*-arylamino) are used, as Z groups, for stabilization.[137] Unfortunately these Z groups mentioned for more and less activated monomer groups respectively cannot stabilize the other monomer group, thus copolymerization of a more activated monomer with a less activated monomer or vice versa is troublesome. However, Z groups containing some dithiocarbamates can polymerize both more and less activated monomer groups.[141]

The R group used on the CTA must be a good leaving group as well as a good reinitiating group towards the monomer added in the chain, to ensure growth of the chain at the same time. It should also stabilize the intermediate formed.[127,139,142,143] It is shown that R groups that have a tertiary carbon, are from a polarity, sterically and radical stability point of view able to fulfil these prerequisites of good stabilization and reinitiation.[139,142,144]

In general *N*-vinyl monomers are difficult to polymerize, even with radical polymerization due to the structure. These monomers have strong electron donating groups and small resonance stabilization, which makes them poor homolytic leaving groups.[132] Thus, the radical species formed will be highly reactive, leading to uncontrollable polymerizations, which in any polymerization of a monomer leads to uncontrollable polymer chains with undesirable molecular weight and dispersity[145].

Due to NVP, being a less activated monomer, xanthates are used as CTA, for its stabilization effect on NVP during the polymerization of NVP.[126,137,142] Xanthates are possess an alkoxy substituent (–OR), where the alkyl R can have any chain length.[132] An example of a xanthate can be seen in Figure 2.6. This xanthate must be used to ensure the correct reactivity towards the thiocarbonyl double bond on the CTA, for the polymerization of NVP.

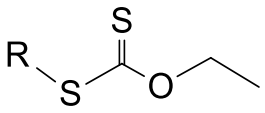

Figure 2.6: Xanthate RAFT agent.[132]

As R (leaving) groups for the use in NVP polymerizations various functionalities can be used, which meet the prerequisites as described. A nitrile, phenyl or carboxylic group attached to the central carbon atom (Figure 2.7) gives satisfactory control over the NVP polymerization. Nitrile and carboxylic groups obtain better results than phenyl groups. Polarity and steric effects play a role in the addition and fragmentation of the radicals. Electron withdrawing groups increase the rate of fragmentation and decrease rates of addition to the thiocarbonyl group. More steric molecules have a better CTA activity. Methyl and hydrogen substituent on the central carbon also plays a role in activity. The activity increase in the series tertiary> secondary>primary.[142,145,146]

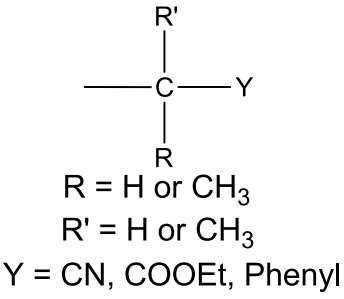

Figure 2.7: Possible R groups for NVP polymerization.

In their study Wan *et al*.[126] used a CTA containing an alkoxy group on the Z group, forming a xanthate and a phenyl as R group with hydrogen and methyl groups for the RAFT polymerization of NVP. The polymerization was conducted at 60 °C with AIBN as initiator in bulk, achieving control over both the molecular weight and dispersity, in the polymerization of NVP.

2.7 References

(1) Keogh, E. V; Walsh, R. J. *Nature* **1965**, *207*, 877–878.

(2) Pandhi, D.; Khanna, D. *Indian J. Dermatol. Venereol. Leprol.* **2013**, *79*, 641–653.

(3) Arck, P. C.; Overall, R.; Spatz, K.; Liezman, C.; Handjiski, B.; Klapp, B. F.; Birch-Machin, M. A.; Peters, E. M. J. *FASEB J.* **2006**, *20*, 1567–1569.

(4) Nordlund, J, J.; Boissy, R, E.; Hering, V, J.; King, R, A.; Ortonne, J, P. *The Pigmentary System*; Oxford University Press, 1998.

(5) Wood, J, M.; Spencer, J, D.; Thornton, M, J.; Decker, H.; Schallreuter, K, U.; Hartmann, H.; Chavan, B.; Rokos, H.; Hasse, S.; Paus, R.; Shalbaf, M. *FASEB J.* **2009**, *23*, 2065–2075.

(6) Bull, J. J.; Müller-Röver, S.; Patel, S. V.; Chronnell, C. M. T.; McKay, I. a.; Philpott, M. P. *J. Invest. Dermatol.* **2001**, *116*, 617–622.

(7) Millar, S. *J. Investig. dermatology*. **2002**, *118*, 216–255.

(8) Cooper, G. M. *The Cell: Approach*; Sinauer Associates: Sunderland, 2000.

(9) Schönbein, C. F. *J. fur Prakt. Chemie*. **1863**, *98*, 323–344.

(10) Loew, O.; Loew, O. U. S. *Dept. Agric. Report.* **1901**, *68*, 47–55.

(11) Wieland, H.; Franke, W. *Liebigs Ann. der Chemie.* **1927**, *457*, 1–70.

(12) Gaetani, G. F.; Ferraris, A. M.; Rolfo, M.; Mangerini, R.; Arena, S.; Kirkman, H. N. *Blood* **1996**, *87*, 1595–1599.

(13) Mueller, S.; Riedel, H. D.; Stremmel, W. *Anal. Biochem.* **1997**, *245*, 55–60.

(14) Deutsch, H. F. *Acta Chem. Scand.* **1951**, *5*, 815–819.

(15) Sumner, J, B.; Dounce, A, L. *J. Biol. Chem.* **1937**, *121*, 417–424.

(16) Schroeder, W. A.; Shelton, J. R.; Shelton, J. B.; Robberson, B.; Apell, G.; Fang, R. S.; Bonaventura, J. *Arch. Biochem. Biophys.* **1982**, *214*, 397–421.

(17) Herbert, D.; Pinsent, J. *Biochem. J.* **1948**, *43*, 193–202.

(18) Hartig, A.; Ruis, H. *Eur. J. Biochem.* **1986**, *160*, 487–490.

(19) Clayton, R, K. *Biochim. Biophys. Acta*. **1959**, *36*, 40–47.

(20) Buzy, A.; Bracchi, V.; Sterjiades, R.; Chroboczek, J.; Thibault, P.; Gagnon, J.; Jouve, H. M.; Hudry-Clergeon, G. *J. Protein Chem.* **1995**, *14*, 59–72.

(21) Galston, A, W.; Bonnichsen, R, K.; Arnon, D, I. *Acta Chem. Scand.* **1952**, *5*, 781–790.

(22) Guan, L.; Scandalios, J. G. *Proc. Natl. Acad. Sci. U. S. A.* **1995**, *92*, 5930–5934.

(23) Belal, R.; Momenteau, M.; Meunier, B. *New J. Chem.* **1989**, *13*, 853–862.

(24) Murthy, M. R. N.; Reid, Thomas J., I.; Sicignano, A.; Tanaka, N.; Rossmann, M. G. *J. Mol. Biol.* **1981**, *52*, 465–499.

(25) Fita, I.; Silva, A. M.; Murthy, M. R. N.; Rossmann, M. G. *Acta Crystallogr. B.* **1986**, *42*, 497–515.

(26) Nicholls, P.; Fita, I.; Loewen, P. C. *Adv. Inorg. Chem.* **2000**, *51*, 51–106.

(27) Chance, B. *Acta Chem. Scand.* **1947**, *1*, 236–267.

(28) Chance, B. *J. Biol. Chem.* **1949**, *179*, 1299–1309.

(29) Northrop, J. H. *J. Gen. Physiol.* **1925**, *7*, 373–387.

(30) Maehly, A, C.; Chance, B. *Methods Biochem Anal.* **1954**, *7*, 357–424.

(31) Stern, K. G. *J. Biol. Chem.* **1936**, *112*, 661–669.

(32) Torii, K.; Iizuka, T.; Ogura, Y. *J. Biochem.* **1970**, *68*, 837–841.

(33) Theorrll, H. B.; Agner, K. *Ark. Ark. foer Kemi, Mineral. och Geol.* **1943**, *16A*, 1–14.

(34) Waldo, G, S.; Fronko, R, M.; Penner-Hahn, J, E. *Biochemistry.* **1991**, *30*, 10486–10490.

(35) Allgood, G, S.; Perry, J, J. *J. Bacteriol.* **1986**, *168*, 563–567.

(36) Kono, Y.; Fridovich, I. *J. Biol. Chem.* **1983**, *258*, 6015–6019.

(37) Vainshtein, B. K.; Melik-Adamyan, W. R.; Barynin, V. V; Vagin, A. A.; Grebenko, A. I. *Nature*. **1981**, *293*, 411–412.

(38) Vainshtein, B. K.; Melik-Adamyan, W. R.; Barynin, V. V; Vagin, A. A.; Grebenko, A. I.; Borisov, V. V; Bartels, K. S.; Fita, I.; Rossmann, M. G. *J. Mol. Biol.* **1986**, *188*, 49–61.

(39) Ko, T. P.; Safo, M. K.; Musayev, F. N.; Di Salvo, M. L.; Wang, C.; Wu, S. H.; Abraham, D. J. *Acta Crystallogr. D. Biol. Crystallogr.* **2000**, *56*, 241–245.

(40) Putnam, C. D.; Arvai, A. S.; Bourne, Y.; Tainer, J. A. *J. Mol. Biol.* **1999**, *296*, 295–309.

(41) Raven, P, H.; Johnson, G, B.; Losos, J, B.; Singer, S, R. *Biology*; McGraw-Hill higher education: Boston, 2011; pp 34–40.

(42) Alberts, B.; Johnson, A.; J, L.; Morgan, D.; Raff, M.; Roberts, K.; P., W. *Molecular Biology of the Cell*; Garland Science: New York, 2002.

(43) Kasaharas, M.; Hinkle, P, C. *J. Biol. Chem.* **1977**, *252*, 7384–7390.

(44) LeFevre, P, G. *J. Gen. Physiol.* **1948**, *31*, 505–527.

(45) Widdas, W, F. *J. Physiol.* **1952**, *118*, 23–39.

(46) Baldwin, J, M.; Gorga, J, C.; Lienhard, G, E. *J. Biol. Chem.* **1981**, *256*, 3685–3689.

(47) Gorga, F. R.; Baldwin, S. A.; Lienhard, G. E. *Biochem. Biophys. Res. Commun.* **1979**, *91*, 955–961.

(48) Sogin, D. C.; Hinkle, P. C. *J. Supramol. Struct.* **1978**, *8*, 447–453.

(49) Baldwin, S, A.; Baldwin, J, M.; Gorga, F, R.; Lienhard, G, E. *Biochim. Biophys. Acta.* **1979**, *552*, 183–188.

(50) Dominguez, R.; Holmes, K, C.; Lodish, H.; Berk, A.; Zipursky, S. L. *Annu. Rev. Biophys.* **2011**, 169–186.

(51) Cooper, G. M. *The Cell Approach*; Sinauer Associates; Sunderland, 2000.

(52) Bragulla, H. H.; Homberger, D. G. *J. Anat.* **2009**, *214*, 516–559.

(53) Banting, F, G.; Best, C, H.; Collip, J, B.; Campbell, W, R.; Fletcher, A, A. *Can. Med. Assoc. J.* **1991**, *145*, 1281–1286.

(54) Goeddel, D. V; Kleid, D. G.; Bolivar, F.; Heyneker, H. L.; Yansura, D. G.; Crea, R.; Hirose, T.; Kraszewski, A.; Itakura, K.; Riggs, A. D. *Proc. Natl. Acad. Sci. U. S. A.* **1979**, *76*, 106–110.

(55) Lawrence, E. *Henderson's dictionary of biology*; Pearson Education Ltd, 2008.

(56) Tanaka, H.; Okada, Y.; Kawagishi, M.; Tokiwa, T. *J. Pharmacol. Exp. Ther.* **1989**, *251*, 1199–1203.

(57) Baumgarten, W. *Vox Sang.* **1967**, *13*, 84–85.

(58) Marlborough, D. I.; Miller, D. S.; Cammack, K. A. *Biochim. Biophys. Acta* **1975**, *386*, 576–589.

(59) Mashbum, L, T.; Wriston, J, C. *Arch. Biochem. Biophys.* **1964**, *105*, 450–453.

(60) Duncan, R. *Nat. Rev. Drug Discov.* **2003**, *2*, 347–360.

(61) Park, E. Y.; Ishikiriyama, M.; Nishina, T.; Kato, T.; Yagi, H.; Kato, K.; Ueda, H. *J. Biotechnol.* **2009**, *139*, 108–114.

(62) Leader, B.; Baca, Q. J.; Golan, D. E. *Nat. Rev. Drug Discov.* **2008**, *7*, 21–39.

(63) Kaneda, Y.; Yamamoto, Y.; Kamada, H.; Tsunoda, S.; Tsutsumi, Y.; Hirano, T.; Mayumi, T. *Cancer Res.* **1998**, *58*, 290–295.

(64) Tsutsumi, Y.; Kihira, T.; Tsunoda, S.; Kamada, H.; Nakagawa, S.; Kaneda, Y.; Kanamori, T.; Mayumi, T. *J. Pharmacol. Exp. Ther.* **1996**, *278*, 1006–1011.

(65) Tsutsumi, Y.; Tsunoda, S.; Kamada, H.; Kihira, T.; Kaneda, Y.; Ohsugi, Y.; Mayumi, T. *Thromb. haemostasis.* **1997**, *77*, 168–173.

(66) Abuchowski, A.; van Es, T.; Palczuk, N. C.; Davis, F. F. *J. Biol. chem.* **1977**, *252*, 3578–3581.

(67) Chen, R.; Abuchowski, A.; van Es, T.; Palczuk, N, C, D.; Frank, F. *Biochim. Biophys. Acta.* **1981**, *660*, 293–298.

(68) Soares, A. L.; Guimarães, Manso, G.; Polakiewicz, B.; Pitombo, R. N. D. M.; Abrahão-Neto, J. *Int. J. Pharm.* **2002**, *237*, 163–170.

(69) Ashihara, Y.; Kono, T.; Yamazaki, S.; Inada, Y. *Biochem. Biophys. Res. Commun.* **1978**, *83*, 385–391.

(70) Abuchowski, A.; McCoy, J. R.; Palczuk, N. C.; van Es, T.; Davis, F. F. *J. Biol. Chem.* **1977**, *252*, 3582–3586.

(71) Koide, A.; Kobayashi, S. *Biochem. Biophys. Res. Commun.* **1983**, *111*, 659–667.

(72) Jackson, C.; Charlton, J.; Lang, G.; Sehon, A.; Kuzminski, K. *Anal. Biochem.* **1987**, *165*, 114–127.

(73) Buckmann, A. F.; Morr, M.; Johansson, G. *Makromol. Chemie.* **1981**, *182*, 1379–1384.

(74) Joppich, M.; Luisi, P, L. *Makromol. Chemie.* **1979**, *180*, 1381–1384.

(75) Abuchowski, A.; Kazo, G. M.; Verhoest, C. R.; Van Es, T.; Kafkewitz, D.; Nucci, M. L.; Viau, A. T.; Davis, F. F. *Cancer Biochem. Biophys.* **1984**, *7*, 175–186.

(76) Harris, J.; Struck, E.; Case, M.; Paley, M.; van Alstine, J.; Brooks, D.; Yalpani, M. *J. Polym. Scieince Polym. Chem. Ed.* **1984**, *22*, 341–352.

(77) Chamow, S. M.; Kogan, T. P.; Venuti, M.; Gadek, T.; Harris, R. J.; Peers, D. H.; Mordenti, J.; Shak, S.; Ashkenazi, A. *Bioconjug. Chem.* **1994**, *5*, 133–140.

(78) Jentoft, N. *J. Biol. Chem.* **1979**, *254*, 4359–4365.

(79) Nishikawa, M.; Tamada, A.; Kumai, H.; Yamashita, F.; Hashida, M. *Int. J. cancer.* **2002**, *99*, 474–479.

(80) Nishikawa, M.; Tamada, A.; Hyoudou, K.; Umeyama, Y.; Takahashi, Y.; Kobayashi, Y.; Kumai, H.; Ishida, E.; Staud, F.; Yabe, Y.; Takakura, Y.; Yamashita, F.; Hashida, M. *Clin. Exp. metastasis.* **2004**, *21*, 213–221.

(81) Hyoudou, K.; Nishikawa, M.; Umeyama, Y.; Kobayashi, Y.; Yamashita, F.; Hashida, M. *Clin. cancer Res.* **2004**, *10*, 7685–7691.

(82) Hyoudou, K.; Nishikawa, M.; Kobayashi, Y.; Umeyama, Y.; Yamashita, F.; Hashida, M. *Free Radic. Biol. Med.* **2006**, *41*, 1449–1458.

(83) Shi, B.; Zhu, M.; Liu, S.; Zhang, M. *Biomed Res. Int.* **2013**, *2013*, 1–4.

(84) Bayramoglu, G.; Karagoz, B.; Yilmaz, M.; Bicak, N.; Arica, M. Y. *Bioresour. Technol.* **2011**, *102*, 3653–3661.

(85) Riccardi, C. M.; Cole, K. S.; Benson, K. R.; Ward, J. R.; Bassett, K. M.; Zhang, Y.; Zore, O. V; Stromer, B.; Kasi, R. M.; Kumar, C. V. *Bioconjugate Chem.* **2014**, *25*, 1501–1510.

(86) Alptekin, Ö.; Tükel, S, S.; Alagöz, D.; Yildirim, D. *J. Mol. Catal. B Enzym.* **2009**, *58*, 121–131.

(87) Yoshimoto, M.; Sakamoto, H.; Shirakami, H. *Colloids surfaces. B, Biointerfaces.* **2009**, *69*, 281–287.

(88) Yoshimoto, M.; Sakamoto, H.; Yoshimoto, N.; Kuboi, R.; Nakao, K. *Enzym. Microb. Technol.* **2007**, *41*, 849–858.

(89) Yoshimoto, K.; Setoyama, Y.; Tsuzaka, K.; Abe, T.; Takeuchi, T. *J. Biomed. Biotechnol.* **2010**, *2010*, 1–6.

(90) Abdel-mageed, H, M.; El-laithy, H, M.; Mahran, L, G.; Fahmy, A, S.; Mäder, K.; Mohamed, S, A. *Process Biochem.* **2012**, *47*, 1155–1162.

(91) Cengiz, S. Çavaş, L. Yurdakoç, K. *Appl. Clay Sci.* **2012**, *65 – 66*, 114–120.

(92) Chin, W.; Heng, P.; Lau, W.; Bhuvaneswari, R.; Olivo, M. *Photochem. Photobiol. Sci.* **2006**, *5*, 1031–1037.

(93) Sairam, M.; Babu, V, R.; Rao, K, S, V, K.; Aminabhavi, T, M. *J. Appl. Polym. Sci.* **2007**, *104*, 1860–1865.

(94) Bailly, N.; Pound-Lana, G.; Klumperman, B.; J. *Aust. J. Chem.* **2012**, *65*, 1124–1131.

(95) Kaneda, Y.; Tsutsumi, Y.; Yoshioka, Y.; Kamada, H.; Yamamoto, Y.; Kodaira, H.; Tsunoda, S.; Okamoto, T.; Mukai, Y.; Shibata, H.; Nakagawa, S.; Mayumi, T. *Biomaterials.* **2004**, *25*, 3259–3266.

(96) Kamada, H.; Tsutsumi, Y.; Yamamoto, Y.; Kihira, T.; Kaneda, Y.; Mu, Y.; Kodaira, H.; Tsunoda, S. I.; Nakagawa, S.; Mayumi, T. *Cancer Res.* **2000**, *60*, 6416–6420.

(97) Tsunoda, S.; Kamada, H.; Yamamoto, Y.; Ishikawa, T.; Matsui, J.; Koizumi, K.; Kaneda, Y.; Tsutsumi, Y.; Ohsugi, Y.; Hirano, T.; Mayumi, T. *J. Control. release* **2000**, *68*, 335–341.

(98) Monfardini, C.; Veronese, F. M. *Bioconjugate Chem.* **1998**, *9*, 418–450.

(99) Haaf, A. S.; Straub, F. *Polym. J.* **1985**, *17*, 143–152.

(100) Ravin, H. A.; Seligman, A. M.; Fine, J. N. *Engl. J. Med.* **1952**, *247*, 921–929.

(101) Reppe, W. *Angew. Chemie.* **1954**, *65*, 577–604.

(102) Hueper, W, C. *Cancer.* **1957**, *10*, 8–18.

(103) Hueper, W, C. *Arch. Path.* **1959**, *67*, 589–617.

(104) Hueper, W, C. *J. Natl. Cancer Inst.* **1961**, *26*, 229–237.

(105) Higa, O. Z.; Rogero, S, O.; Machado, L, D, B.; Mathor, M, B.; Lugão, A, B. *Radiat. Phys. Chem.* **1999**, *55*, 705–707.

(106) Bindu, N. *Int. J. Toxicol.* **1998**, *17*, 95–130.

(107) Kirsh, Y. E.; Chichester, U. K. *Water Soluble Poly-N-Vinylamides: Synthesis and Physicochemical Properties; Wiley*: Chichester, 1998; pp 129–215.

(108) D'Souza, A, J, M.; Schowen, R, L.; Topp, E, M. *J. Control. Release.* **2004**, *94*, 91–100.

(109) Pretula, J.; Kaluzynski, K.; Wisniewski, B.; Szymanski, R.; Loontjens, T.; Penczek, S. *J. Polym. Sci. Part a-Polymer Chem.* **2008**, *46*, 830–843.

(110) Lugão, A, B.; Machado, L, D, B.; Miranda, L, F.; Alvarez, M, R.; Rosiak, J. M. *Radiat. Phys. Chem.* **1998**, *52*, 319–322.

(111) Lugão, A. B.; Rogero, S. O.; Malmonge, S. M. *Radiat. Phys. Chem.* **2002**, *63*, 543–546.

(112) Banwell, H. *Dermatology* **2006**, *212*, 66–76.

(113) Ignatova, M.; Stoilova, O.; Manolova, N.; Markova, N.; Rashkov, I. *Macromol. Biosci.* **2010**, *10*, 944–954.

(114) Davies, W. L.; Gloor, W. T. *J. Pharm. Sci.* **1972**, *61*, 618–622.

(115) Lee, S. *Sci. Aging Knowledge Environ.* **2005**, *35*, 26–34.

(116) Santanakrishnan, S.; Hutchinson, R, A.; Učňova´, L.; Stach, M.; Lacík, I.; Buback, M. *Macromol. Symp.* **2011**, *302*, 216–223.

(117) Santanakrishnan, S.; Tang, L.; Hutchinson, R, A.; Lacík, I.; Stach, M.; Schrooten, J.; Hesse, P.; Buback, M. *Macromol. React. Eng.* **2010**, *4*, 499–509.

(118) Fikentscher, H.; Herrle, K. *Mod. Plast.* **1943**, *23*, 157–163.

(119) Kern, W.; Chedron, H. *Houben Weyl methoden der Org. chemie* **1962**, *Vol. XIV/1*.

(120) Breitenbach, W.; Schmidt, A. *Monatsch Chem.* **1952**, *83*, 1288.

(121) Breitenbach, W. *J. Polym. Sci.* **1957**, *23*, 949.

(122) Buhler, V. *Polyvinylpyrrolidone for Pharmaceuticals*; Springer: Berlin, 2005.

(123) Teodorescu, M.; Bercea, M. *Polym. Technol. Eng.* **2015**, *54*, 923–943.

(124) Kumbar, S.; Laurencin, C.; Deng, M. *Natural and Synthetic Biomedical Polymers*; Elsevier Inc: Burlington, 2014.

(125) Schuster, C.; Fikentscher, H. Polymerization of n-vinyl lactams. U.S. Patent 2335454, November1943.

(126) Wan, D.; Satoh, K.; Kamigaito, M.; Okamoto, Y. *Macromol. ,* **2005**, *38*, 10397–10405.

(127) Moad, G.; Rizzardo, E.; Thang, S. H. *Aust. J. Chem.* **2005**, *58*, 379–410.

(128) Szwarc, M. *Nature.* **1956**, *178*, 1168–1169.

(129) Chiefari, J.; Chong, Y, K.; Le, T, P, T.; Mayadunne, R, T, A.; Kristina, J.; Jeffrey, J.; Ercole, F.; Meijs, G, F.; Moad, C, L.; Thang, S, H.; Rizzardo, E.; Moad, G.; Postma, A. *Macromolecules.* **1998**, *31*, 5559–5562.

(130) Moad, V. G.; Solomon, D. H. *The Chemistry of Free Radical Polymerization.*; Pergamon-Elsevier Science Ltd., Ed.: Oxford, 1995.

(131) Mayadunne, R. T. A.; Rizzardo, E.; Chiefari, J.; Chong, Y. K.; Moad, G.; Thang, S. H. *Macromolecules.* **1999**, *32*, 6977–6980.

(132) Barner-Kowollik, C. *Handbook of RAFT polymerization.*; John Wiley & Sons: Hoboken, 2007.

(133) Jenkins, S. J.; Allen, J. E. *J. Biomed. Biotechnol.* **2010**, *2010*, 1–14.

(134) Mayadunne, R. T. A.; Rizzardo, E.; Chiefari, J.; Krstina, J.; Moad, G.; Postma, A.; Thang, S. H. *Macromolecules.* **2000**, *33*, 243–245.

(135) Chong, Y. K.; Le, T. P. T.; Moad, G.; Rizzardo, E.; Thang, S. H. *Macromolecules.* **1999**, *32*, 2071–2074.

(136) Rodriguez, A. R.; Choe, U.-J.; Kamei, D. T.; Deming, T. J. *Macromol. Biosci.* **2012**, *12*, 805–811.

(137) Tsarevsky, N, V.; Sumerlin, B, S. *Fundamentals of Controlled/Living Radical Polymerization.*; Royal Society of Chemistry: London, 2012; pp 78 –283.

(138) Moad, G.; Rizzardo, E.; Thang, S. H. *Acc. Chem. Res.* **2008**, *41*, 1133–1142.

(139) Moad, G.; Rizzardo, E.; Thang, S. H. *Chem. Asian J.* **2013**, *8*, 1634–1644.

(140) Rodriguez, C.; Weintrob, A. C.; Dunne, J. R.; Weisbrod, A. B.; Lloyd, B.; Warkentien, T.; Malone, D.; Wells, J.; Murray, C. K.; Bradley, W.; Shaikh, F.; Shah, J.; Carson, M. L.; Aggarwal, D.; Tribble, D. R. *J. Trauma Acute Care Surg.* **2014**, *77*, 769–773.

(141) Benaglia, M.; Chiefari, J.; Chong, Y. K.; Moad, G.; Rizzardo, E.; Thang, S. H. *J. Am. Chem. Soc.* **2009**, *131*, 6914–6915.

(142) Keddie, D, J.; Moad, G.; Rizzardo, E.; Thang, S. H. *Macromolecules.* **2012**, *45*, 5321–5342.

(143) Perrier, S.; Tokalpuckdee, P. *J. Polym. Chem.* **2005**, *43*, 5347–5393.

(144) Chong, Y, K.; Kristina, J.; Le, T, P, T.; Moad, G.; Postma, A.; Rizzardo, E.; Thang, S, H. *Macromolecules.* **2003**, *36*, 2256–2272.

(145) Nakabayashi, K.; Mori, H. *Eur. Polym. Journal.* **2013**, *49*, 2808–2838.

(146) Moad, G.; Rizzardo, E.; Thang, S. H. *Polymer* **2008**, *49*, 1079–1131.

Chapter 3: Synthesis

3.1 Introduction

Radical polymerization is a widely used process for the production of polymers with high molecular weights.[1] Reversible addition fragmentation chain transfer (RAFT) mediated polymerization is one of the radical polymerization techniques used.[2,3] For this polymerization technique a chain transfer agent (CTA) is used. The CTA has the structural design as depicted in Figure 3.1. The CTA consists of a free radical leaving R group, stabilizing Z group and thiocarbonyl thio group connecting the R and Z groups.

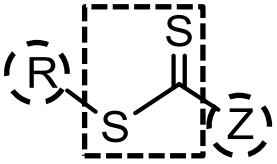

Figure 3.1: Structural design of a RAFT CTA with R-, Z- and thiocarbonyl thio groups indicated.[2,4,5]

CTAs are used due to the advantageous effect of controlling the polymerization of various monomers. This control during the polymerization reaction, includes the molecular weight and dispersity (*Đ*) of the polymer.[2,6,7]

Control over the polymerization reaction needs to be achieved. Due to the length of the polymer chains (average number of monomers per chain, defined as average degree of polymerization DP_n (Equation 3.1)) and the molecular weight distribution, also known as dispersity, variations in the properties of the polymer can be found.[8–11]

$$DP_n = \frac{M_{\text{Average molar mass of polymer}}}{M_{\text{molecular weight of monomer}}} \qquad (3.1)$$

It has been shown that a well-known monomer, *N*-vinylpyrrolidone (NVP), can be polymerized with good results, through the use of CTAs.[5,7] NVP is predominantly polymerized through xanthate based thiocarbonyl thio CTAs (Figure 3.2),[12,13] due to stabilization effect these CTAs have during polymerization.[14] This stabilization is needed due to the NVP monomer being non-conjugated. The propagating radical thus is very reactive and poorly stabilized,[15] which is countered by these xanthate CTAs.[16,17] The intermediate radical formed during polymerization of NVP is described as to possess a poor homolytic leaving group, which is stabilized and retarded by these xanthate CTAs.[14] New research has been done into more versatile switchable CTAs.[4,18–20] Examples of these CTAs are dithiocarbamate functionalities on the Z group.[21] Xanthate CTAs are however, easier to synthesise and polymerization through xanthate mediated RAFT of NVP is easier and better controlled.

Xanthates are thiocarbonyl thio compounds with an alkoxy group ($O-R'$, where R' can be any alkyl) attached to the central carbon between the sulphur atoms.[12] The general structures for these compounds are shown in Figure 3.2. The activating Z group on the structure is the alkoxy group, which forms a xanthate due to the $-S(S)C-O-R'$ group.[22]

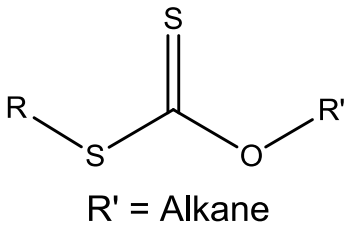

Figure 3.2: General structure of xanthates.[23]

Monomer is inserted between the R group and the single bonded sulphur on the CTA (Scheme 3.1). Insertion takes place when the R group acts as a good leaving and reinitiating group. The R group on the CTA should also stabilize the radical formed during polymerization and have no retardation effect on the polymerization[4].

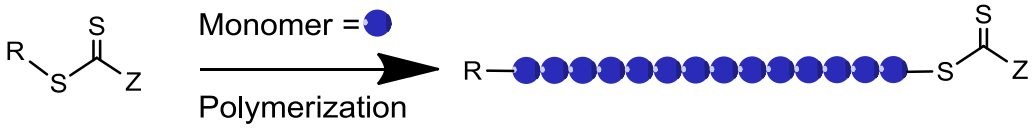

Scheme 3.1: General polymerization scheme.

The aim of this chapter is the description of the CTA synthesis and the polymerization of NVP.

3.2 Experimental

3.2.1 Materials

N-vinylpyrrolidone (Sigma Aldrich, >99 %, sodium hydroxide as inhibitor) was distilled under reduced pressure before use, to remove impurities and inhibitors, and stored over molecular sieves, at -20 °C, to minimise side reactions which consume the monomer.[24] 2,2'-Azobisisobutyronitrile (AIBN) (Riedel de Haën) was recrystallized twice from methanol. Potassium *O*-ethyl xanthate (Adrich, 96%), potassium iodide (Riedel de Haën) and iodine (Fluka) were used without any purification. Anhydrous magnesium sulphate (Merck) was used as drying agent. Toluene (Sigma Aldrich, anhydrous, 99.8%), pentane, diethyl ether, chloroform and ethyl acetate (KIMIX) were used without re-distillation. Distilled deionized water was obtained from an OLGA Purelab option water filtration system set up. Silica gel (Fluka, particle size 0.063 – 0.2 mm, Brockmann 2-3) was used for column chromatography. TLC analysis was done using Machery-Nagel pre-coated TLC aluminium sheets (DC-Fertigfolien ALUGRAM® Xtra SIL G/UV_{254}). Snakeskin dialysis tubing (Thermo

Scientific, 3500 MWCO, 22mm × 35 feet diameter) was used for dialysis. Freeze drying was done using a Virtus BenchTop 2K freeze dryer coupled to an Edwards vacuum pump.

3.2.2 Synthesis of CTA *S*-(2-cyano-2-propyl), *O*-ethyl xanthate (R1)

The synthesis of *S*-(2-cyano-2-propyl), *O*-ethyl xanthate was adapted from a method as described by Pound *et al*.[25] This is done in a two-step process. *O*,*O*-diethyl bisxanthate was prepared by dissolving potassium *O*-ethyl xanthate (5.03 g, 31.3 mmol) in distilled water (50 mL). Iodine (1.7 g, 13.4 mmol) and potassium iodide (0.86 g, 0.518 mmol) dissolved in water (50 mL) was added dropwise to the yellow potassium *O*-ethyl xanthate solution. This was left to stir for 48 hours at room temperature. The product formed was extracted with diethyl ether (3 × 50 mL) and the combined ether fractions where washed with distilled water (3 × 50 mL) to remove any unwanted salts. Anhydrous magnesium sulphate was used to dry the ether solution. The solvents were removed under vacuum and a yield of 1.55 g of the yellow oil was found. Yield = 41 %. Purity > 97 % by NMR. ^{1}H-NMR ($CDCl_3$): δ [ppm] = 1.43 (CH_2-$\underline{CH_3}$, 6H, t, ^{3}J = 7.1 Hz), 4.69 (O-$\underline{CH_2}$-CH_3, 4H, q, ^{3}J = 7.1 Hz).

Subsequently, *O*,*O*-diethyl bisxanthate (1.15 g, 4.75 mmol), and AIBN (1.57 g, 9.54 mmol) were dissolved in toluene (40 mL) and placed in a three-neck round bottom flask at room temperature. The solution was degassed by purging with argon for 30 min, whilst stirring. The flask was placed in an oil bath preheated to 80 °C and the reaction ran for 8 hours. After the reaction reached completion the solvent was removed under reduced pressure. Purification was performed using column chromatography with a solvent composition of pentane: ethyl acetate solution of 70:30 (*v/v*). After removal of the solvents, 1.49 g of a yellow oil was found. (Yield = 83%). Purity > 97 % as determined by NMR. ^{1}H-NMR ($CDCl_3$): δ[ppm] = 1.47 (CH_2-$\underline{CH_3}$, 3H, q, ^{3}J = 7.1 Hz), 1.78 (C(CN)$\underline{(CH_3)_2}$, 6H, s), 4.76 (O-$\underline{CH_2}$-CH_3, 2H, q, ^{3}J = 7.1 Hz)

^{13}C-NMR δ[ppm] = 208.02 (O$\underline{C}$(S)S), 121.12 (C($\underline{CN}$)$(CH_3)_2$), 71.09 (O-$\underline{CH_2}$-CH_3), 41.20 ($\underline{C}$(CN)$(CH_3)_2$);, 25.19 (C(CN)$\underline{(CH_3)_2}$), 13.17 (CH_2-$\underline{CH_3}$).

3.2.3 Polymerization of NVP

A typical polymerization of NVP, targeting a molecular weight of 20 000 g/mol, with R1 as CTA was described by Pound *et al*.[25] The molar ratios of monomer to CTA was determined from Equation 3.1. As an example a target polymerization of $M_{n,target}$ = 50% conversion ~ 10 000 g/mol (DP_{target} ~ 10 000/111.1 = 90) is used. To determine the required ratio, this value has to be doubled, which gives a mole ratio NVP: CTA of 180:1 is. The mole ratio of CTA: initiator was 1:0.1.

For a typical polymerization targeting a molecular weight of 20 000 g/mol, the following procedure was followed. CTA R1 (47.3 mg, 0.25 mmol), AIBN (4.1 mg, 0.025 mmol) and NVP (5 g, 25 mmol) were placed in a 50 mL pear shaped Schlenk flask containing a magnetic stirrer bar. This solution was degassed via 3 freeze-pump-thaw cycles. Argon was used to back-fill the reaction vessel before the

reaction. Subsequently, the flask was placed in an oil bath preheated at 60 °C. This was left to polymerize under these conditions with stirring. The reaction was considered as complete when the stirrer bar was immobile. After the polymerization and cooling of the polymer solution, chloroform was added as diluent. This solution was precipitated dropwise in diethyl ether so as to isolate the polymer. This was centrifuged at 1789 × g for 4 min separating the precipitated polymer out of the diethyl ether. The diethyl ether solution was decanted and replaced with clean diethyl ether, and the centrifugation was repeated. This process was repeated twice. The polymer was dried overnight under vacuum at room temperature and the yield determined from this dry polymer mass.

3.3 Analysis

3.3.1 NMR

All of the NMR spectra were recorded using either a Varian Gemini 300 MHz NMR spectrometer, Varian VXR-Unity 400 MHz spectrometer or a Varian Inova 600 MHz NMR spectrometer. Chemical shifts of the spectra are reported in ppm. Deuterated chloroform ($CDCl_3$) was used as solution for all of the NMR analyses on low molecular weight compounds and deuterated dimethyl sulfoxide (DMSO-d_6) was used for all polymer NMR analyses without further purification.

3.3.2 SEC

All SEC analyses were done in *N*,*N*-dimethylacetamide (DMAc) (Sigma-Aldrich, Chromosolv® Plus, for HPLC ≥ 99.9%) solution and was performed on a setup consisting of a Waters 717 plus auto sampler with a Waters In-line degasser AF connected to a Shimadzu LC-10AT pump with the following column configuration: as a precolumn a 1×PSS GRAM column (10 µm particle size, 8.0×50 mm), as analytical columns 1×PSS GRAM (10 µm particle size, 100 Å pore size, 8.0×300 mm) and 2×PSS GRAM columns (10 µm particle size, 3000 Å pore size, 8.0×300 mm). A Waters 410 differential refractometer and a Waters 2487 dual wavelength absorbance detector were connected in series as detectors. The SEC system was calibrated using low dispersity poly(methyl methacrylate) standards.

3.4 Results and discussions

3.4.1 Synthesis of CTA *S*-(2-cyano-2-propyl), *O*-ethyl xanthate (R1)

The first step in the synthesis of CTA R1 is the formation of a disulphide. This is done through an oxidative reaction of thiols.[26] In the second step the AIBN decomposes in the presence of heat. This subsequently forms a nitrogen gas and a radical which reacts with the disulphide to from the CTA *S*-(2-cyano-2-propyl), *O*-ethyl xanthate (R1) (Scheme 3.2).

This specific CTA R1 was chosen due to previous research,[25,27] where it was shown to have good control over the polymerization with NVP with good correlation between the theoretical and

experimental molecular weights and ease of post polymerization reaction to an aldehyde ω functionalized end group.[28]

After synthesis and purification of *S*-(2-cyano-2-propyl), *O*-ethyl xanthate CTA ^{1}H-NMR and ^{13}C-NMR analyses were carried out and the results are shown in Figure 3.3. All of the peaks for both of ^{1}H-NMR and ^{13}C-NMR are accounted for and correlate with other literature.[25]

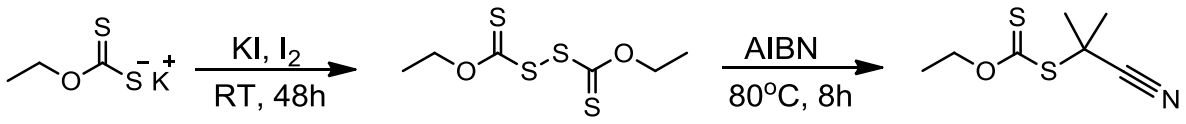

Scheme 3.2: *S*-(2-cyano-2-propyl), *O*-ethyl xanthate synthesis procedure.

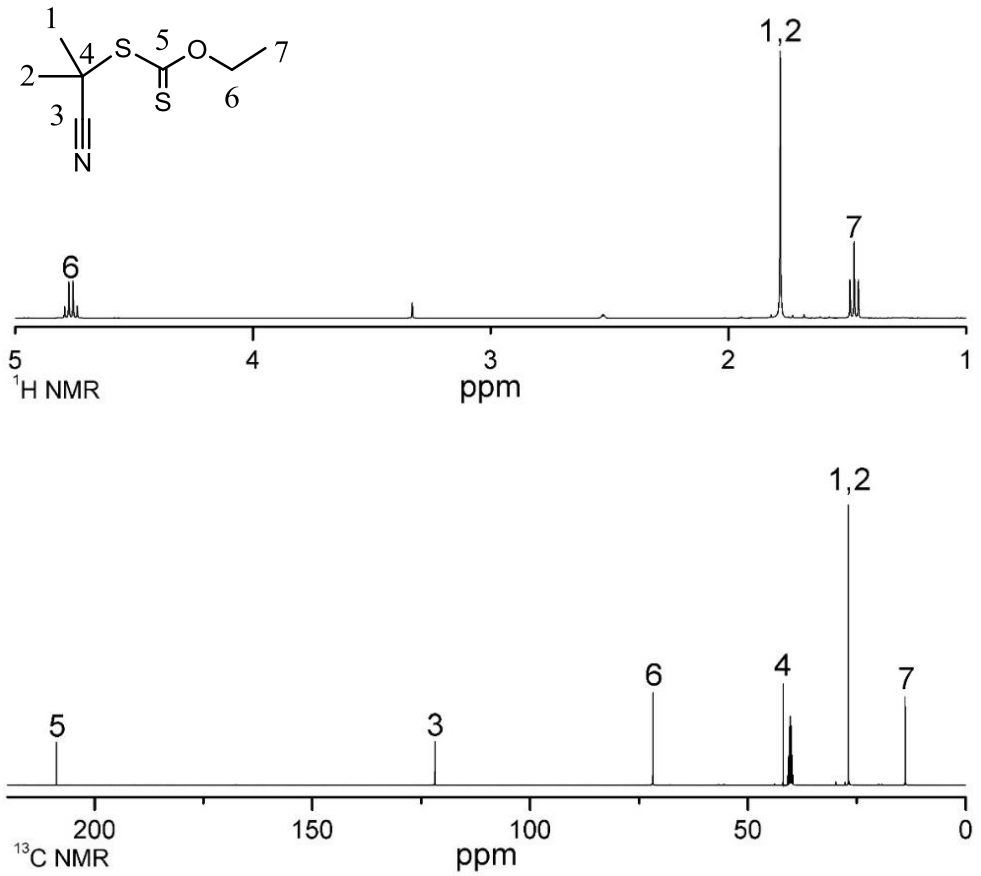

Figure 3.3 ^{1}H-NMR and ^{13}C-NMR spectra of *S*-(2-cyano-2-propyl), *O*-ethyl xanthate in DMSO-d_6 with carbon and hydrogen number identifiers.

3.4.2 Polymerization of NVP

The aim of the synthesis of PVP with CTA R1 was access to well-defined PVP with different molecular weights, and low molar mass dispersities. For the general polymerizations of NVP, Table

3.1 describes the ratios used for the polymerization and molecular weights as determined from ^{1}H NMR spectroscopy and SEC.

For the polymerization of NVP, controlled by a CTA, an initiator is needed in the reaction to form the radicals.[7] Radicals are formed by the thermal decomposition of AIBN. These radicals initiate the polymerization and form a radical on the CTA, which is the start of the polymerization. Pound *et al*.[25] determined that the most successful polymerizations of NVP with this R1 CTA were found at 60 °C in bulk with AIBN. Pound *et al*. also determined that the narrowest molecular weight distribution is found when the conversion of polymerization is between 40 % and 60 % conversion.

Table 3.1: Summary regarding the PVP prepared via CTA mediated bulk polymerization

PVP	Time (h)	[a]Mole ratio	[b]$M_{n,Target}$ (g/mol)	[c]Conv. (%)	[d]$M_{n,\ NMR}$ (g/mol)	$M_{n,\ SEC}$ (g/mol)	$Đ$
1	3	180:1:0.1	20×10^3	51	11×10^3	10×10^3	1.16
2	4	360:1:0.1	40×10^3	43	18×10^3	18×10^3	1.16
3	5	540:1:0.1	60×10^3	49	28×10^3	26×10^3	1.16
4	4	720:1:0.1	80×10^3	53	40×10^3	37×10^3	1.26

[a] The mole ratio is as follow: M_0: CTA: Initiator

[b] Molecular weight at 100% conversion as determined from Equation 3.1

[c] Conversion was determined gravimetrically

[d] Molecular weight as determined from ^{1}H-NMR using Equation 3.2

To ensure the control over the molecular weight and dispersity of the polymerization of NVP is acceptable, a set time cannot be used, but rather a targeting of a conversion between 40 % and 60%.[25] If the polymerization reaction mixture becomes too viscous, no stirring is possible due to the stirrer bar becoming immobilized. This leads to an uncontrolled polymerization, with higher molecular weight and high dispersity.

The values from Table 3.1 for the molecular weights as determined from SEC and ^{1}H-NMR, are in excellent agreement, confirming the polymerization of PVP with these molecular weights. The agreement between the two different techniques for molecular weight determination is quite remarkable if the potential sources of inaccuracies are considered. The most important ones are discussed in the next paragraphs.

With SEC, poly(methyl methacrylate) (PMMA) molecular weight standards are used in the calibration of the SEC instrument that have a different hydrodynamic volume to that of PVP. The molecular weight of PVP is thus measured in relation to PMMA and not PVP.

With NMR, inaccuracies are attributed to integration inaccuracies as a result of end group peak and polymer peak overestimations. With impurities, unwanted reactions, chain breaking and non-ideal termination reactions of the polymer chains, such as disproportionation also give rise to overestimations such as described by Pound *et al.*[25]

These overestimations are due to the process of RAFT polymerization and the NVP monomer. The polymerization of NVP through RAFT polymerization is a rather difficult monomer to polymerize due to it being a less activated monomer.[4] This difficulty arises from the double bond on the monomer conjugated to the lone pair of electrons on the nitrogen. Monomers that fall into this less activated monomer group possess a poor homolytic leaving group and a highly reactive radical addition reaction. This highly reactive radical that is formed with unconjugated monomers leads to a large number of disadvantages when polymerizing. First, due to a higher reactivity the rate constant of polymerization increases, which leads to a possibility of inefficient deactivation of the reactive end groups to unreactive species, which in turn leads to an uncontrollable polymerization.[29,30] The second disadvantage is that side reactions can take place. Due to the lack in stabilization of these radicals, chain transfer reactions, disproportionation and head-head insertions can take place when polymerizing. This effect becomes more prevalent with the increase in conversion.[31,32] Last is the problem of side reactions, such as dimerization, that take place in the presence of impurities, especially with NVP.[24] Pound *et al.*[24] observed dimerization and various side products through NMR when polymerizing NVP. Dimerization of NVP takes place via a cationic mechanism with the addition of heat. This is initiated by protonation of the double bond on the NVP monomer.

These problems are however, mostly overcome by using the correct CTA with suitable R and Z groups, such as the R and Z groups on the CTA as shown in this chapter. This stabilization has been accomplished with the CTA used in this study. Table 3.1 shows the low dispersity values of the polymerizations. These low dispersities are indicative of good stabilization during polymerization. The R group chosen in this instance as shown from literature is a good leaving group and the Z group a good stabilizing group.[25] Finally the problem of impurities can be overcome by removing protic functional groups in solvents and reagents and ensuring all chemicals used for the polymerization reactions are very pure.

Although good control has been accomplished during the polymerizations, the problems of polymerization with a less activated monomer can be seen in Table 3.1 and as explained above. All of the polymerizations were done with conversions between 40% and 60% and the molecular weights close to 50% conversion of the targeted molecular weights, some comparison can be drawn between the time, conversion and molecular weight achieved from the polymerizations. All of the polymerizations are polymerized in just a few hours while achieving about 45 - 55% conversion for each of the polymerizations. Very good dispersities are found for these polymerization due to the

short reaction time used for the polymerization reactions. PVP-3's polymerization reaction time does not compare nicely to the trend as followed by that of the other polymerization in Table 3.1. Comparisons among the polymerization reactions are difficult due to experimental error. During the freeze-pump-thaw process, a small amount of oxygen could be present when the polymerization starts, thus removing some radicals when polymerizing. The heat applied to the system has an effect on the constant initiation of the reaction. When a change in the heating takes place, the constant initiation is altered, changing the growth of the chain, which has an effect on the molecular weight and dispersity.

For the polymerizations indicated in Table 3.1, different molecular weights were targeted. For the PVP's 1-4 a large difference among the molecular weights was seen, each with low dispersity values except for PVP 4 which had a slightly higher dispersity. This is most likely due to loss of control over reaction of the polymerization process targeting higher molecular weights. The molecular weight distributions for these polymers are shown in Figure 3.4.

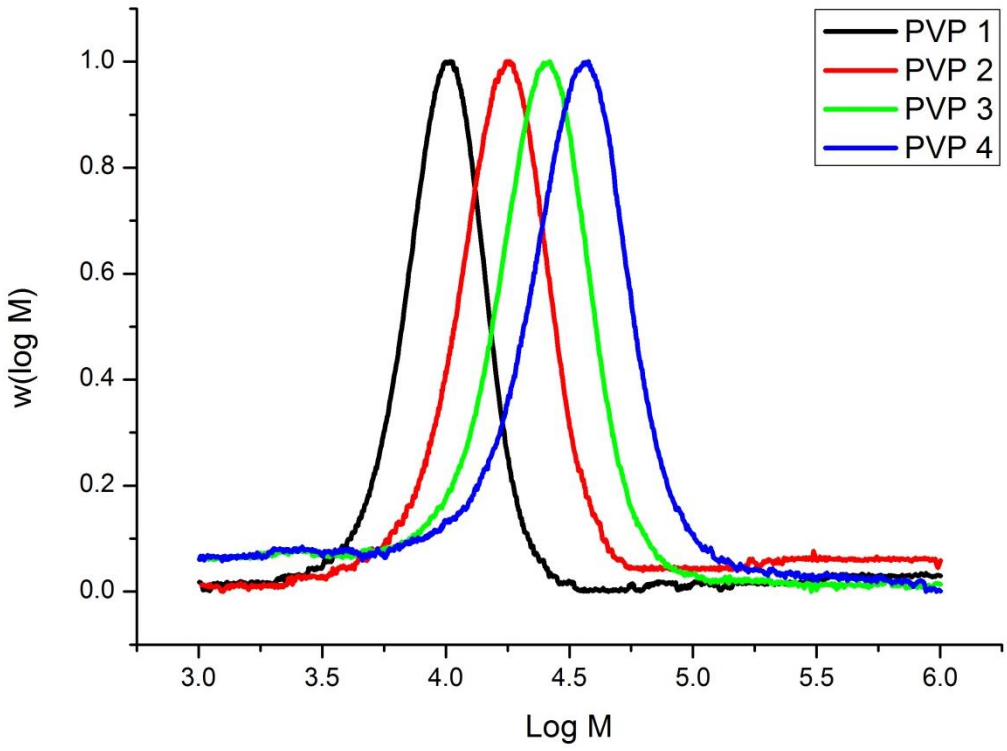

Figure 3.4 Normalized molecular weight distribution of the polymerizations PVP 1-4.

Figure3.4 indicates a typical ^{1}H-NMR spectrum of PVP mediated by CTA R1. All of the peaks corresponding to the polymers are broad and upfield. The structure corresponding to the PVP polymer is inserted in Figure 3.6. The peaks are numbered following this structure. The backbone repeat units of the PVP are seen in Figure 3.5, between the values of 1.3 – 2.6 ppm and 3.1 – 3.8 ppm.[25,33–35] The CTA end group peaks are very small in comparison to that of the polymer due to lower concentration

of end groups compared to the repeat units. The $–CH_2–$ moiety of the xanthate ω end group can be seen at 4.6 ppm. The integration values corresponding to the $–CH_2–$ on the backbone as shown on Figure 3.5 and the $–CH_2–$ moiety of the xanthate ω end group are used to determine the number average molecular weight (M_n). Equation 3.2 is used to describe this molecular weight determination from ^{1}H-NMR spectrum. The integration value of peak 2 is divided by the xanthate ω end group peak at 4.6 ppm, which was arbitrarily set to 2, to account for the two protons. The values are shown in Table 3.1 for all of the polymerizations as determined from NMR. The mass of one NVP monomer unit is 114.1 g/mol and the mass of the CTA end groups are 189.3 g/mol.

$$M_{n,NMR} = (\text{Peak 2})/2 \times 114.1 + 189.3 \qquad (3.2)$$

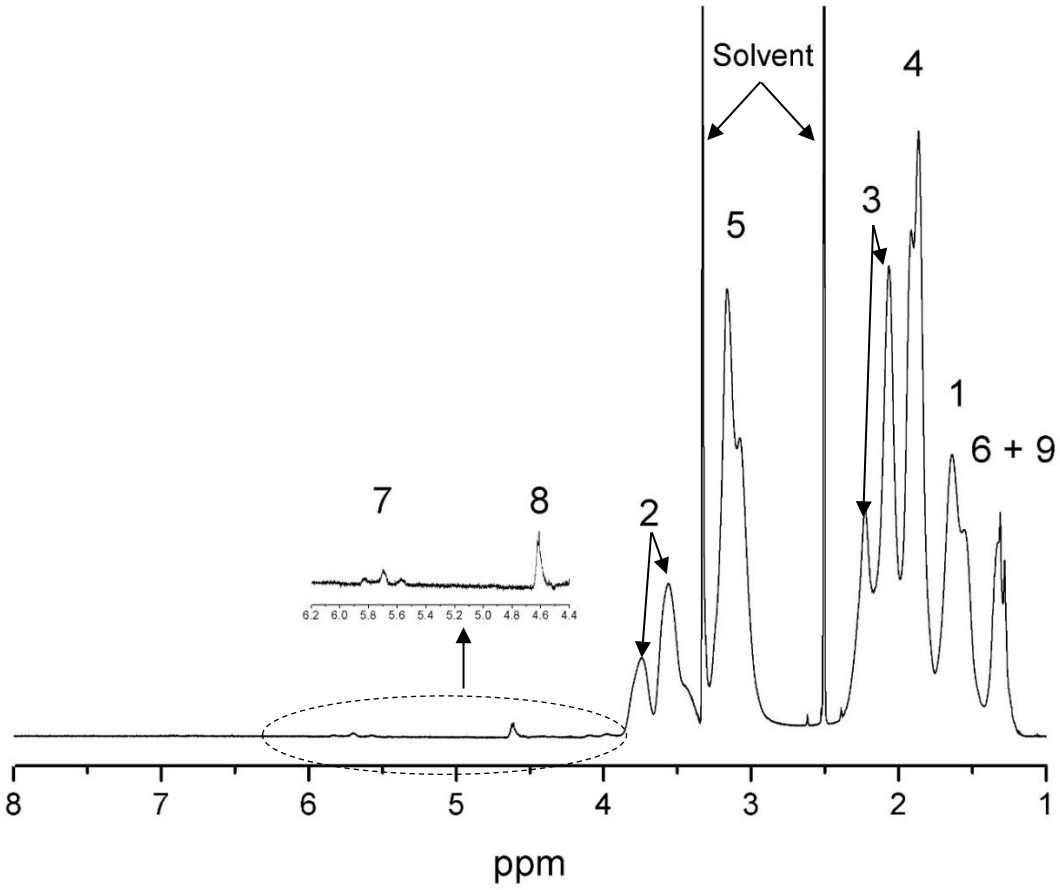

Figure 3.5: General ^{1}H NMR spectrum of a 10×10^3 g/mol polymer after RAFT polymerization.

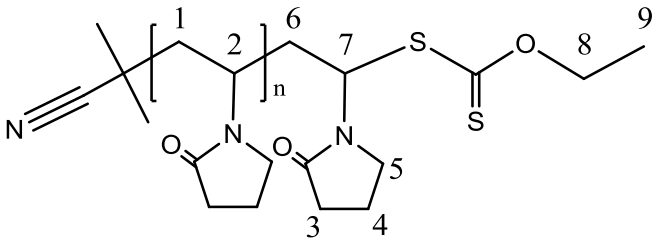

Figure 3.6: PVP with peak numbering

3.5 Conclusion

The synthesis and purification of the CTA *S*-(2-cyano-2-propyl), *O*-ethyl xanthate (R1) was successfully performed. After purification a yield of 83% was found. From Figure 3.3, the purity of the CTA R1 is seen. All the peaks in the ^{1}H-NMR and ^{13}C-NMR spectra were accounted for and correlated with the structure, based on literature. The subsequent polymerizations of NVP with this CTA R1 were demonstrated with four different molecular weights of PVP, each with narrow molecular weight distributions as seen in Table 3.1. The polymers were characterized via ^{1}H NMR spectroscopy and SEC. The values as determined from these two analytical techniques were compared and are seen in Table 3.1. The agreement between the values for these analysis techniques is excellent.

3.6 References

(1) Moad, G.; Solomon, D. H. *The Chemistry of Free Radical Polymerization*; Pergamon, 1995.

(2) Chiefari, J.; Chong, Y, K.; Le, T, P, T.; Mayadunne, R, T, A.; Kristina, J.; Jeffrey, J.; Ercole, F.; Meijs, G, F.; Moad, C, L.; Thang, S, H.; Rizzardo, E.; Moad, G.; Postma, A. *Macromolecules.* **1998**, *31*, 5559–5562.

(3) Jenkins, A. D.; Jones, R. G.; Moad, G. *Pure Appl. Chem.* **2010**, *82*, 483–491.

(4) Keddie, D. J.; Moad, G.; Rizzardo, E.; Thang, S. H. *Macromolecules* **2012**, *45*, 5321–5342.

(5) Moad, G.; Chong, Y. K.; Postma, A.; Rizzardo, E.; Thang, S. H. *Polymer* **2005**, *46*, 8458–8468.

(6) Chong, B. Y. K.; Le, T. P. T.; Moad, G.; Rizzardo, E.; Thang, S. H. *Macromolecules* **1999**, *32*, 2071–2074.

(7) Moad, G.; Rizzardo, E.; Thang, S. H. *Aust. J. Chem.* **2005**, *58*, 379–410.

(8) Su, W. F. *Principles of Polymer Design and Synthesis*, Springer-Verlag: Berlin, 2013.

(9) Perkins, W. G.; Capiati, N. J.; Porter, R. S. *Polym. Eng. Sci.* **1976**, *16*, 200–203.

(10) G. C. East, D. M. and E. P. *Trans. Faraday Soc.* **1966**, *62*, 1301–1307.

(11) Szycher, M. *High Performance Biomaterials: A Complete Guide to Medical and*

Pharmceutical Applications; CRC Press: Lancastar, 1991; pp 287–312.

(12) Wan, D.; Satoh, K.; Kamigaito, M.; Okamoto, Y. *Macromolecules.* **2005**, *38*, 10397–103405.

(13) Nguyen, T. L. U.; Eagles, K.; Davis, T. P.; Barner-Kowollik, C.; Stenzel, M. H. J. *Polym. Sci. Part A Polym. Chem.* **2006**, *44*, 4372–4383.

(14) Barner-Kowollik, C. *Handbook of RAFT polymerization.*; Wiley-VCH: Hoboken, 2007.

(15) Keddie, D, J.; Moad, G.; Rizzardo, E.; Thang, S, H. *Macromolucules.* **2012**, *45*, 5321–5342.

(16) Moad, G.; Rizzardo, E.; Thang, S. H. *Aust. J. Chem.* **2005**, *58*, 379–410.

(17) Perrier, S.; Takolpuckdee, P. *J. Polym. Sci. Part A Polym. Chem.* **2005**, *43*, 5347–5393.

(18) Moad, G.; Rizzardo, E.; Thang, S. H. *Aust. J. Chem.* **2009**, *62*, 1402–1472.

(19) Benaglia, M.; Chiefari, J.; Chong, Y. K.; Moad, G.; Rizzardo, E.; Thang, S. H. *J. Am. Chem. Soc.* **2009**, *131*, 6914–6915.

(20) Moad, G.; Rizzardo, E.; Thang, S. H. *Chem. Asian J.* **2013**, *8*, 1634–1644.

(21) Gardiner, J.; Martinez-Botella, I.; Tsanaktsidis, J.; Moad, G. *Polym. Chem.* **2016**, *7*, 481–492.

(22) Chiefari, J.; Mayadunne, R, T, A.; Moad, C, L.; Skidmore, M, A.; Thang, S, H.; Moad, G.; Rizzardo, E.; Postma, A. *Macromolecules.* **2003**, *36*, 2273–2283.

(23) Chong, Y, K.; Chiefari, J.; Le, T, P, T.; Mayadunne, R, T, A.; Kristina, J.; Jeffrey, J.; Ercole, F.; Meijs, G, F.; Moad, C. L.; Thang, S, H.; Moad, G.; Rizzardo, E. *Macromolecules.* **1998**, *31*, 5559–5562.

(24) Pound, G.; Eksteen, Z.; Pfukwa, R.; McKenzie, J. M.; Lange, R. F. M.; Klumperman, B. *J. Polym. Sci. Part A Polym. Chem.* **2008**, *46*, 6575–6593.

(25) Pound, G. Reversible Addition Fragmentation Chain Transfer (RAFT) Mediated Polymerization of N -vinylpyrrolidone, University of Stellenbosch, 2008.

(26) Danehy, J, P.; Doherty, B, T.; Egan, C, P. *J. Org. Chem.* **1971**, *36*, 2525–2530.

(27) Giliomee, J.; Pfukwa, R.; Gule, N. P.; Klumperman, B. *Polym. Chem.* **2016**, *7*, 1138–1147.

(28) Pound, G.; McKenzie, J. M.; Lange, R. F. M.; Klumperman, B. *Chem. Commun.* **2008**, *27*, 3193–3195.

(29) Goto, A.; Fukuda, T. *Prog. Polym. Sci.* **2004**, *29*, 329–385.

(30) Fukuda, T. *J. Polym. Sci. Part A Polym. Chem.* **2004**, *42*, 4743–4755.

(31) Haaf, F.; Sanner, A.; Straub, F. *Polym. J.* **1985**, *17*, 143–152.

(32) Ray, B.; Kotani, M.; Yamago, S. *Macromolecules* **2006**, *39*, 5259–5265.

(33) Sesta, B.; Segre, A. L.; Aprano, A. D.; Proietti, N.; Chimica, D.; Uni, V.; Sapienza, L.; Moro,

P. A.; Ricerca, A.; Roma, C. N. R.; Nmr, S. V; Salaria, V. *J. Phys. Chem. B.* **1997**, *2*, 198–204.

(34) Dutta, K.; Brar, A. S. *J. Polym. Sci. Part A Polym. Chem.* **1999**, *37*, 3922–3928.

(35) Pfukwa, R. Synthesis and Characterization of Telechelic Hydroxyl Functional Poly (*N*-vinylpyrrolidone), University of Stellenbosch, 2008.

Chapter 4: End functionalization

4.1 Introduction

There are three reversible deactivation radical polymerization techniques that are widely used for polymerization, one of these is reversible addition–fragmentation chain transfer (RAFT) polymerization.[1] RAFT polymerization is used due to the wide variety of vinyl monomers polymerized, with control over molecular weight, dispersity and chain end functionality during polymerization.[2] RAFT polymerization uses a suitable chain transfer agent (CTA) for each monomer,[3] which possesses the structural design as seen in Scheme 4.1. A basic representation of the polymerization is seen, accompanied by the end polymer displaying the different sections of the polymer.

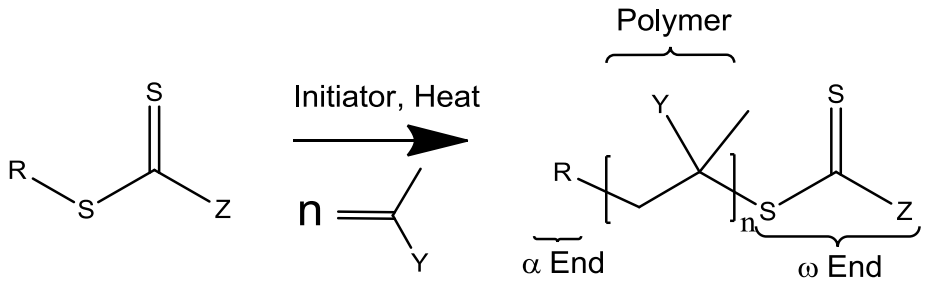

Scheme 4.1: Schematic representation of RAFT mediate polymerization indicating the end groups after polymerization.[4]

The CTA, used in the RAFT mediated polymerization, has end groups labelled as R and Z groups; and these are respectively retained as α and ω end groups after polymerization as shown in Scheme 4.1. For every vinyl monomer polymerized with a CTA, the end groups have a wide variety of functional groups, which allows for the convenient installation of functionalities on the final polymer. Both the α and ω end groups of the polymer functionalities can be used for these post polymerization reactions.[5–8]

Depending on the end functionality selected on the polymer, the R and Z groups can be chosen, before polymerization, to possess the required functionality without further post polymerization reactions, [9,10] or the functionality can be achieved through post polymerization reactions of the α and ω end groups, on the polymer.[11–13] Post polymerization functionalizations is used when a specific functionality is required, but cannot be used for the RAFT polymerization process of the monomer chosen for the polymerization. For post polymerization end functionalization, due to the large range of functional groups that can be chosen for the R and Z of CTA, the polymers are able to be modified in a variety of ways.[7,8,14,15]

Various R groups can be chosen on the CTA with various end functionalities. These include dyes,[16,17] PEG,[18] polyethylene[19] and pyridine.[20,21] Depending on the polymer and R group, various α end group functionalities can be placed on the polymer. These include the functionalization of acetal,[22] carboxyl groups,[23–25] hydroxyl groups,[26] activated esters,[27,28] azide,[29] amide,[30] primary amine groups[31,32] and alkynyl[33,34].

On the ω end group of the polymer, in general, four types of reactions are performed, namely thermolysis[14,15,35–40] yielding alkenes, radical induced reactions[14,15,41,42] where the product is dependent on the radical used, nucleophilic and reduction reactions,[14,15,35,37,43–55] producing thiols at the ω end of the polymeric chain (Scheme 4.2).

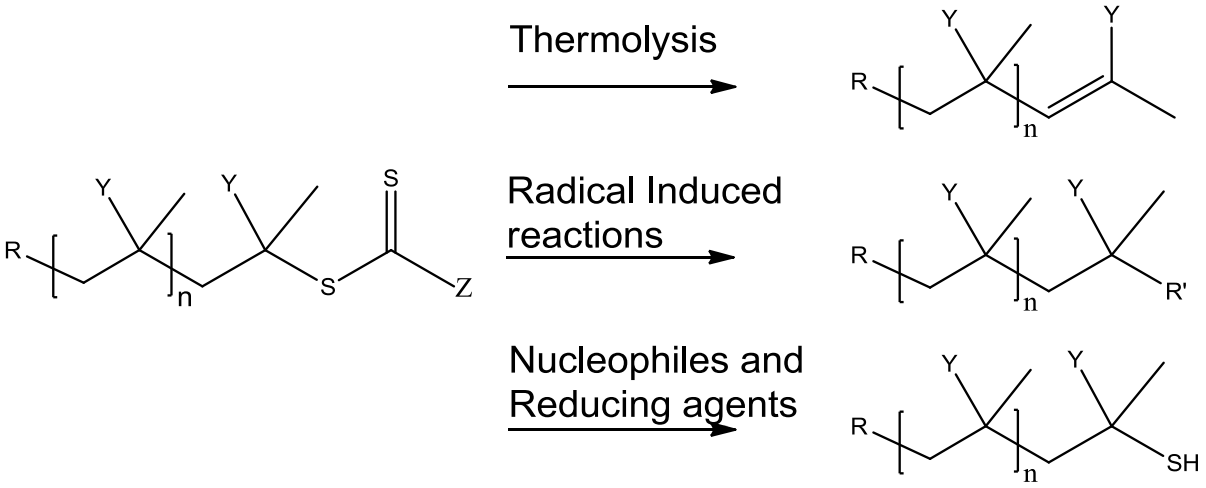

Scheme 4.2: End group functionalization of *ω* end group.

Thermolysis is the elimination of the thiocarbonyl thio group from the polymer, leading to the formation of an alkene group[36–41]. Radical induced reactions are the removal of the *ω* end groups through the use of a radical. An example is the use of 2,2-azo(bis)isobutyronitrile (AIBN) as radical for the removal of dithiobenzoate from poly(methyl methacrylate).[56] Nucleophiles such as amines,[1,44,45,57] thiols[58] or hydroxides[51] and reducing agents[51,55] form thiols on the ω end groups. For a full review of ω end group functionalization reviews by Willcock *et al.*[14] and Moad *et al.*[15] should be consulted.

In their publication Reader *et al.*[22] synthesised a CTA with which PVP was polymerized. In the post polymerization both the α and ω end groups were functionalized to different end groups. α Acetal and ω xanthate end groups were functionalized to aldehyde and thiol end groups respectively.

An application where the end functionalization, on the polymer, is of importance, is the bioconjugation of polymers to a bioactive molecule[35]. An example which is very close to the work done in this thesis is the conjugation of polyethylene glycol to catalase and superoxide dismutase.[59] In

their study, Pound *et al.*[35] conjugated lysozyme to PVP through the use of a ω aldehyde end functional group on the PVP. For the conjugation of catalase to PVP this ω aldehyde end functional group is targeted.

It has been shown that aldehydes are a suitable end functionalized group for bioconjugation reactions, since they readily react with amine functionality of the lysine amino acid residue.[35] In this chapter we will describe the formation of this aldehyde end functional group from xanthate CTA used in the polymerization of PVP as shown in Scheme 4.3.

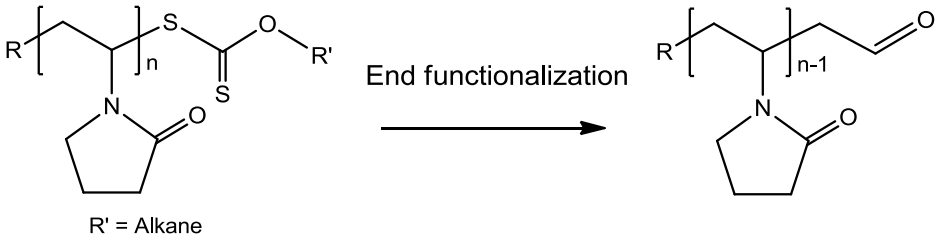

Scheme 4.3: General structure after polymerization of PVP and ω aldehyde end functionalization.

4.2 Experimental

4.2.1 Materials

HCl 32% (Sigma Aldrich), chloroform and diethyl ether were used without further purification (KIMIX). For dialysis, Snakeskin dialysis tubing (Thermo Scientific, 3500 MWCO, 22 mm × 35 feet diameter) was used. Distilled deionized water was obtained from an OLGA Purelab option water filtration system set up. Freeze drying was performed using a Virtus BenchTop 2K Freeze dryer coupled to an Edwards vacuum pump.

4.2.2 End functionalization

End functionalization of the xanthate ω end functional PVP as polymerized in Chapter 3 is described.

4.2.2.1 Direct aldehyde functionalization

This method was adapted from Ilchev *et al.*[60] PVP as polymerized with CTA R1, with a molecular weight of 10×10^3 g/mol (2 g), was dissolved in an aqueous HCl solution (1 M). This is reacted at 40 ℃ for 20 hours (Scheme 4.4). After this it was dialysed against distilled water, for 24 hours at room temperature. After dialysing the solution, freeze drying was used to remove the water from the polymer.

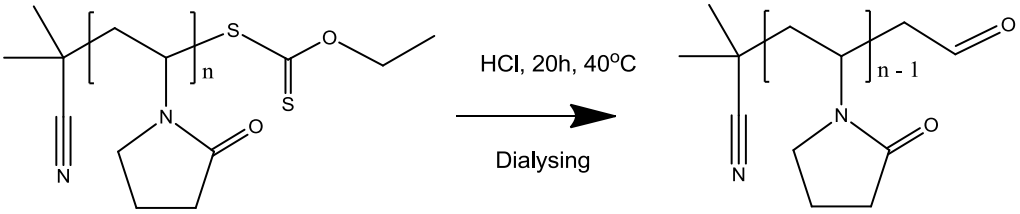

Scheme 4.4: Direct aldehyde functionalization of xanthate end functional group on PVP.

4.2.2.2 Indirect aldehyde functionalization

The end functionalization of the ω end group on the polymer was adapted from a method as described by Pound *et al.*[35] (Scheme 5.5). The different molecular weight PVPs synthesized in Chapter 3 (2 g) was dissolved separately in distilled deionized water (20 mL). This was stirred for 20 h at 40 °C. After the hydrolysis end functionalization, dialysis was applied for 24 h in distilled deionized water. After dialysis, the newly functionalized polymer was freeze drying for 24 h, removing the water and recovering the hydroxyl functionalized PVP. The freeze dried polymer was dissolved in chloroform and re-precipitated in diethyl ether. To separate the polymer from the diethyl ether, centrifugation was applied for 4 minutes at 4000 RPM. The diethyl ether was decanted and the polymer vacuum dried overnight. SEC and ^{1}H-NMR was done on all of the samples.

After drying of the polymer, aldehyde end functionalization was performed. The polymer was heated to 120 °C for 24 h under vacuum. SEC and ^{1}H-NMR spectroscopy was done to determine functionality and molecular weight after functionalization.

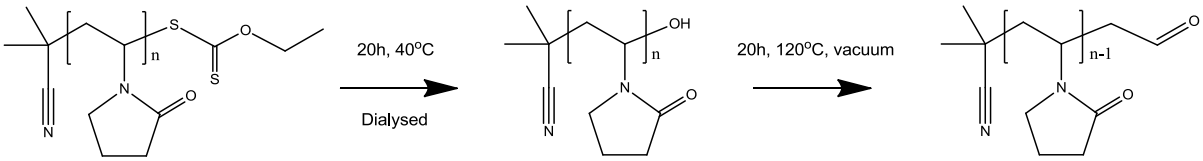

Scheme 4.5: Indirect aldehyde functionalization of xanthate end functional group on PVP.

4.3 Analysis

4.3.1 NMR

NMR spectra were recorded using either a Varian Gemini 300 MHz NMR spectrometer, Varian VXR-Unity 400 MHz spectrometer or a Varian Inova 600 MHz NMR spectrometer. Chemical shifts of the spectra are reported in ppm. Deuterated dimethyl sulfoxide (DMSO-d_6) was used for all polymer NMR analyses without further purification.

4.3.2 SEC

All SEC analyses were done in *N*,*N*-dimethylacetamide (DMAc) (Sigma-Aldrich, Chromosolv® Plus, for HPLC ≥ 99.9%) solution and was performed on a setup consisting of a Waters 717 plus

auto sampler with a Water In-line degasser AF connected to a Shimadzu LC-10AT pump with the following column configuration: As a precolumn a 1×PSS GRAM column (10 µm particle size, 8.0×50 mm), as analytical columns 1×PSS GRAM (10 µm particle size, 100 Å pore size, 8.0×300 mm) and 2×PSS GRAM columns (10 µm particle size, 3000 Å pore size, 8.0×300 mm.) A Waters 410 differential refractometer and a Waters 2487 dual wavelength absorbance detector were connected in series as detectors. The SEC system was calibrated using low dispersity poly(methyl methacrylate) standards.

4.4 Results and discussion

The end group functionalizations of polymerizations PVP 1-4, were determined using ^{1}H-NMR spectroscopy. An aldehyde ω end group was targeted. First a direct aldehyde functionalization was used, which was not successful. Subsequently an indirect aldehyde functionalization method was used. This is shown to be successful and the results of the study shown below.

4.4.1 Direct aldehyde functionalization

Ilchev *et al.*[60] used this direct approach for their functionalization to an aldehyde ω end functional group. In this one-step reaction, a hydroxyl end group is formed, followed by aldehyde end functionalization, all in one solution, without characterization of the intermediate hydroxyl end group. The ^{1}H-NMR spectra before and after the end functionalization are shown in Figure 4.1.

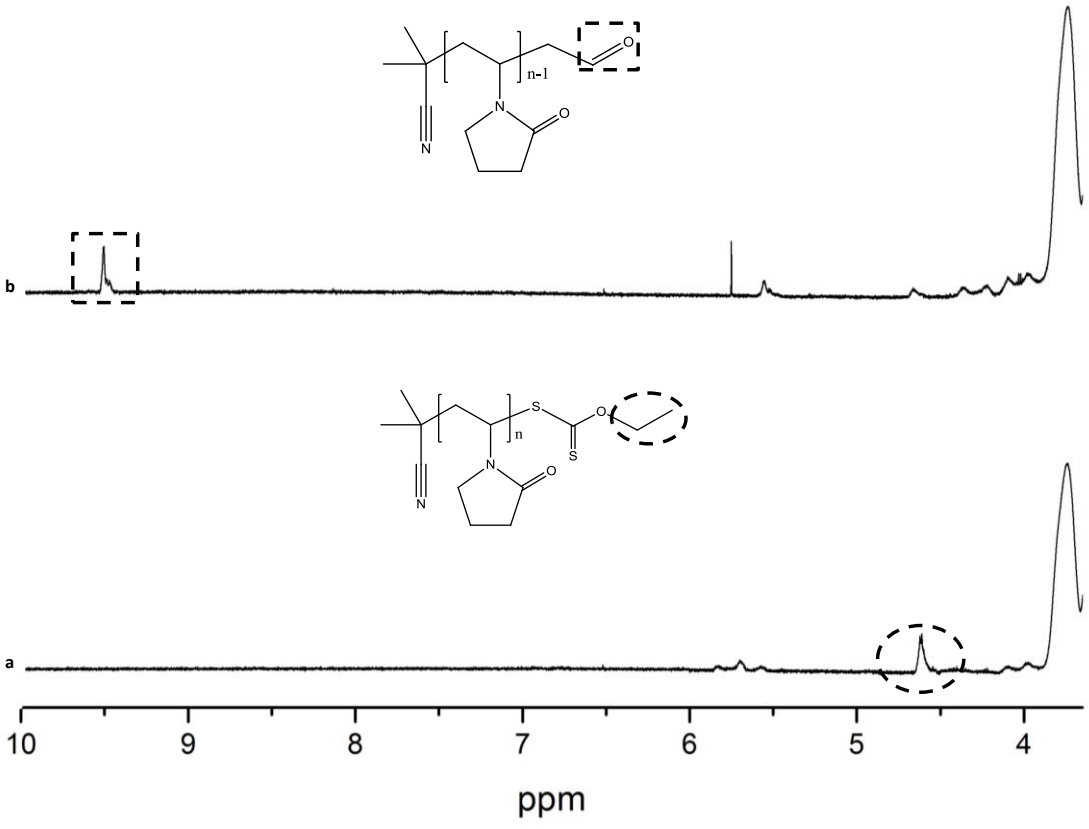

Figure 4.1 ^{1}H-NMR spectra of (a) xanthate ω end group PVP and (b) aldehyde ω end group PVP.

This reaction was successful in changing the xanthate ω end group to an aldehyde as seen from the ^{1}H-NMR spectrum in Figure 4.1b at 9.5 ppm. However, there are some problems with this method. First, unknown peaks, at 4.6 ppm and 5.7 ppm are seen. These peaks are could be due to unfunctionalized xanthate groups still present on some of the polymer chains. Also the reaction used a 1 M hydrochloric solution which was not fully compatible with the dialysis tubing used for the experiment. The HCl dissolved the tubing, releasing the polymer solution into the water solution, making it difficult to recover.

4.4.2 Indirect aldehyde functionalization

In a second approach, the method introduced by Pound *et al*.[35] was used for the end functionalization of the polymer. ω End group functionalization of xanthate to hydroxyl end group on PVP was done via hydrolysis as shown Scheme 4.5. In Figure 4.2 the ^{1}H-NMR spectra for the xanthate ω end group functional PVP and hydroxyl ω end group functional PVP is shown. Figure 4.3 is the ^{1}H-NMR spectra after aldehyde functionalization.

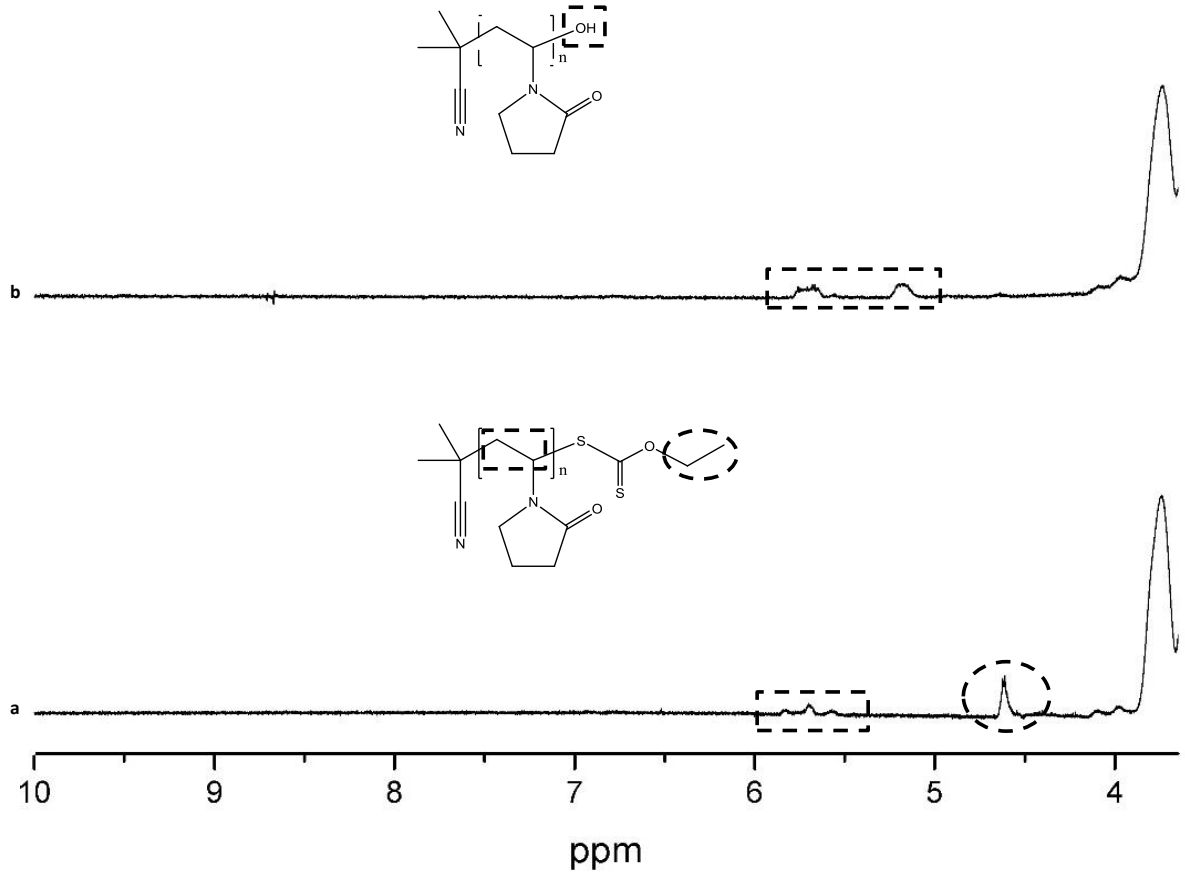

Figure 4.2: ^{1}H-NMR spectra of (a) xanthate ω end group PVP and (b) hydrolysed ω end group PVP.

Figure 4.2a shows the ^{1}H-NMR spectrum containing the xanthate ω end functionalised PVP. Figure 4.2b is the ^{1}H-NMR spectrum after hydrolysis of the xanthate ω chain end. After hydrolysis, no change was detected in the polymer itself, only the ω end group. The change in the ω end group can

be seen between 4.4 ppm and 6 ppm. From Figure 4.2a the peak at 4.6 ppm, which is indicative of the xanthate ω end group as shown in the insert, is present. In Figure 4.2b this is not present anymore, indicating the removal of the xanthate groups as shown in literature.[61] There is a change in the peaks between 5.5 and 6 ppm due to the ω end group changing to a hydroxyl group. The peak between 4.4 ppm and 6 ppm has been changed to the two peaks from 5 ppm to 6 ppm. This is due to the hydroxyl group having an effect on the backbone chain on the PVP.[61] The peak at 5.2 ppm is that of the $–CH_2–$ on the CTA[61] and the peak at 5.8 ppm is that of –CH – backbone.[62] It is shown from literature that the xanthate at the PVP chain end readily reacts to introduce this hydroxyl functionality on the end group and so removing the xanthate end group.[61,63]

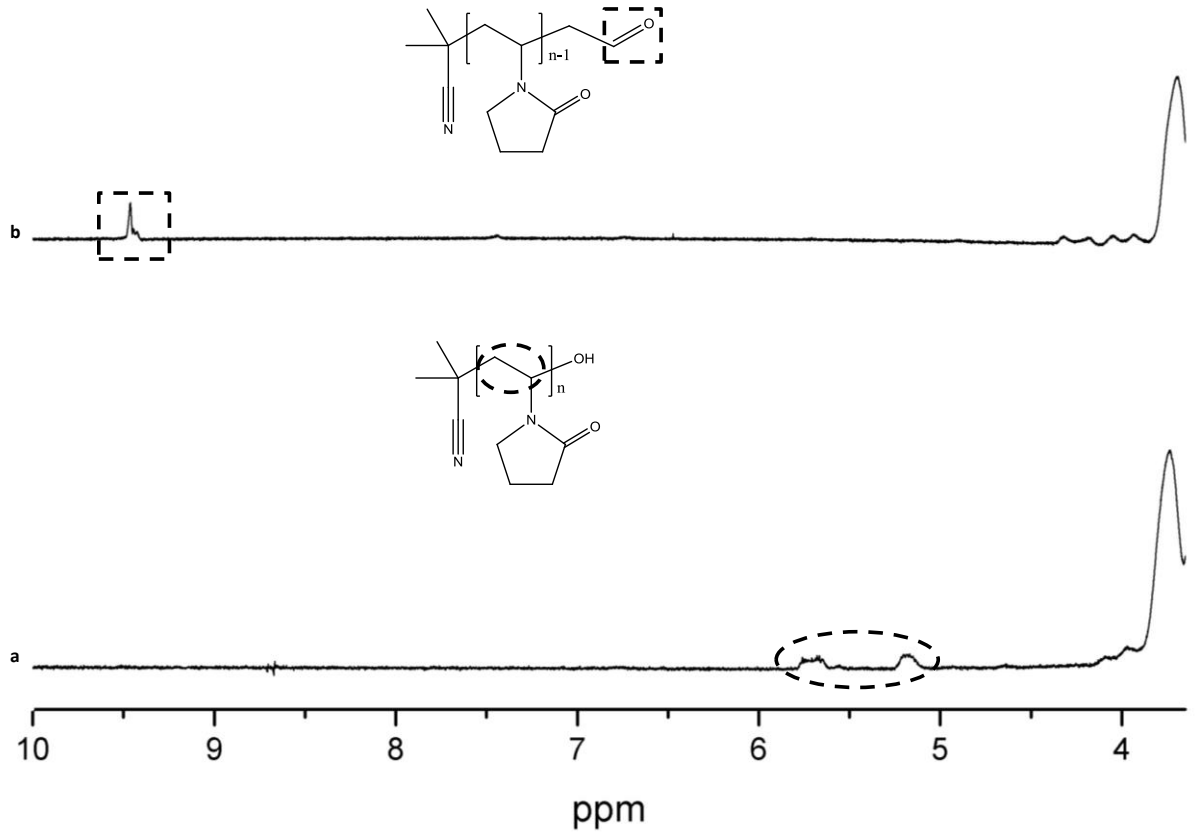

Figure 4.3: ^{1}H-NMR spectra of (a) hydrolysed ω functionalised PVP and (b) aldehyde ω functionalised functionalized PVP.

Figure 4.3 shows the ^{1}H-NMR spectrum after the conversion of the hydroxyl group into an aldehyde at the ω end group. With this second end functionalization step, no change in the polymer itself was seen. In Figure 4.3a between 5 ppm and 6 ppm the peaks of the hydroxyl ω end group on the PVP is seen. In Figure 4.3b these peaks between 5 ppm and 6 ppm are removed and replaced with a peak at 9.5 ppm. The loss of these two peaks indicates the loss of the hydroxyl functional group on the ω end group of the polymer. The new peak at 9.5 ppm is a clear signature of the new aldehyde functional

group formed after functionalization as shown in Scheme 4.5. According to literature when heat is applied to a ω hydroxyl end functionalized PVP group, the terminal pyrrolidone unit is lost.[61] Table 4.1 summarizes the SEC results before and after each end functionalization step following the indirect method as adapted from Pound *et al*.[35]

Table 4.1: Molecular weights of the four polymer after hydrolysis and aldehyde functionalization using the indirect aldehyde functionalization method as described

PVP	Xanthate end group $M_{n,SEC}$ (g/mol)	$Đ$	Hydrolysed end group $M_{n,SEC}$ (g/mol)	$Đ$	Aldehyde end group $M_{n,SEC}$ (g/mol)	$Đ$
1	10×10^3	1.16	10×10^3	1.13	10×10^3	1.15
2	18×10^3	1.16	19×10^3	1.17	17×10^3	1.20
3	26×10^3	1.16	26×10^3	1.20	25×10^3	1.22
4	37×10^3	1.26	37×10^3	1.20	37×10^3	1.23

Table 4.1 contains the molecular weights as determined from SEC after the end functionalization processes. This change in the hydrolysis end functionalization and followed the aldehyde functionalization is small over the four polymers used for this end functionalization. The molecular weights are thus still close to that of the starting molecular weights. The changes in molecular weights are very small due to only changing the end groups on the polymer and not the polymer itself. The size of the end groups is relatively small compared to the polymer. There is however, a small change that took place in the polymer dispersities. The post polymerization modifications did not alter the molecular weight and dispersity of the polymer significantly.

4.5 Conclusion

In conclusion, the end functionalization of the ω end group on the PVP polymer was successful using the method as adapted from Pound *et al.*[61] This shows the successful functionalization of the ω end group of this particular CTA and PVP as would be expected from literature[61]. The successful end functionalization of the ω end group from a xanthate to a hydroxyl functional group is shown via ^{1}H NMR spectroscopy in Figure 4.2. In a similar way in Figure 4.3 the successful end modification of this hydroxyl group into an aldehyde end functional group on the polymer is shown. During this end functionalization no change took place on the polymer chains itself.

From Table 4.1, containing the SEC results for the indirect aldehyde functionalization, it is seen that there is no significant change in the molecular weights of the polymers after both functionalization

steps. The dispersities of the polymers are very good with the values of the 4 polymers around 1.2 after the aldehyde ω end group functionalization. These 4 polymers will be used in the bioconjugation of catalase in Chapter 5.

4.6 References

(1) Moad, G.; Rizzardo, E.; Thang, S. H. *Aust. J. Chem.* **2005**, *58*, 379–410.

(2) Chiefari, J.; Chong, Y, K.; Le, T, P, T.; Mayadunne, R, T, A.; Kristina, J.; Jeffrey, J.; Ercole, F.; Meijs, G, F.; Moad, C, L.; Thang, S, H.; Rizzardo, E.; Moad, G.; Postma, A. *Macromolecules.* **1998**, *31*, 5559–5562.

(3) Perrier, S.; Takolpuckdee, P. *J. Polym. Sci. Part, A Polym. Chem.* **2005**, *43*, 5347–5393.

(4) Chong, Y, K.; Chiefari, J.; Le, T, P, T.; Mayadunne, R, T, A.; Kristina, J.; Jeffrey, J.; Ercole, F.; Meijs, G, F.; Moad, C. L.; Thang, S, H.; Moad, G.; Rizzardo, E. *Macromolecules.* **1998**, *31*, 5559–5562.

(5) Canalle, L. a.; Löwik, D. W. P. M.; van Hest, J. C. M. *Chem. Soc. Rev.* **2010**, *39*, 329–353.

(6) Nicolas, J.; Mantovani, G.; Haddleton, D. M. *Macromol. Rapid Commun.* **2007**, *28*, 1083–1111.

(7) Boyer, C.; Bulmus, V.; Davis, T. P.; Ladmiral, V.; Liu, J.; Perrier, S. *Chem. Rev.* **2009**, *109*, 5402–5436.

(8) Barner-Kowollik, C. *Handbook of RAFT*; Wiley-VCH: Hoboken, 2007.

(9) Liu, J.; Bulmus, V.; Barner-Kowollik, C.; Stenzel, M. H.; Davis, T. P. *Macromol. Rapid Commun.* **2007**, *28*, 305–314.

(10) Boyer, C.; Liu, J.; Bulmus, V.; Davis, T, P.; Barner-Kowollik, C.; Stenzel, M, H. *Macromolecules* **2008**, *41*, 5641–5650.

(11) Moad, G.; Rizzardo, E.; Postma, A.; Thang, S. *Polymer* **2005**, *46*, 8458–8468.

(12) de Brouwer, H.; Schellekens, M, A, J.; Klumperman, B.; Monteiro, M, J.; German, A, L. *J. Polym. Sci. Part A Polym. Chem.* **2000**, *38*, 3596–3603.

(13) Postma, A.; Davis, T, P.; O'Shea, M, S.; Moad, G. *Macromolecules.* **2005**, *38*, 5371–5374.

(14) Willcock, H.; O'Reilly, R. K. *Polym. Chem.* **2010**, *1*, 149–157.

(15) Moad, G.; Rizzardo, E.; Thang, S. H. *Polym. Int.* **2011**, *60*, 9–25.

(16) Geelen, P.; Klumperman., B. *Macromolecules. 40*, 3914–3920.

(17) Such, G. K.; Evans, R. A.; Davis, T. P. *Macromolecules.* **2006**, *39*, 9562–9570.

(18) dos Santos, A. M.; Le Bris, T.; Graillat, C.; D'Agosto, F.; Lansalot., M. *Macromolecules.*

2009, *42*, 946–956.

(19) Briquel, R.; Mazzolini, J.; Bris, T. L.; Boyron, O.; Boisson, F.; Delolme, F.; D'Agosto, F.; Boisson, C.; Spitz., R. *Angew. Chem., Int. Ed. Engl.* **2007**, *47*, 9311–9313.

(20) Zhou, G. C.; Harruna, I, I. *Anal. Chem.* **2007**, *79*, 2722–2727.

(21) Zhou, G.; He, J.; Harruna., I. I. *J. Polym. Sci., Part A, Polym. Chem. 45*, 4225–4239.

(22) Reader, P. W.; Pfukwa, R.; Jokonya, S.; Arnott, G. E.; Klumperman, B. *Polym. Chem.* **2016**, *7*, 6450–6456.

(23) Lai, J.; Filla, D.; Shea, R. *Macromolecules* **2002**, *35*, 6754–6756.

(24) Stenzel, M. H.; Davis, T. P.; Fane, A. G. *J. Mater. Chem.* **2003**, *13*, 2090–2097.

(25) Wang, R.; McCormick, C. L.; Lowe, A. B. *Macromolecules.* **2005**, *38*, 9518–9525.

(26) Lima, V.; Jiang, X. L.; Brokken-Zijp, J.; Schoenmakers, P. J.; Klumperman, B.; Van Der Linde, R. *J. Polym. Sci., Part A Polym. Chem* **2005**, *43*, 959–973.

(27) Bathfied, M. .; D'Agosto, F. .; Spitz, R. .; Charreye, M.-T.-; Delair, T. *J. Am. Chem. Soc.* **2006**, *128*, 2546–2547.

(28) Wiss, K. T.; Krishna, O. D.; Roth, P. J.; Kiick, K. L.; Theato, P. *Macromolecules.* **2009**, *42*, 3860–3863.

(29) Gondi, S. R.; Vogt, A. P.; Sumerlin, B. S. *Macromolecules.* **2007**, *40*, 474–481.

(30) Takolpuckdee, P.; Mars, C. A.; Perrier, S.; Archibald, S. J. *Macromolecules.* **2005**, *38*, 1057–1060.

(31) Postma, A.; Davis, T, P.; Evans, R, A.; Li, G.; Moad, G.; O'Shea, M. *Macromolecules.* **2006**, *39*, 5293–5306.

(32) Postma, A.; Davis, T, P.; Moad, G.; Li, G.; O'Shea, M. *Macromolecules* **2006**, *39*, 5307–5318.

(33) Nasrullah, M. J.; Vora, A.; Webster, D. C. *Polym. Prepr.* **2007**, *48*, 128–129.

(34) Ranjan, R.; Brittain, W. J. *Macromolecules.* **2007**, *40*, 6217–6223.

(35) Pound, G.; McKenzie, J, M.; Lange, R, F. M.; Klumperman, B. *Chem. Commun.* **2008**, *27*, 3193–3195.

(36) Postma, A.; Davis, T, P.; Evans, R, A.; Li, G.; Moad, G.; O'Shea, M. *Macromolecules.* **2006**, *39*, 5293–5306.

(37) Xu, J.; He, J.; Fan, D.; Tang, W.; Yang, Y. *Macromolecules.* **2006**, *39*, 3753–3759.

(38) Chong, B.; Moad, G.; Rizzardo, E.; Skidmore, M.; Thang, S, H. *Aust. J. Chem.* **2006**, *59*, 755–762.

(39) Destarac, M.; Kalai, C.; Petit, L.; Wilczewska, A, Z.; Zard, S, Z.; Mignani, G. *ACS Symp. Ser.* **2006**, *944*, 564–577.

(40) Chen, M.; Ghiggino, K, P.; Smith, T, A.; Thang, S, H.; Wilson, G, J. *Aust. J. Chem.* **2004**, *57*, 1175–1177.

(41) Chen, M.; Ghiggino, K, P.; Thang, S, H.; Wilson, G, J.; White, J. *J. Org. Chem.* **2005**, *70*, 1844–1852.

(42) Rizzardo, E.; Chen, M.; Chong, B.; Moad, G.; Skidmore, M.; Thang, S, H. *Macromolekular Symp.* **2007**, *248*, 104–116.

(43) Mayadunne, R. T. a; Rizzardo, E.; Chiefari, J.; Krstina, J.; Moad, G.; Postma, A.; Thang, S. H. *Macromolecules* **2000**, *33*, 243–245.

(44) Wang, Z, M.; He, J, P.; Tao, Y, F.; Jiang, H, J.; Yang, Y, L. *Macromol. .* **2003**, *36*, 7446–7452.

(45) Favier, A.; Ladaviere, C.; Charreyre, M, T.; Pichot, C. *Macromolecules.* **2004**, *37*, 2026–2034.

(46) Lima, V.; Jiang, X, L.; Schoenmakers, P, J.; Brokken-Zijp, J.; Klumperman, B.; Van Der Linde, R. *J. Polym. Scieince Part, A Polym. Chem.* **2005**, *43*, 959–973.

(47) Thomas, D, B.; Convertine, A, J.; Hester, R, D.; Lowe, A, B.; McCormick, C, L. *Macromolecules.* **2004**, *37*, 1735–1741.

(48) Schilli, C.; Lanzendoerfer, M, G.; Mueller, A, H, E. *Macromolecules.* **2002**, *35*, 6819–6827.

(49) Llauro, M, F.; Loiseau, J.; Boisson, F.; Delolme, F.; Ladaviere, C.; Claverie, J.; Part, A. *J. Polym. Sci. Part A Polym. Chem.* **2004**, *42*, 5439–5462.

(50) Scales, C, W.; Convertine, A, J.; McCormick, C, L. *Biomacromolecules.* **2006**, *7*, 1389–1392.

(51) Sumerlin, B, S.; Lowe, A, B.; Stroud, P, A.; Urban, M, W.; McCormick, C, L.; Zhang, P. *Langmuir* **2003**, *19*, 5559–5562.

(52) Patton, D, L.; Advincula, R, C.; Mullings, M.; Fulghum, T. *Macromolecules.* **2005**, *38*, 8597–8602.

(53) Plummer, R.; Goh, Y, K.; Whittaker, A, K.; Monteiro, M, J. *Macromolecules.* **2005**, *38*, 5352–5355.

(54) Qiu, X, P.; Winnik, F, M. *Macromol. Rapid Commun.* **2006**, *27*, 1648–1653.

(55) Kabachii, Y, A.; Kochev, S, Y. *Polym. Sci. Ser. A* **2006**, *48*, 717–722.

(56) Perrier, S.; Takolpuckdee, P.; Mars, C. A. *Macromolecules.* **2005**, *38*, 2033–2036.

(57) Mayadunne, R, T, A.; Jeffery, J.; Moad, G.; Rizzardo, E. *Macromolecules.* **2003**, *36*, 1505–1513.

(58) Harrisson S. *Macromolecules* **2009**, *42*, 897–898.

(59) Beckman, J. S.; Minor, R. L.; White, C. W.; Repine, J. E.; Rosen, G. M.; Freeman, B. a. *J. Biol. Chem.* **1988**, *263*, 6884–6892.

(60) Ilchev, A. Amine End-Functional Poly(*N*-vinylpyrrolidone) as a Macroinitiator for L-lysine *N* -carboxyanhydride Polymerization - Towards the Preparation of pH-Responsive Micelles for Drug Delivery, University of Stellenbosch, 2014.

(61) Pound, G. Reversible Addition Fragmentation Chain Transfer (RAFT) Mediated Polymerization of N -vinylpyrrolidone, University of Stellenbosch, 2008.

(62) Pfukwa, R. Synthesis and Characterization of Telechelic Hydroxyl Functional Poly (*N*-vinylpyrrolidone), University of Stellenbosch, 2008.

(63) Marten, F. L. *Encyclopedia of Polymer Science and Engineering*; John Wiley and Sons, Inc.; 1989.

Chapter 5: Bioconjugation

5.1 Introduction

The act of conjugating bioactive compounds to polymers was introduced in 1955, when poly(*N*-vinylpyrrolidone) (PVP) was conjugated to glycyl-L-leucine-mescaline.[1–3] In 1990 the first three polymer protein conjugates approved by the Food and Drug Administration were styrene maleic anhydride neocarzinostain, poly(ethylene glycol) (PEG) conjugated to adenosine deaminase and PEG conjugated to L-asparaginase.[3,4]

Polymer therapeutics is the term used to describe the use of water soluble and biocompatible polymers attached to a bioactive compound. Different methods of conjugation with polymer exist. These methods include polymer-protein conjugates,[5,6] polymer-drug conjugates,[7,8] and self-assembled micelles[9]

Studies have been performed in order to determine the effect of native unconjugated bioactive compounds, such as proteins and enzymes for medical purposes. However, most have been proven to be unsuccessful due to a few short comings. These short comings include the short life it has in the body which leads to over dosing and side effects.[10,11] These compounds also have limited success due to it not being target specific towards the infected tissue.[12,13] It has been shown that conjugation to synthetic polymers especially PVP has a longer circulation half-life and limited tissue distribution, which makes it ideal as drug carrier, due to its longer circulation times and ability to be functionalized into targeting the specific tissue.[14–16]

For polymer-protein conjugates covalent linkages are required between the polymer and protein. On these proteins, targeted for conjugation, certain functionalities on the amino acids can be targeted. The functionalities targeted on the amino groups are amine(lysine), carboxylic acids (aspartic and glutamic), thiols(cysteine), and hydroxyl groups(serine and tyrosine).[17]

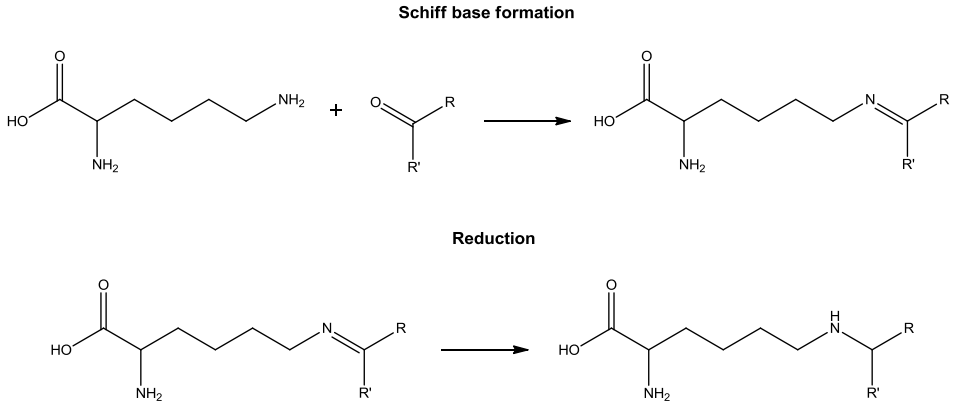

Scheme 5.1: Aldehyde/ ketone conjugation to a lysine.

Because of the amino group present, lysine amino acids are the amino acid mostly conjugated to. This is due to the availability and ease of conjugation. Aldehydes or ketones can easily be conjugated to these lysine amine acid groups. This conjugation takes place via reductive amination where a carbonyl group reacts with the primary amine, forming a Schiff base reaction with an imine functionality. Subsequently followed by reduction of the imine functionality to an amine functionality in the second step. A covalent bond is formed during this reduction (Scheme 5.1).[18–20]

The enzyme catalase originally from the bovine liver, used in this study, consists of four subunits (Figure 5.1a) combined to form a tetramer (Figure 5.1b). These subunits consist of the same amino acid sequence and arrangement for the formation of secondary α helix structures.[21,22] The molecular weight of the tetrameric enzyme is 256 kDa containing 2108 amino acids in the enzyme polymer chain of which 112 are L-lysine.[22–26] Catalase decomposes hydrogen peroxide to water and oxygen (Equation 5.1).

$$2\ H_2O_2 \xrightarrow{\text{Catalase}} 2\ H_2O + O_2 \qquad (5.1)$$

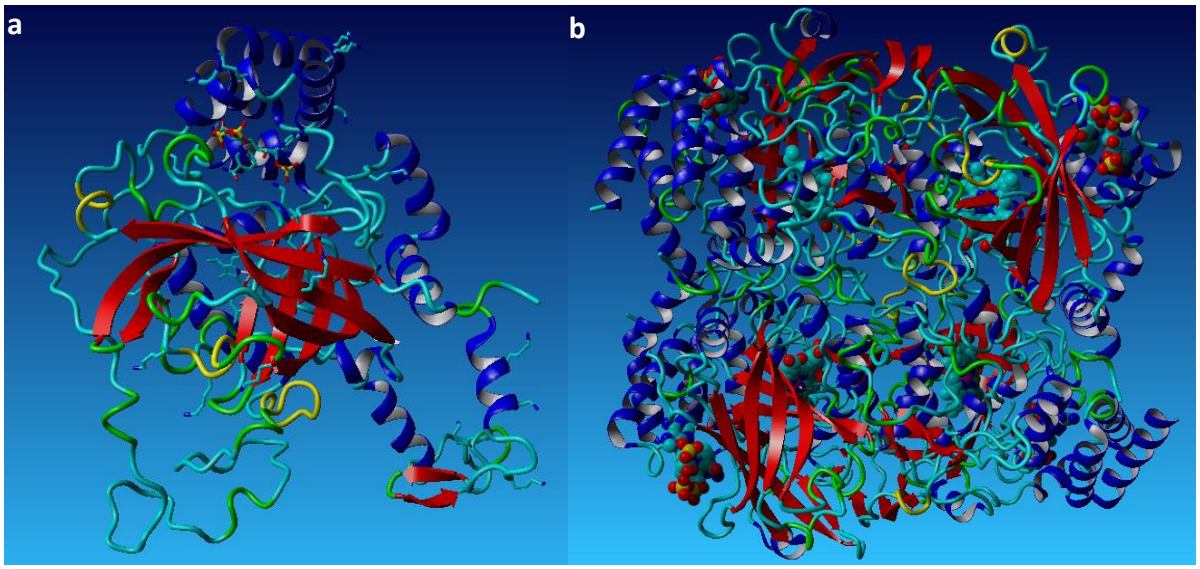

Figure 5.1: Catalase subunit (a) and tetramer (b).[23,27]

For the conjugation of catalase to PVP the procedure as described by Pound *et al.*[18], Chamow *et al.*[19] and Jentoft *et al.*[28] will be used. The L-lysine amino acid residue, abundantly present in catalase, will be covalently conjugated to PVP, through an aldehyde functional group present on the PVP. A Schiff base is formed, which is reduced to form the covalent bond. After conjugation the success and effect of conjugation will be determined using an enzymatic assay, SDS-PAGE analysis and circular dichroism.

5.2 Experimental

5.2.1 Materials

Catalase from bovine liver (powder, 2,000-5,000 units/mg protein, Sigma Aldrich) (1 unit will decompose 1μM hydrogen peroxide, at a pH of 7 and 25 °C, per minute) was used as received. Picrylsulfonic acid solution (5 % (w/v) in H_2O, Sigma Aldrich) was used as is. Distilled deionized water was obtained from an OLGA Purelab option water filtration system set up. Sodium hydrogen phosphate (Dibasic anhydrous, Fluka), Sodium hydrogen carbonate (≥99.7%, Sigma Aldrich), HCl 32% (Sigma Aldrich), H_2O_2 30% (Sigma Aldrich) was used without further purification. Sodium chloride (99.99 Suprapur®, Merck), potassium chloride (99.99 Suprapur®, Merck), potassium dihydrogen phosphate (99.995 Suprapur®, Merck), sodium cyanoborohydride (Merck), dibasic potassium phosphate (99.995 Suprapur®, Merck), sodium dodecyl sulphate (10% in H_2O, Merck), sodium dihydrogen phosphate (99.995 Suprapur®, Merck), bromophenol blue indicator (ACS,Reag. Ph Eur. Merck), β-mercaptoethanol (≥99%, Merck), glycerol (ACS,Reag. Ph Eur. Merck), glycine (≥99%, Sigma Aldrich) tris, hydrochloride (≥99%, Merck), ammonium persulfate (Merck), tetramethylethylenediamine (Merck), Coomassie® Brilliant blue R 250 (Merck), acetic acid (glacial, ≥100%, Merck),, methanol (≥99%, Sigma Aldrich), tris base (≥99%, Merck), acrylamide: bis-acrylamide solution (Merck) were used without further purification.

5.2.2 Conjugation

Conjugation of the polymer to catalase was adapted from a procedure described by Pound *et al.*[18] Catalase was dissolved, to a concentration of 1 mg/mL in a phosphate buffered saline (PBS) solution (pH of 7.0) at 4 °C. A stock solution was made from which 2ml of the solution was used for each conjugation. The catalase was reacted with the aldehyde functionality on the ω end of PVP (PVP 1 – 4 as functionalized in chapter 4) at 4 °C for 5 days while slowly shaking the solution. The mass of polymers used for the two reactions are shown in Table 5.1 and Table 5.2. After 1 hour, 0.25 mL of a 0.25 M sodium cyanoborohydride ($NaBH_3CN$) solution was added as a reducing agent in order for the intermediate imine functionality to reduce to an amine (as seen in Scheme 5.1). The concentration of catalase was not determined after conjugation. It was assumed that no the concentration would still be the same after conjugation.

The first conjugation with catalase involved PVP with a molecular weight of 10×10^3 g/mol (PVP 1). The effect of increasing the polymer concentration on the enzymatic activity was analysed using this polymer-conjugate. An increase in polymer concentration increases the number of polymer chains conjugated to a single catalase molecule. Table 5.1 shows the mass of polymer used in this conjugation.

Table 5.1: Mass of a 10×10^3 g/mol (PVP 1) PVP polymer conjugated to catalase in 2 mL PBS solution (1 mg/mL)

Conjugates	Mass Polymer (g)
1	0
2	0.009
3	0.035
4	0.088
5	0.117
6	0.176
7	0.351

In the second conjugation study, PVP with different molecular weights were used (PVP 1 – 4) in order to determine the effect of PVP molecular weight on the enzymatic activity of the catalase. To ensure that the results are able comparable, the concentration of polymer end groups to catalase was kept constant, while the molecular weight of PVP was varied. Table 5.2 shows the molecular weights and mass of each PVP used.

Table 5.2: Mass of the different molecular weight PVP polymers (PVP 1 – 4) conjugated to catalase in 2 ml PBS solution (1 mg/mL)

Conjugates	PVP	Molecular weight $M_{n,SEC}$ (g/mol)	Mass polymer (g)
1	-	0	0
2	1	10×10^3	0.117
3	2	17×10^3	0.199
4	3	25×10^3	0.293
5	4	37×10^3	0.433

5.3 Analysis

5.3.1 TNBSA assay

To determine the concentration of primary amine groups (such as those present in lysine) in enzymes or in small molecules, a trinitrobenzene sulfonic acid (TNBSA) assay is used, as described in literature.[29–31] The reaction between primary amines and TNBSA is shown in Scheme 5.2. The primary amine attacks the sulphonate group on the TNBSA molecule, forming the chromogenic product, which can be measured with UV-vis spectroscopy. The concentration of amines present in

catalase is very important as they are targeted during the conjugation reaction. Therefore, knowing the exact concentration of amino groups in the catalase is paramount to the conjugation parameters.

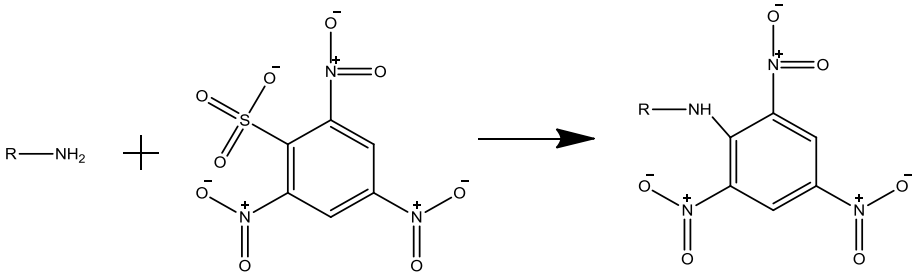

Scheme 5.2: TNBSA reaction scheme.

The TNBSA analysis of primary amines was adapted from literature. [29–31] The TNBSA analysis of catalase was performed with the aim of determining the concentration of primary amine groups present in catalase. The same TNBSA analysis was performed with butyl amine in order to calculate the molar extinction coefficient for the chromogenic product at a wavelength of 335 nm. This value is necessary for calculations using the Beer Lambert Law (Seen in Equation 5.2). The absorbance at 335 nm of each TNBSA solution was measured with an Analytik Jena specord 210 plus UV-vis instrument, using a Hellma QS 10.00 mm cuvette.

$$A = \varepsilon c l \qquad (5.2)$$

For catalase, the concentration of primary amines present was determined by mixing 0.25 mL of a 0.01 % (*w/v*) 2,4,6-trinitrobenzene sulfonic acid solution (in a 0.1 M sodium carbonate buffer at pH 8.5) with 0.5 mL of a 0.1 mg/mL catalase solution, dissolved in the same sodium carbonate buffer solution. It was then incubated at 37 °C for 2 hours. A 10 % sodium dodecyl sulphate (SDS) solution (0.25 mL) and 0.125 mL of a 1 M HCl solution was added to the incubated solutions and absorbance was measured at 335 nm. Sodium carbonate buffer solution was used as a reference. This analysis was repeated for all catalase solutions (0.1 mg/mL to 0.4 mg/mL). From these measurements a graph was drawn describing the absorbance at 335 nm vs the concentration of each catalase solution. The same analysis was repeated for four butyl amine solutions (0.015 mg/mL to 0.04 mg/mL). From these measurements a calibration curve was drawn describing the absorbance at 335 nm vs the concentration of each butyl amine solution.

5.3.2 SDS-PAGE

For Sodium dodecyl sulphate - polyacrylamide gel electrophoresis (SDS-PAGE) analysis, four solutions are used, namely the sample loading gel, separation gel, stacking gel running buffer, stain solution, destain solution 1 and destain solution 2. For each of these four solutions the following compositions are used.

2× Sample loading gel: 0.1% (*w/v*) bromophenol blue, 5% (*w/v*) SDS, 2% (*v/v*) β-mercaptoethanol, 20 % (*v/v*) glycerol and 100 mM Tris-HCl (pH 6.8) are mixed and used in a 1:1 dilution ratio with the sample to be analysed. This is placed in boiling water for 10 min to ensure the protein is denatured.

Separation gel: 7.9 mL water, 6.7 mL acrylamide/bis-acrylamide (30 %/0.8 % *w/v*), 5.0 mL of 1.5 M Tris-HCl (pH = 8.8), 0.2 mL of 10 % (*w/v*) SDS and 0.2 mL 10 % (*w/v*) ammonium persulfate are mixed together. This was degassed to ensure oxygen is removed from the solution. Subsequently, 0.008 mL tetramethylethylenediamine is added and placed between 2 glass plates

Stacking gel: 5.50 mL distilled water, 1.00 mL of a 1M Tris (pH 8.8), 0.08 mL 10 % (*w/v*) SDS, 1.30 mL acrylamide/bis-acrylamide (30 %/0.8 % *w/v*) and 0.08 mL 10 % (*w/v*) ammonium persulfate is added and mixed together. Just before adding this gel between the glass plates 0.008 mL tetramethylethylenediamine is added to the solution.

Running buffer: 250 mM Tris, 1.92 M glycine and 35 mM SDS are mixed together.

Stain solution: 0.125 % Coomassie Brilliant Blue R250, 50 % methanol and 10 % glacial acetic acid is dissolved with distilled water to a final volume of 500 mL.

Destain Solution 1: 50 % methanol and 10 % glacial acetic acid are dissolved in distilled water to a final volume of 500 mL.

Destain Solution 2: 5 % methanol and 7 % glacial acetic acid dissolved are with distilled water to a final volume of 500 mL.

Analysis: The two glass plates are clamped together between casting frames on the casting stand. The separating gel is prepared and pipetted between the glass plates. To ensure the gel is horizontal isopropanol is added on top. After polymerization of the separation gel (30 minutes) the isopropanol is decanted. The stacking gel is pipetted on top of this and the spacer comb is placed in before polymerization starts. This is left to polymerize (30 minutes). The comb is removed and the plates removed from the casting frame. The glass plates are placed in the cell buffer reservoir, running buffer is inserted in the inner chamber of the dam until the desired level is reached. The sample solution(s), protein marker and reference(s) are added into separate lanes. The reservoir is placed inside the outer chamber and this is also filled with running buffer until the required level. This is enclosed and the anodes connected. The SDS-PAGE was set to 100 V for 15 minutes followed by 200 V for 1 hour. After an hour the gels are removed, followed by staining of the gels for 1 hour with the staining solution at room temperature. This is followed by destaining with destain solution 1 for an hour and lastly destaining with solution 2 overnight, all at room temperature. For the SDS-PAGE analysis a Mini-PROTEAN Tetra Cell SDS-PAGE apparatus was used with a PowerPac™ power supply.

5.3.3 Enzymatic activity assay of catalase

The decomposition of hydrogen peroxide, through catalase, is measured with an enzymatic activity assay. UV-vis spectroscopy was used to measure the decrease in absorbance at 240 nm relating to the decrease in hydrogen peroxide concentration The procedure was followed as described in literature.[32,33] For the analysis a hydrogen peroxide and a catalase solution is prepared separately in a 20 mM sodium phosphate buffer solution adjusted to a pH of 7 with 1 M HCl. The hydrogen peroxide is dissolved until a concentration of 0.036M. After the conjugation experiment the catalase conjugates is dissolved until a concentration of 0.01 μM. 2.9 mL of the hydrogen peroxide solution is placed in the UV-vis cuvette. 0.1 mL of the catalase solution is added into the cuvette and the absorbance measured at 240 nm every second after addition for 400 seconds. For the PVP reference, 0.0125g of the 10 x 10^3 g/mol (PVP 1), PVP polymer is dissolved in 1 mL sodium phosphate buffer solution and the decomposition of hydrogen peroxide determined in the same way. For this analysis an Analytik Jena specord 210 plus UV-vis instrument is used, using a Hellma QS 10.00 mm cuvette with sodium phosphate buffer solution as reference.

5.3.4 Circular dichroism

CD spectra were acquired using a Chirascan-plus CD Spectrometer which has a 150 W xenon lamp light source. As detector, a UV-vis photomultiplier was used. Pro-Data control and viewer software are used for the analysis. Samples were scanned between 190 and 350 nm. For the cuvette a Hellma 115F-QS (10.00 mm) was used. The catalase concentration was dissolved until a concentration of 0.0625 mg/mL in a 20 mM sodium phosphate buffer solution adjusted to a pH of 7.

5.4 Results and discussion

5.4.1 Concentration of lysine groups on catalase

Before conjugation, the concentration of primary amine groups, which equate to the concentration of lysine residues on the catalase, was determined. The concentration of primary amine groups are required in order to target selected amine concentrations with PVP during conjugation.

In order to determine the concentration of primary amines in catalase two UV-vis analyses are required, using two TNBSA assays. The first establishes the relationship between the concentration of catalase and the absorbance. The second is a calibration analysis whereby the n-butyl amine is used to calculate the extinction coefficient of the chromogenic product (Scheme 5.2). This will later be used in order to determine the relationship between absorbance and the free amines in catalase.

The TNBSA assay was used to determine primary amines present in catalase. This method utilizes the absorbance of the chromogenic product measured at 335 nm after the TNBSA reaction.[29–31] Figure 5.2 shows the absorbance at 335 nm of the chromogenic product, as a function of the catalase concentration. From literature[31] a linear increase in the absorbance measured is expected with the

increase in primary amine concentration. In Figure 5.2 this is observed. Deviations, of the measured values, from the linear regression line are observed. These deviations are however, very close to the regression line. Figure 5.2 only describes the relationship between the absorbance and catalase concentration. Further calculations, using the Beer Lambert Law (Equation 5.2) are necessary in order to determine the concentrations of primary amines in the catalase solutions.

The Beer Lambert law is used to describe the relationship between absorbance measured (A), length of the cuvette (l) and concentration (c) of the substrate. A molar extinction coefficient (ε) is a constant, used to describe how a molecule absorbs light at the given wavelength in relation to the concentration.[34] In order to calculate the molar extinction coefficient of the TNBSA chromogenic product, a calibration curve is used (Figure 5.3).

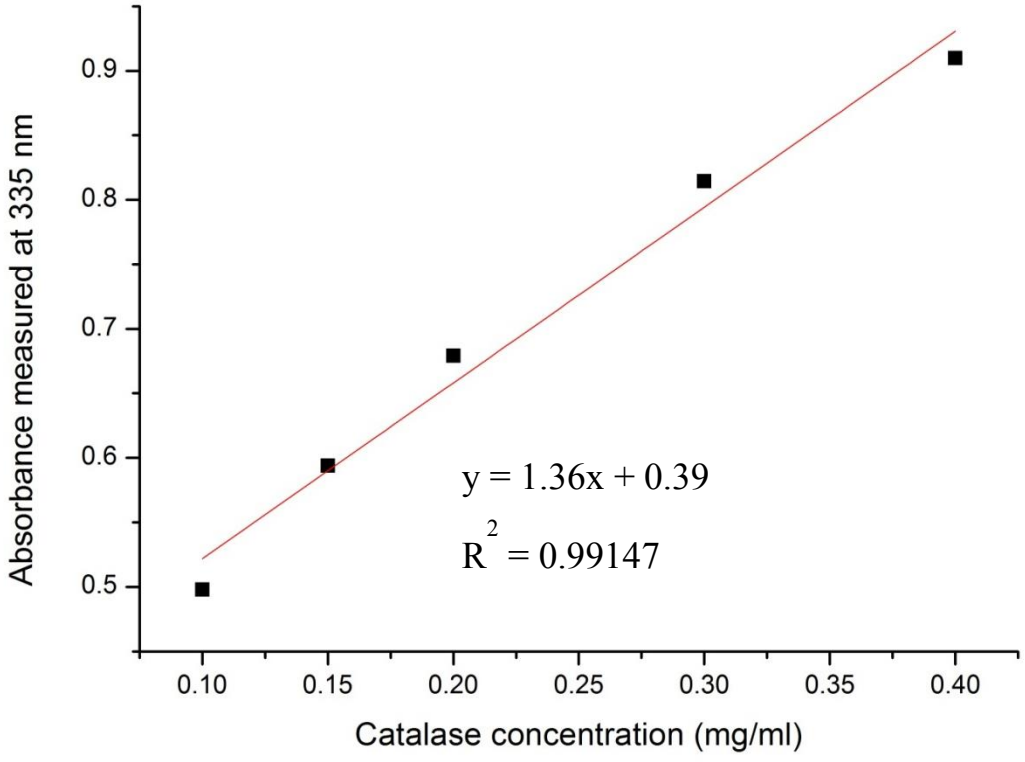

Figure 5.2: TNBSA assay absorbance at 335 nm measured as a function of catalase concentration.

Different concentrations of butyl amine were analysed and plotted in Figure 5.3. For the calibration curve in Figure 5.3 a linear regression line is also expected and is observed. Very small deviations of the measured values from the regression line are observed. Using the Beer Lambert law, the molar extinction coefficient was determined as 12×10^3 L/mol·cm, for primary amines reacted with TNBSA at 335 nm as determined from Figure 5.3.

From the TNBSA assay (Figure 5.2) and knowledge obtained about the TNBSA chromogenic product's molar extinction coefficient determined from Figure 5.3, the primary amine concentration of 1 mg catalase was found to be 4.4×10^{-4} mol /mL, using the Beer Lambert law.

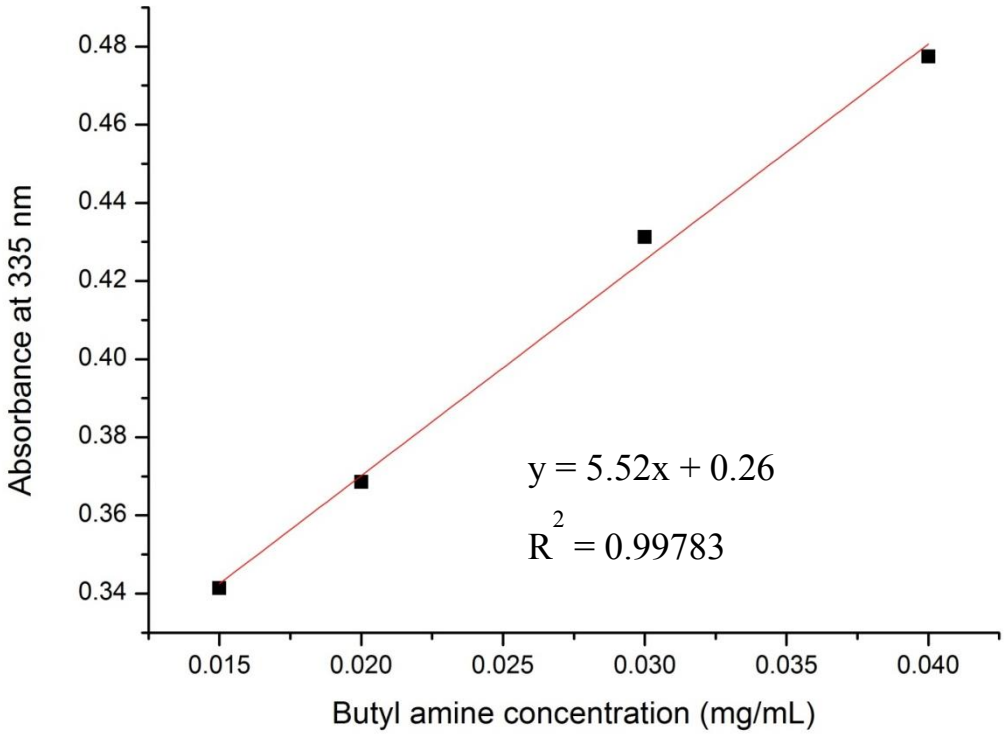

Figure 5.3: TNBSA assay absorbance at 335 nm measured as a function of butyl amine concentration.

The concentration as determined from the Beer Lambert law correlates very well with the amount of L-lysine present in catalase in the following way: Catalase with a molecular weight of 256 kDa has 112 lysines present in the enzyme. Lysine residue has a molecular weight of 128.09 Da, therefore, the total mass of lysine present in catalase is ~ 14300 Da. For 1 Da of catalase, 0.056 Da of lysine group are present. Thus, using Equation 5.3, 4.38×10^{-4} mol /mL Lysine amine groups are present in 1Da of catalase. The concentration of the four α amino groups must be brought into consideration, increasing the concentration to 4.45×10^{-4} mol /mL amine groups are present in 1Da of catalase. This concentration is very close to the value as calculated from the TNBSA assay.

$$n = m/m_r \qquad (5.3)$$

The TNBSA assay could not be performed on the PVP-catalase conjugates, due to the TNBSA reacting with PVP to form chromogenic products. The chromogenic products formed were directly related to the concentration of PVP added. The chromogenic products absorb at 335 nm, resulting in unreliable values of free amine concentration after conjugation. No other methods were used in determining the lysine amino acid concentration after conjugation.

5.4.2 Effect of PVP concentration on catalase

The consequence of conjugating different concentrations of aldehyde functional ω end group PVP to the lysine present on catalase was studied. For the conjugation reactions PVP with a molecular weight of 10 x 10^3 g/mol (PVP 1) was used. Scheme 5.3 schematically represents the conjugation of PVP to catalase through reductive amination as described in the experimental section. As can be seen in the scheme, sodium cyanoborahydride was used as the reducing agent in these conjugation reactions.

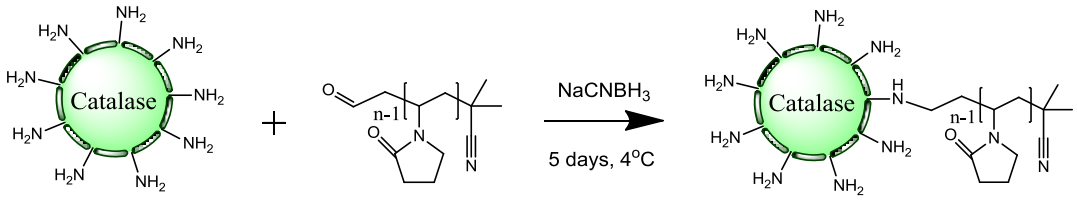

Scheme 5.3: Conjugation of catalase to aldehyde end functionalized PVP.

A summary of the ratio of lysine groups to PVP aldehyde end groups for the conjugation, the PVP end group concentration and amount of PVP used for each conjugation can be seen in Table 5.3. Theoretically 4.38 × 10^{-4} mol /mL lysine groups are present on 1 mg of catalase as determined from the TNBSA assay; this value is however not targeted for the conjugations. The theoretical lysine groups will not be targeted and concentration of PVP kept low, to minimalize the effect of PVP on the conjugated catalase.

Table 5.3: Ratio lysine groups to polymer end groups in a 2 mL PBS solution

Conjugates	Lysine groups: Polymer end groups	Polymer end group concentration (M)	Mass polymer (g)
1	1:0	0	0
2	1000:1	4.93×10^{-7}	0.009
3	100:1	4.93×10^{-6}	0.035
4	75:1	5.85×10^{-6}	0.088
5	50:1	8.78×10^{-6}	0.117
6	25:1	1.76×10^{-6}	0.176
7	12.5:1	3.5×10^{-5}	0.351

Conjugate 1 seen in Table 5.3 was used as a control in the study and is not conjugated to the PVP polymer. This unconjugated catalase can be thought of as a baseline to which the conjugated catalase can be compared. The concentrations of PVP for conjugates 2 and 3 are chosen to be less than the

concentration of the lysine groups present in catalase. This ensures that unconjugated catalase can still be detected via SDS-PAGE analysis, if present, after conjugation. Since each catalase contains more than one free-amine available for conjugation, excess PVP will be used for samples 4 to 7 to ensure that each catalase is conjugated. SDS-PAGE analysis, enzymatic activity and circular dichroism analysis techniques were used to study the properties of the conjugates.

5.4.2.1 SDS-PAGE analysis of conjugations

Sodium dodecyl sulphate - polyacrylamide gel electrophoresis (SDS-PAGE) is a common technique used to separate biomolecules such as proteins.[35,36] The separation occurs through differences in the electrophoretic mobility of the biomolecules, which is a function of the charge, conformation and size of the molecule. Since the method of separation of the molecules is by electrical charge, the process is referred to as electrophoresis and takes place on a polyacrylamide gel. Sodium dodecyl sulphate (SDS), an anionic detergent, is used as a denaturing agent, which applies a negative charge to the proteins proportional to the size of the protein.[35,36] A conductive buffer is used and a potential difference placed over the system ensuring that the negatively charged proteins move from the cathode to the anode. Smaller macromolecules move faster through the matrix than the larger molecules, allowing for separation according to size.[35,36] Bromophenol blue dye indicates the presence of proteins on the SDS-PAGE. In the solution the Bromophenol blue is negatively charged, moving with the protein. After removing the potential difference, the acidity of the proteins are decreased when the SDS-PAGE is stained with the Coomassie Brilliant Blue R250 staining solution. At a pH below the isoelectric point of proteins, the dye reacts with the carboxylic, phenolic and sulfhydryl groups on the protein to form blue markers which are observed on the SDS-PAGE.[37–40] These blue markers are the points of interest in the analysis, as they represent the positions of the proteins, as well as are an indication of the separation.

Figure 5.4 depicts the SDS-PAGE of the samples of catalase after conjugation with different concentrations of PVP, as described in Table 5.3.

From Figure 5.4, the first signs of successful conjugation are seen. In the lane labelled “Pol”, containing the polymer reference, a clear lane is seen indicating that the polymer and bromophenol blue dye do not react. This is due to bromophenol blue dye reacting exclusively with carboxylic, phenolic and sulfhydryl groups,[38] which are not present on the conjugated or unconjugated PVP polymer. Therefore, as was expected no blue band will be observed on the SDS-PAGE, and only a clear lane remains. The conjugated and unconjugated catalase still has these functional groups available to react with the dye, and therefore, the blue bands at the expected 64 kDa of the monomer can be seen on the SDS-PAGE (green highlight). The lane labelled “Cat” corresponds to the position of the unconjugated catalase and was used as a reference for the conjugates. A blue line is expected at ~ 64 kDa which corresponds to the molecular weight of the catalase subunit.[41,42] As can be expected,

there is no difference between Conjugate 1, the unconjugated catalase reference, and the reference catalase "Cat" in Figure 5.4. The difference between these references is Conjugate 1 took part in the experiment and "Cat" did not.

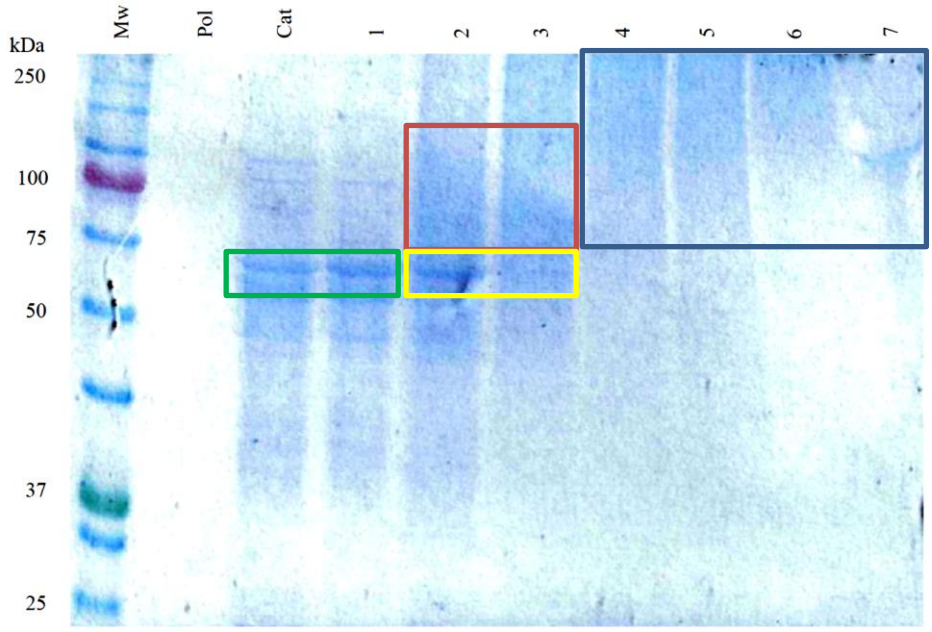

Figure 5.4: SDS-PAGE analysis of catalase conjugated to different concentrations of PVP with molecular weight of 10 × 10^3 g/mol. Where Mw is the molecular weight marker, Pol the polymer reference, Cat the catalase reference and 1-7 the conjugations as labelled in Table 5.3.

In conjugate 2 only a small fraction of the lysine groups have been conjugated with PVP. Thus, the line indicating ~ 64 kDa is still present on the SDS-PAGE (yellow highlight). This indicates the presence of the unconjugated protein, as expected. A dark blue area is seen above the ~ 64 kDa line (red highlight), indicating a small increase in the molecular weight due to the conjugated catalase. This smudge is a clear indication that conjugation with PVP has taken place. In conjugate 3, the dark blue smudge was also observed with a feint band at ~ 64 kDa (yellow highlight), showing the presence of small amount of unconjugated catalase in the solution. A smudge above this line indicates conjugation has taken place (red highlight). As stated earlier, the concentration of PVP for conjugates 2 and 3 are less than concentration of catalase as seen in Table 5.3. These two conjugates were included in order to determine if unconjugated catalase will still be detected when only partial conjugation has taken place. In conjugates 4 to 7, the band at ~ 64 kDa is lost indicating that there is no unconjugated catalase remaining. Also the darker blue smudges, representing the conjugates, are observed above 100 kDa (blue highlight) nearing the resolution limit of the SDS-PAGE. This indicates that there was a significant increase in the size of the conjugates, suggesting that one catalase molecule is indeed able to conjugate to multiple PVP molecules. The concentration of PVP conjugated to catalase was not determined.

5.4.2.2 Catalase activity after conjugation

The enzymatic activity of the conjugates was studied by assessing the conjugate's ability to decompose hydrogen peroxide. The disappearance of the hydrogen peroxides concentration was followed by UV-vis spectroscopy at 240 nm for 400 seconds, tracking the decrease in absorbance as a function of time. The polymer conjugates as seen in Table 5.3 were used in the same concentration for the study. Figure 5.5 contains the information pertaining to the enzymatic activity of the conjugates. Conjugate 1 is used as a baseline for comparison.

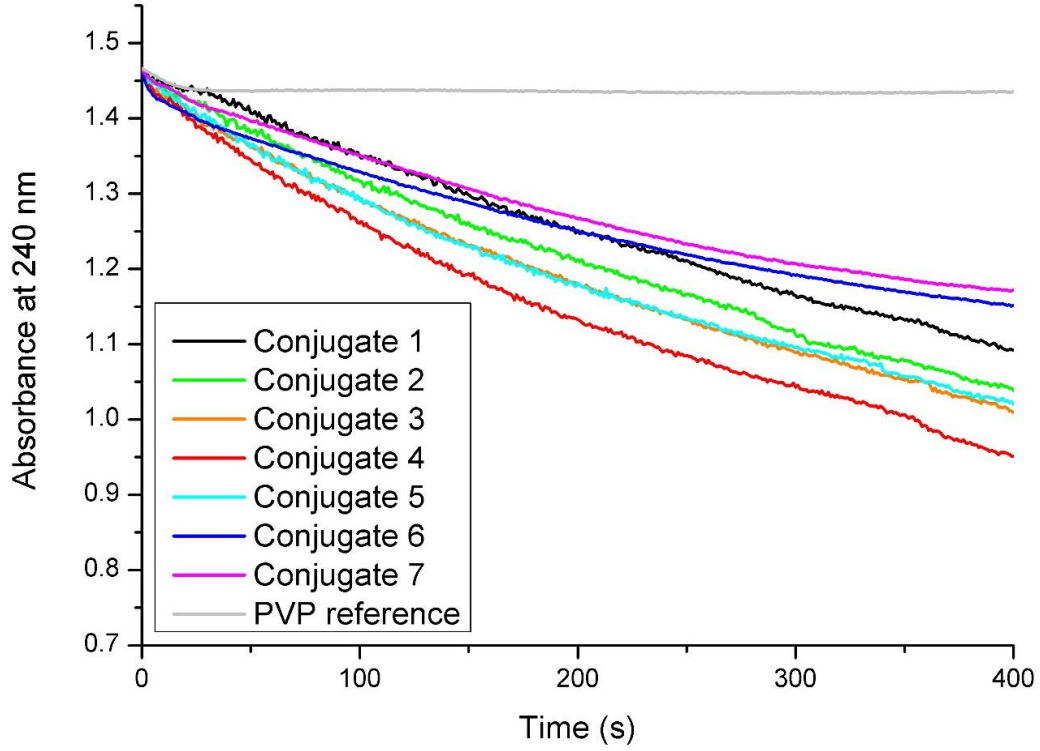

Figure 5.5: Enzymatic activities of different concentrations 10 x 10^3 g/mol PVP polymer conjugated to catalase, as stated in Table 5.3, measured with UV-vis spectroscopy at 240 nm over time.

From Figure 5.5, decomposition of hydrogen peroxide after conjugation is evident. For the first four conjugates (conjugates 2 – 5) the activity of the catalase increases with respect to the unconjugated catalase. However, with conjugates 6 and 7 the activity of the conjugates is lower with respect to unconjugated catalase. Therefore, it can be concluded that conjugation to PVP does not interfere with the active group or structure of catalase to such an extent that activity is lost; a change in the activity is, however, observed. At low to moderate degrees of conjugation, it has a positive effect on the activity. A trend in the conjugates is observed with an increase in PVP concentration. The activity of the conjugates increases with an increase in PVP concentration until a maximum is reached in the activity for conjugate 4. After which, a decrease is seen in the activity for conjugates 5, 6 and 7. The difference between unconjugated catalase and Conjugate 4 is large, as observed from Figure 5.5. The decomposition of hydrogen peroxide with PVP without any conjugated catalase is determined as seen

from Figure 5.5. This PVP reference is analysed to determine if the PVP on its own will have an effect on the decomposition of hydrogen peroxide. From Figure 5.5 it is observed that the PVP has a small effect in decreasing the absorbance at the beginning of the analysis for a few seconds, but does not alter the concentration of hydrogen peroxide after this alteration. Takada *et a.l*[43] determined the same effect for PVP in their study. For the conjugations the same concentrations was used and the same concentration for each conjugate's enzymatic analysis. Aggregation of the conjugates after conjugation was not determined.

Using Figure 5.5, the enzymatic activity parameters can be determined for these conjugates. These parameters are determined to show, mathematically, the change in the enzymatic activity that has taken place with the conjugations. Using the Beer Lambert law (Equation 5.2) and a molar extinction coefficient of 43.6 L/mol·cm[44] the decrease in hydrogen peroxide concentration was determined. A second order rate law (Equation 5.4) was applied to the decrease in the concentration of hydrogen peroxide ([S]) over time (t). For this a second order rate constant (k) is required for each conjugate. The constant is determine as the slope of $\frac{1}{[S]_t}$ versus the time for each conjugate. With Equation 5.4 and the second order rate constant (k) the hyperbolic relationship between the reaction rate and hydrogen peroxide concentration can be determined for each conjugate. V_{max} can be determined from this relationship and is defined as the maximum asymptotic value approached by the curve, but never intersects.[45] The turnover number (k_{cat}) can be determined using V_{max} (Equation 5.5). This is defined as the conversation of substrate per second for a certain enzyme concentration (E_T).[45] For Catalase a concentration of 3.9×10^{-10} M is found. The values for these variables are shown in Table 5.4.

$$\text{Rate} = -\frac{\Delta [S]}{\Delta t} = k[S]^2 \qquad (5.4)$$

$$k_{cat} = \frac{V\text{max}}{E_T} \qquad (5.5)$$

Table 5.4: Enzymatic activity parameters, for the conjugates 1 – 7 as described in Table 5.3

Conjugate	V_{max} (M/s)	k_{cat} (s^{-1})
1	0.0155	4.0×10^7
2	0.0165	4.4×10^7
3	0.0175	4.6×10^7
4	0.0185	4.9×10^7
5	0.0165	4.4×10^7
6	0.0155	4.0×10^7
7	0.015	3.8×10^7

From Table 5.4 the change in the enzymatic activity of catalase as described in Figure 5.5 is described mathematically. An increase in the activity is found with conjugations 2 – 5 in comparison with conjugate 1 with conjugate 4 the maximum, with a value of 4.9×10^7 s^{-1}. Conjugate 5 – 7 has a decrease in the enzymatic activity when compared to conjugate 4, with conjugate 6 having the same value as conjugate 1 and 7 having a lower enzymatic activity than conjugate 1. The value used to describe the enzymatic activity is the turnover number or k_{cat} and as determined from literature is 4.0×10^7 s^{-1} for catalase,[46,47] which is the same as for conjugate 1, the unconjugated catalase, as seen in Table 5.4. Conjugate 4 has a value of 4.9×10^7 s^{-1}, and conjugate 7 a value of 3.8×10^7 s^{-1}. These turnover numbers for the conjugates describes the change in the enzymatic activity of catalase in the same way as Figure 5.5.

The increase in the activity of catalase with the conjugation of a polymer has been observed before. In their study, Beckman *et al.*[48] showed that with the conjugation of PEG, with a molecular weight of 5000 Da, to 60% - 80% of the lysine amino groups present in catalase, an increase in the activity of catalase was found with better oxidative stress handling capabilities. Thus, the increase in catalytic activity was not unexpected and can take place. Riccardi *et al.*[41] determined in their study that with an increase in conjugation with poly(acrylic acid) a decrease in the enzymatic activity of catalase is observed. Ashihara *et al.*[49] studied the conjugation of α-methoxy-poly(ethylene glycol) (MPEG) to L-asparaginase. In their conjugations with the increase in concentration of MPEG a decrease in the activity of the enzyme was observed. These studies indicate that with the increase in concentration of the polymer a decrease in enzymatic activity can be found.

5.4.2.3 Circular dichroism of catalase

Amino acids, forming proteins, are covalently bonded through peptide bonds to form polymer chains, called polypeptides.[50] When the correct sequence of amino groups are present in these polymer peptide chains, different structures within the enzyme are formed. These structures are grouped into primary, secondary, tertiary and quaternary structures. Circular Dichroism (CD) is an analytical tool used to determine and detect these structures. One of the secondary structures formed, with the correct sequence, is α-helixes, which is present in catalase. This secondary structure of catalase was detected with CD because of the chirality of the carbonyl groups present in the helix, which absorb in the far-UV region (190 -250 nm). Two minimum ellipticities are typically seen at 208 nm and 222 nm. These helixes are stabilized by the hydrogen bonding which takes place between the carbonyl groups and amine group, four amino acids away from the carbonyl group of the same polymer peptide chain (Figure 5.6).[21,22,50–52] From the CD spectrum at the near UV region (250 -300) aromatic amino acids, present in the catalase enzyme, can be detected.[52]

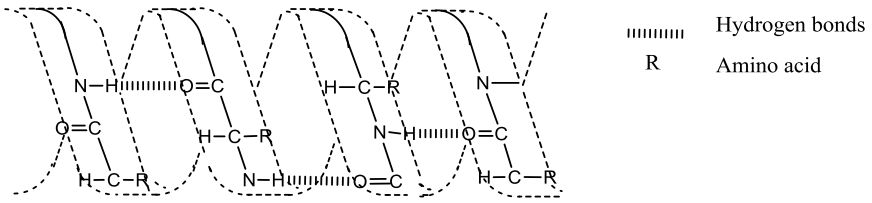

Figure 5.6: α Helix configuration showing hydrogen bonds between amino acids.

CD is a spectroscopy method used in the analysis of chiral (asymmetrical) molecules. Amino acids within proteins contain chiral carbons, making it easy for them to be analysed by CD.[52–55] The properties of proteins that can be determined from CD include the secondary structure, binding properties, folding and denaturing of the proteins.[54] As in the case of UV-vis spectroscopy, CD uses a light source for the analyses of the samples, due to the sample's ability to separate a right handed and left handed circular polarized light. A light beam contains an electric and magnetic field, both of which are time dependent. The light source is polarized, forming a sinusoidal wave in the direction of the beam. Due to filters and prism the sinusoidal wave is converted into an oscillating sinusoidal electric field with both clockwise direction (E_R) and counter clockwise direction (E_L), of equal intensity. When these two oscillating waves reach the sample, they are absorbed with different intensities and refraction. These two waves are precisely 90 ^{0} out of phase and are separated after the sample through prisms and electronic devices followed by detection. The two waves are rotated differently and combination of two sinusoidal waves after the sample forms an ellipse. Giving rise to the term ellipticity polarization of the light and is reported in molar ellipticity ([θ] deg cm^2 dmol^{-1}).

Figure 5.7 contains the CD spectra for catalase after conjugation with different concentrations PVP with a molecular weight of 10 x 10^3 g/mol. The same enzyme concentration was used for this analysis. As mentioned above, CD reveals information about the structure of an enzyme containing chiral centres. In the CD analysis for this study, the change in the micro structure of catalase is measured with the increase in polymer concentration. The CD spectrum of unconjugated catalase (conjugate 1) was obtained as a baseline for comparison. All spectra were normalized according to the concentration of protein and path length.

When comparing the CD spectra in Figure 5.7, especially the unconjugated catalase (conjugate 1), to CD spectra of catalase found in literature,[56,57] a difference is observed in the minimum ellipticity. A bimodular band, with a minimum ellipticity at 208 and 222 nm, is expected. These two ellipticity minima correspond to the α helix in the structure.[54,58,59] Conjugate 1, with a minimum ellipticity of ~ 220 nm, in Figure 5.7 corresponds with that of catalase at higher temperature, where denaturing of the enzyme takes place, as seen in literature.[59] The origin of this denaturalization is not known, however, handling of the enzymes could have had an effect. Although this is not conducive to protein studies, these spectra are still valuable to the study as they display evidence of a change in the secondary

structure of catalase conjugated to PVP compared to unconjugated catalase, albeit slightly different from literature. The spectrum for unconjugated catalase (conjugate 1) has a lower ellipticity minima compared to that of conjugated catalase. A change in the Figure 5.7 is observed for conjugates 2 – 7, where conjugation to PVP took place.

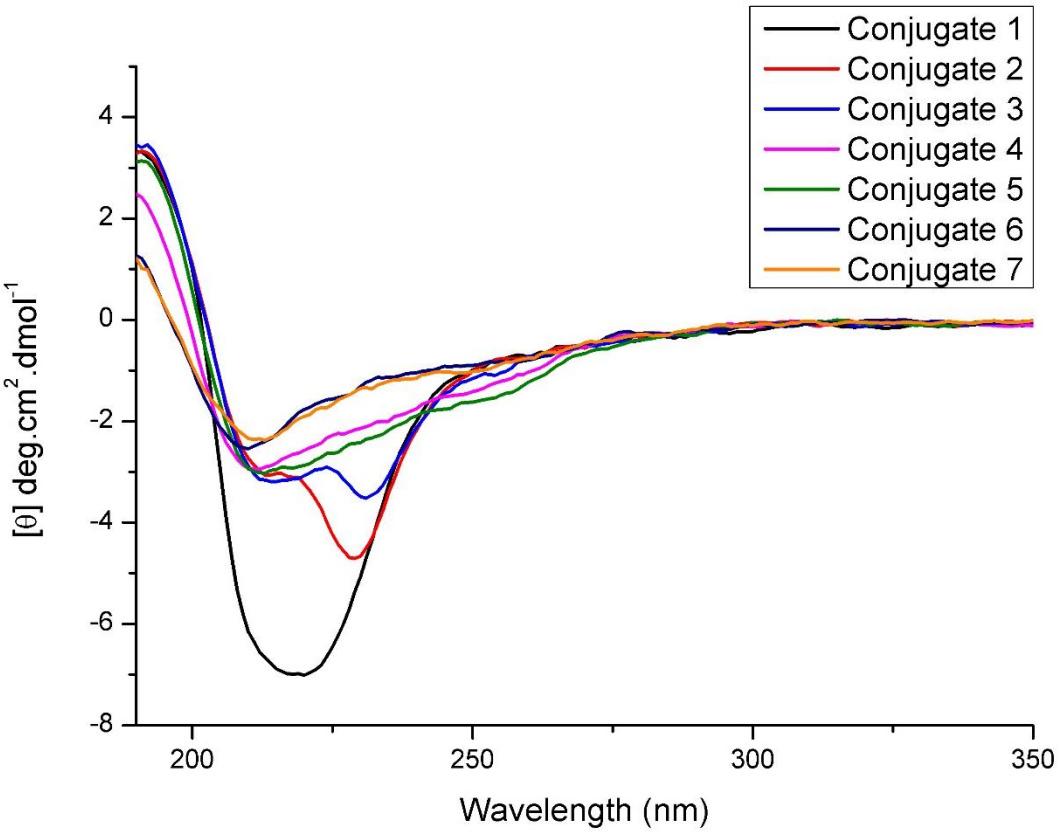

Figure 5.7: Circular dichroism of catalase conjugated with different concentrations of PVP with a molecular weight of 10 x 10^3 g/mol.

From Figure 5.7 bimodular bands are seen at ~ 210 nm and ~ 230 nm for conjugates 2 and 3, but not for conjugates 4 – 7, where conjugation to every catalase in the solution took place. The bands at ~ 210 nm and ~ 230 nm, for these two conjugates, could be due to the unconjugated catalase. As described in Table 5.3 and evident from the SDS-PAGE (Figure 5.4) unconjugated catalase is present after conjugation. For conjugates 4 and 5, the bands at ~ 210 nm are present with the same negative ellipticity as conjugates 2 and 3. Conjugates 6 and 7 has a decrease in the minimum ellipticity value at ~ 210 nm and ~ 230 nm. A decrease in the ellipticity at 190 nm for conjugates 4, 6 and 7 is also seen in this Figure 5. 7. From the changes in the spectra, for all of the conjugates, a change in the micro structure of the enzyme is seen. A decrease in the ellipticiy at 190 nm for conjugates 4, 6 and 7 and increase in the negative ellipyicity at ~ 210 nm, for the conjugates with an increase in PVP concentration, indicates possible denaturing of the enzyme, with the denaturing of conjugates 6 and 7, where a higher concentration of PVP is added in this study, having the most denaturing of the

enzyme. From the enzymatic activity the conjugates 6 and 7 have lower activity than unconjugated catalase. However, the reason for conjugates 2, – 5 having an increase in the enzymatic activity, with denaturing of the enzyme taking place, is not known. Further studies are required into this peculiar finding.

Furthermore, a change in the ellipticity is seen between the wavelengths of ~ 250 nm to ~ 275 nm for two of the conjugations. For Conjugates 1 (unconjugated catalase), 2, 3, 6 and 7 the ellipticity is the same, Conjugates 4 and 5 have lower minimum ellipticity compared to the other conjugates. The reason for these two conjugates having this minimum ellipticity is not known.

In their study Aubin-Tam *et al.*[60] cytochrome C was labelled with negatively charged Au nanoparticles. From CD they determined that a loss in the α-helix secondary structure took place. They observed a similar disturbance in the CD spectra as we have seen for the catalase-PVP conjugates. It is, therefore, possible that the conjugation has caused a loss in the α-helix secondary structure. However, further investigation is necessary to elucidate this.

After conjugation catalase to of PVP, a change in the molecular weight, enzymatic activity and structure of catalase was found when compared to unconjugated catalase. From Figure 5.4, a change in the molecular weight of catalase is observed when conjugating the PVP. It was also observed that increasing the concentration of PVP ensures conjugation to every catalase present in the solution. From Figure 5.5 the observation is made that conjugating PVP to catalase does not remove the enzymatic activity, of catalase. Decomposition of hydrogen peroxide through the conjugated enzyme is still possible. For the enzymatic activity a competing effect is taking place with lower concentration of PVP increasing the activity and higher concentration decreasing the activity, suggesting that a change in the structure of catalase is taking place. It has also been shown that unconjugated PVP does not decompose hydrogen peroxide. From CD analysis (Figure 5.7) it was confirmed that a change in the structure of catalase is taking place with an increase in polymer concentration. \the circular dichroism of PVP was not analysed, but a decrease in ellipticity at 190 nm and increase in ellipticity at ~ 210 nm and ~ 230 nm with the increase in PVP concentration as observed from Figure 5.7. The assumption is made that the PVP is not detected at these wavelengths or the signal is very low. Further studies is required in determining what type of change is taking place in the structure of catalase when conjugation of catalase to PVP and what competing effect is increasing the enzymatic activity of catalase when conjugated to catalase.

5.4.3 Effect of PVP molecular weight on catalase

After conjugation with different concentrations of PVP to catalase, a question arose regarding the extent that the molecular weight of the PVP plays a role in the enzymatic activity and structure of the enzyme. To answer this question, different molecular weights were conjugated to catalase. The concentration of polymer end groups where kept identical for the conjugations. The same method of

conjugating PVP to catalase through reductive amination, as expressed earlier in Scheme 5.3 is followed. Table 5.5 contains the information pertaining to the conjugations whereby the concentration of polymer end groups remained constant.

For these reactions four different molecular weights (PVP 1 – 4) were used. Table 5.5 summarizes the molecular weight, ratio of lysine groups to polymer end groups and mass of each conjugation. As with the previous conjugation experiment, Conjugate 1 indicated in Table 5.5 was used as a reference and is unconjugated. For conjugates 2 – 5 the ratio of lysine groups to polymer end groups were chosen to ensure excess PVP is present in the solution, ensuring that every catalase molecule is conjugated to PVP. As with the previous study SDS-PAGE analysis, enzymatic activity and circular dichroism analysis techniques were used to study the properties of the conjugates.

Table 5.5: Information regarding the polymers used in the conjugation with catalase in a 2 mL PBS solution

Conjugates	PVP	PVP Molecular weight $M_{n,SEC}$ (g/mol)	Lysine groups: Polymer end groups	Polymer end group concentration (M)	Mass of polymer (g)
1	-	0	1:0	0	0
2	1	10×10^3	50:1	8.78×10^{-6}	0.117
3	2	17×10^3	50:1	8.78×10^{-6}	0.199
4	3	25×10^3	50:1	8.78×10^{-6}	0.293
5	4	37×10^3	50:1	8.78×10^{-6}	0.433

5.4.3.1 SDS-PAGE analysis of conjugations

The results of the SDS-PAGE analysis after conjugation of catalase to PVP of 4 different molecular weights, as described in Table 5.5, can be seen in Figure 5.8.

As with the previous SDS-PAGE experiment, as observed in Figure 5.4, the experimental labels in Figure 5.8 are “Pol”, “Cat” and Conjugate 1 correspond to the polymer reference, catalase reference and the unconjugated catalase reference, respectively showing unconjugated catalase (black highlight). As expected, the dye used for this analysis, reacted with the unconjugated catalase and conjugates, but not with the polymer reference, as explained previously in Section 5.4.2.1. From Figure 5.8 it is observe that the lanes corresponding to the conjugates 2 - 5, contain no unconjugated catalase at ~ 64 kDa and an increase in the molecular weights after conjugation is observed (orange highlight), indicating successful conjugation to the catalase.

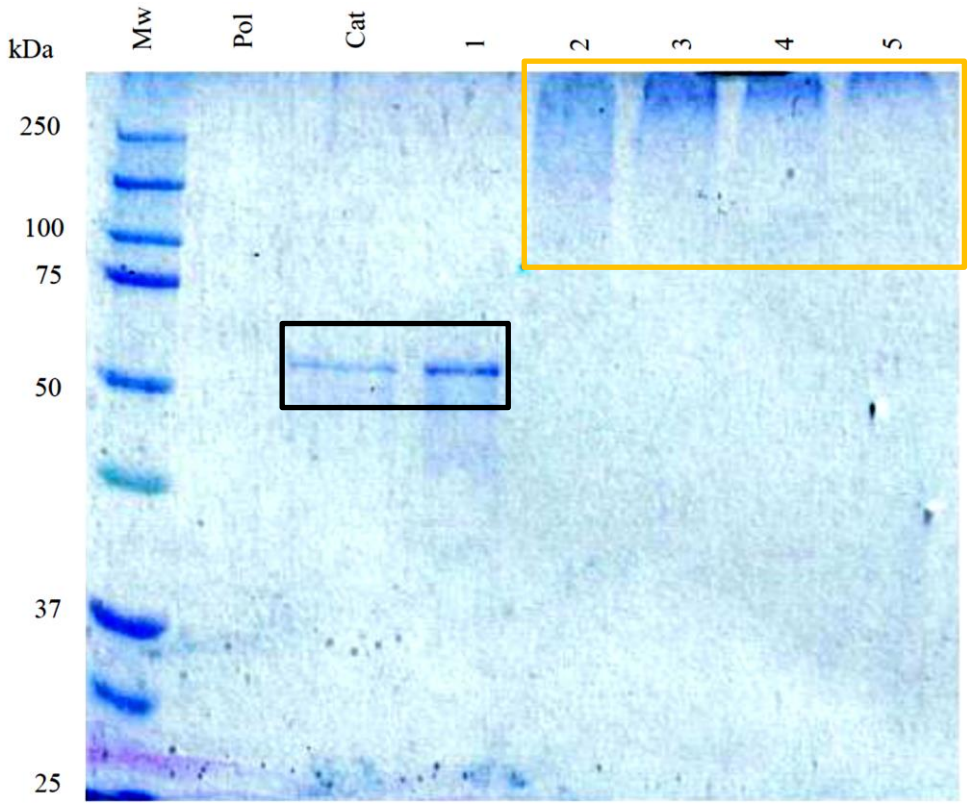

Figure 5.8: SDS-PAGE analysis after the conjugations of PVP with different molecular weights as described in Table 5.5. Where Mw is the molecular weight marker, Pol is the polymer reference, Cat the catalase reference, 1 the unconjugated catalase from the reaction, 2 the 10×10^3 g/mol conjugate, 3 the 17×10^3 g/mol conjugate, 4 the 25×10^3 g/mol conjugate and 5 the 37×10^3 g/mol conjugate.

5.4.3.2 Catalase activity after conjugation

In the same manner as in Section 5.4.2.2, the enzymatic activities of these conjugates were studied with UV-vis spectroscopy at 240 nm for 400 seconds. The conjugate's ability to decompose hydrogen peroxide was measured via the decrease in absorbance at this wavelength. Figure 5.9 represents the enzymatic activity after conjugation with PVP with different molecular weights, as indicated in Table 5.5. The same enzyme concentration is used for the analysis. Conjugate 1, containing unconjugated catalase, was used as a baseline for comparison.

This analysis was performed in order to determine the effect of the molecular weight on the enzymatic activity of catalase. As with the previous enzymatic assays, the polymer does not remove the enzymatic activity of catalase as a function of increase in the molecular weight. In fact, an increase in the enzymatic activity of catalase for these four conjugates was seen when compared to unconjugated catalase. For Conjugate 2 to Conjugate 4 an increase in the decomposition of hydrogen peroxide was observed, while a decrease in activity was seen for conjugate 5. However, the enzymatic activity of conjugate 5 was still higher than that of unconjugated catalase. This suggests that an increase in molecular weight of PVP causes an increase in the enzymatic activity of catalase when the conjugates

contain PVP under 40 × 10^3 g/mol. As described earlier with Figure 5.5 the PVP has little effect on the absorbance measured. An insignificant difference in enzymatic activity was observed for the conjugates below 40 x 10^3 g/mol, especially for Conjugates 2, 3 and 5. Indicating that conjugation of PVP under 40 × 10^3 g/mol to catalase has close to the same effect on the enzymatic activity of catalase. The same concentration of catalase was used for the conjugations and the same concentration of enzyme for each enzymatic analysis of the conjugates. The conjugates were not tested for aggregation

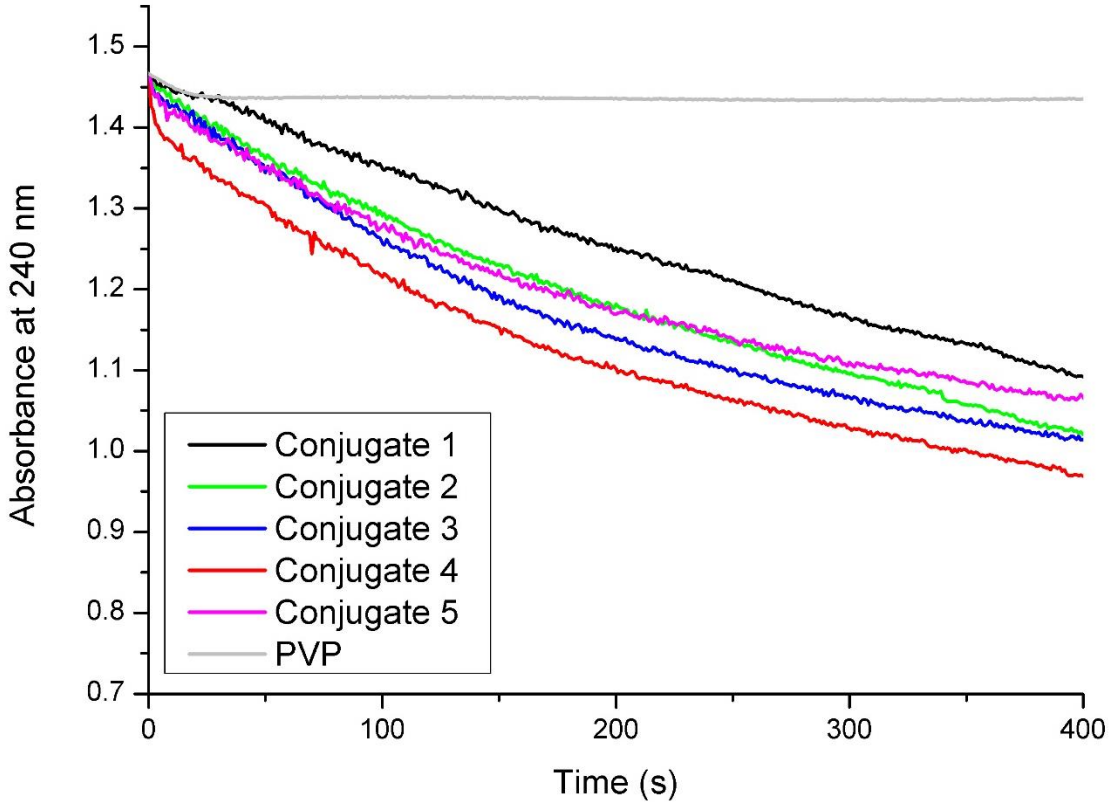

Figure 5.9: Enzymatic activities of the 5 conjugates measured with UV-vis spectroscopy at 240 nm over time, after conjugation as depicted in Table 5.5. With conjugate 1 the unconjugated catalase, conjugate 2 the 10 × 10^3 g/mol conjugate, conjugate 3 the 17 × 10^3 g/mol conjugate, conjugate 4 the 25 × 10^3 g/mol conjugate and conjugate 5 the 37 × 10^3 g/mol conjugate.

As described for Figure 5.5 the enzymatic activity parameters can be determined for Figure 5.9. For conjugates 1– 5, the same molar extinction coefficient for hydrogen peroxide (43.6 L/mol·cm[44]) and second order rate law (Equation 5.4) was applied to the decrease in hydrogen peroxide concentration. The rate constant (k) was determined in the same manner as before and used in determining the hyperbolic relationship between reaction rate and hydrogen peroxide concentration. V_{max} was determined from this relationship and with the same catalase enzyme concentration (3.9 × 10^{-10} M), k_{cat} was determined. The values for V_{max} and k_{cat} as determined for conjugates 1 – 5 is shown in Table 5.6.

Table 5.6: Enzymatic activity parameters, for the conjugates 1 – 5 as described in Table 5.5

Conjugate	V_{max} (M/s)	k_{cat} (s^{-1})
1	0.0155	4.0×10^7
2	0.0165	4.2×10^7
3	0.0165	4.2×10^7
4	0.017	4.4×10^7
5	0.0165	4.2×10^7

In Table 5.6 as with Figure 5.9 an increase is seen in the enzymatic activity with the increase in the enzymatic turnover number in comparison with conjugate 1, the unconjugated catalase. A maximum for conjugate 4 is seen with a decrease in enzymatic activity for conjugate 5. Conjugate 2 and 5 has the same value for the turnover number.

In their study Gaertner *et al.*[61] discovered the same effect when attaching trypsin to PEG. In this study, they determined that an increase in PEG molecular weight caused an increase in the enzymatic activity compared to native trypsin.

5.4.3.3 Circular dichroism of catalase

Figure 5.10 contains the CD spectra for the four different molecular weight polymers conjugated to catalase, with the same end group concentration. As mentioned previously, CD can provide information regarding the secondary structure of catalase. For this analysis the change in secondary structure with an increase in molecular weight was studied, with the same enzyme concentration. As with Figure 5.7, Conjugate 1, the unconjugated catalase, was obtained as a baseline for comparison. All spectra were normalized according to the concentration of protein and path length.

In Figure 5.10, a lower ellipticity minima is observed for the unconjugated catalase (conjugate 1) when compared to the other conjugates (conjugates 2 – 5), where conjugation took place. A decrease in the lower minima ellipticity band at ~ 230 nm is observed after conjugation; however, the band at ~ 210 nm was still present for the PVP-catalase conjugates, indicating possible partial denaturing. The difference in ellipticity between conjugated catalase and unconjugated catalase is substantial, possibly due to change in the micro structure of the enzyme caused by conjugation. A band for each conjugate between ~ 250 nm and ~ 275 nm is previously observed in Figure 5.7, the reason for this band is not known. No logical sequence can be observed between the four conjugates when examining their CD spectra. The conjugates all follow the same curve shape, although small differences in the curves can be seen when comparing them to each other. This is especially true when comparing conjugates 3 to 4 and conjugates 2 to 5. At ~ 210 nm Conjugates 3 and 4 have a lower minimum than Conjugates 2 and

5. It appears that increasing the molecular weight conjugated to the catalase alters the structure of catalase to the same extent. Thus, a wide variety of molecular weights, below 40 × 10^3 g/mol, can be conjugated to catalase while expecting little change in the structure of catalase. As stated above, and shown in Figure 5.9, an insignificantly small difference in the structure and enzymatic activity of catalase was observed for these four conjugates. Thus, it can be concluded that when catalase is conjugated to PVP with a molecular weight below 40 × 10^3 g/mol, a similar change in structure and enzymatic activity can be expected.

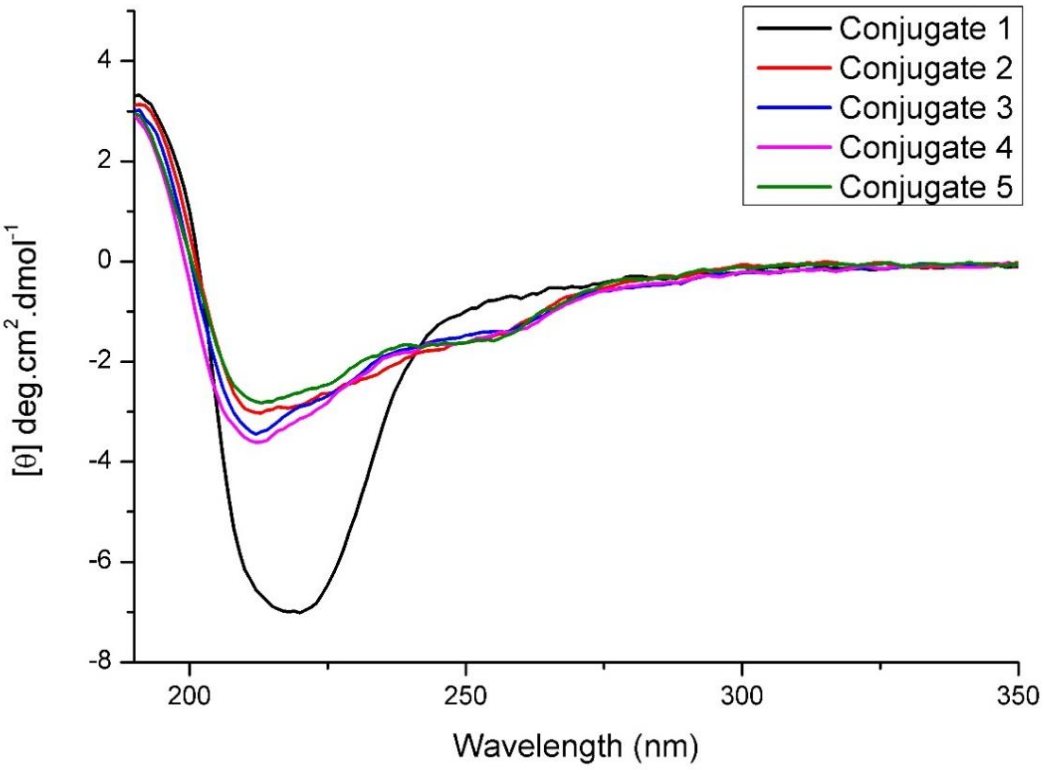

Figure 5.10: Circular dichroism after conjugation as described in Table 5.5. With conjugate 1 the unconjugated catalase, conjugate 2 the 10 × 10^3 g/mol conjugate, conjugate 3 the 17 × 10^3 g/mol conjugate, conjugate 4 the 25 × 10^3 g/mol conjugate and conjugate 5 the 37 × 10^3 g/mol conjugate.

From the SDS-PAGE, an increase in the molecular weight of the enzyme was seen, without any unconjugated catalase still present. After the conjugation, it was determined that the enzymatic activity of catalase increased when PVP was conjugated to catalase, in comparison with unconjugated catalase. Although there is a difference in the activity of catalase when comparing the conjugates to one another, it was very small. Showing that increasing the molecular weight of the polymer below 40 × 10^3 g/mol has little to no effect on the activity of catalase. In the CD spectra of the conjugates, a change in the structure of catalase is observed. The spectra of the 4 conjugates are very close together and there is no trend between the molecular weights.

5.5 Conclusion

In conclusion, it was determined that conjugation of PVP to catalase, was successful. Reductive amination can be used in conjugating an aldehyde ω end group, present on PVP, to the amine, present on the lysine in the catalase enzyme. From literature, the conjugation of an aldehyde to a amine group was expected.[18,19,28] From the SDS-PAGE analysis, a change in the molecular weight of the conjugates is observed. This change was as to be expected when conjugating higher concentrations of PVP to the enzyme. With enough PVP added to the catalase solution, conjugation to every catalase in the solution will take place, and no unconjugated catalase will remain. From UV-Vis it was established that conjugation of the PVP to catalase does not remove the enzymatic activity of the catalase, and the catalase's ability of decomposing hydrogen peroxide is still present. From this UV-vis analysis, it was also determined that conjugating different concentrations, of the same molecular weight PVP to catalase, has an effect on the enzymatic activity of catalase. With an increase in PVP concentration, it was determined that the enzymatic activity of the catalase increases to a maximum, after which a further increase in the PVP concentration decreases the enzymatic activity of catalase. The enzymatic activity becomes lower than unconjugated catalase, if the concentration of PVP is increased further. CD indicates that there is a possible change in the micro structure and possible denaturing of the catalase taking place when conjugating PVP to catalase. The change depends on the concentration of PVP added. It can be concluded that PVP conjugated to catalase does not deactivate the catalase; it rather increases the activity when conjugating low concentrations of PVP, and alters the structure of catalase.

In order to determine the effect the polymer molecular weight would have on the conjugate's enzymatic activity and the secondary structure of catalase, conjugates containing varying molecular weight PVP were tested using. The end group concentration was kept constant in order to ensure that any differences in the conjugates would only be due to molecular weight. The conjugates showed an increase in molecular weight, is seen from SDS-PAGE analysis. No unconjugated catalase was observed indicating that the conjugation reactions were successful. From the enzyme activity assay, it was determined that an increase in molecular weight does not remove the activity of the enzyme. The enzymatic activity of catalase was seen to be directly proportional to an increase in molecular weight, until a value of 25×10^3 g/mol, after which a decrease in activity was seen. However, this slightly lowered activity was higher than unconjugated catalase. The differences in enzymatic activity between the conjugations, compared to each other are small. From the CD spectrum a structural change is observed for the conjugates. Differences were observed in the enzymatic activity and CD spectra when comparing the different conjugates to each other; however the differences are insignificant. It can be concluded that, roughly the same effect in structure alteration and enzymatic activity on the catalase is found for a wide distribution of PVP polymer molecular weights between 10

$\times 10^3$ g/mol and 40 $\times 10^3$ g/mol. The same assumption is made, as with Figure 5.7, that PVP is not detected at the wavelengths analysed.

5.6 References

(1) Jatzkewitz, H. Z. *Naturforsch B.* **1955**, *10*, 27–31.

(2) Istvan Majoros, Baker, Jr.James, R. *Dendrimer-Based Nanomedicine.*; Pan Stanford Publishing; Singapore, 2008; pp 17–34.

(3) Duncan, R. *Nat. Rev. Drug Discov.* **2003**, *2*, 347–360.

(4) Fuertges, F.; Abuchowski, A. *J. Control. Release.* **1990**, *11*, 139–148.

(5) Davis, F. F. *Adv Drug Del Rev.* **2002**, *54*, 457–458.

(6) Harris, J. M.; Chess, R. B. *Nat Rev Drug Discov.* **2003**, *2*, 214–221.

(7) Duncan, R. *Handbook of Anticancer Drug Development*; Lippincott, Williams and Wilkins: Baltimore, 2003.

(8) Ringsdorf, H. *J. Polym. sceince Polym. Symp.* **1975**, *51*, 135–153.

(9) Kakizawa, Y.; Kataoka, K. *Adv Drug Deliv Rev.* **2002**, *54*, 203–222.

(10) Tanaka, T.; Tokiwa., H. *Cancer Res.* **1990**, *50*, 6615–6619.

(11) Donohue, S. A.; Rosenberg., J. H. *J. Immunol.* **1983**, *130*, 2203–2208.

(12) Kimura, K.; Taguchi, T.; Urushizaki, I.; Ohno, R.; Abe, O.; Furue, H.; Hattori, T.; Ichihashi, H.; Inoguchi, K.; Majima, H. *Cancer Chemother. Pharmacol* **1987**, *20*, 223–229.

(13) Rosenberg, S. A.; Lotze, M. T.; Muul, L. M.; Chang, A. E.; Avis, F. P.; Leitman, S.; Linehan, W. M.; Robertson, C. N.; Lee, R. E.; Rubin, J. T. *New Engl. J. Med.* **1987**, *316*, 889–897.

(14) Kaneda, Y.; Tsutsumi, Y.; Yoshioka, H.; Kamada, Y.; Yamamoto, H.; Kodaira, S.; Tsunoda, T.; Okamoto, Y.; Mukai, H.; Shibata, S.; S, N.; Mayumi, T. *Biomaterials.* **2004**, *25*, 3259–3266.

(15) Tsunoda, S.; Kamada, H.; Yamamoto, Y.; Ishikawa, T.; Matsui, J.; Koizumi, K.; Kaneda, Y.; Tsutsumi, Y.; Ohsugi, Y.; Hirano, T.; T. Mayumi. *J. Control. Rel.*, **2000**, *68*, 335–341.

(16) Kamada, H.; Tsutsumi, Y.; Yamamoto, Y.; Kihira, T.; Kaneda, Y.; Mu, Y.; Kodaira, H.; Tsunoda, S. -i.; Nakagawa, S.; Mayumi, T. *Cancer Res.* **2000**, *60*, 6416–6420.

(17) Hoffman, A. *Clin. Chem.* **2000**, *46*, 1478–1486.

(18) Pound, G.; McKenzie, J, M.; Lange, R, F, M.; Klumperman, B. *Chem. Commun.* **2008**, *27*, 3193–3195.

(19) Chamow, S. M.; Kogan, T. P.; Venuti, M.; Gadek, T.; Harris, R. J.; Peers, D. H.; Mordenti, J.; Shak, S.; Ashkenazi, A. *Bioconjug. Chem.* **1994**, *5*, 133–140.

(20) Jentoft, N. *J. Biol. Chem.* **1979**, *254*, 4359–4365.

(21) Murthy, M. R. N.; Reid, Thomas J., I.; Sicignano, A.; Tanaka, N.; Rossmann, M. G. *J. Mol. Biol.* **1981**, *52*, 465–499.

(22) Fita, I.; Rossmann, M. G. *J. Mol. Biol.* **1985**, *185*, 21–37.

(23) Murthy, M. R.; Reid, T. J.; Sicignano, A.; Tanaka, N.; Rossmann, M. G. *J. Mol. Biol.* **1981**, *152*, 465–499.

(24) Nicholls, P.; Fita, I.; Loewen, P. C. *Adv. Inorg. Chem.* **2000**, *51*, 51–106.

(25) Schroeder, W. A.; Shelton, J. R.; Shelton, J. B.; Robberson, B.; Apell, G.; Fang, R. S.; Bonaventura, J. *Arch. Biochem. Biophys.* **1982**, *214*, 397–421.

(26) Sumner, J. B.; Dounce, a L. *Science* **1937**, *85*, 366–367.

(27) I. Fita, A. M. Silva, M. R. N. M. andM. G. R. *Acta Crystallogr. B.* **1986**, *42*, 497–515.

(28) Jentoft, N. *J. Biol. Chem.* **1979**, *254*, 4359–4365.

(29) Habeeb, A. F. S. A. *Anal. Biochem.* **1966**, *14*, 328–336.

(30) Sashidhar, R. B.; Capoor, A. K.; Ramana, D. *J. Immunol. Meth.* **1994**, *167*, 121–127.

(31) Hermanson, G. *Bioconjugate Techniques*; Academic Press: San Diego, CA., 1996; pp112–113.

(32) Stern, K. G. *J. Biol. Chem.* **1937**, *121*, 561–572.

(33) Beers, R.F. Jr., and Sizer, I. W. *J. Biol. Chem.* **1952**, *195*, 133–140.

(34) Pavia , D, L.; Lampman, G, M.; George, S, K.; Vyvyan, J, R. *Introduction to Spectroscopy*; Brooks/Cole, Cengage Learning: Belmont, CA, 2010; pp 353–389.

(35) Garfin, D. E. *Methods Enzymol.* **1990**, *182*, 425–441.

(36) Gallagher, S. R. *Curr. Protoc. Mol. Biol.* **2006**, 75:II:10.2A:10.2.1–10.2A.37.

(37) Wei, Y.; Li, K.; Tong, S. *Talanta* **1996**, *43*, 1–10.

(38) Krishnamurthy, K. V. *Methods in Cell Wall Cytochemistry*; CRC Press: Boca Raton, 1999; pp 1–24.

(39) Ghosh, P. K. *Introduction to Protein Mass Spectrometry*; Academic Press: San Diego, 2015; pp 9–67.

(40) Bonner, P. L. R.; Hargreaves, A. J. *Bioscience Laboratory Techniques*; John Wiley & Sons, Inc.: Chichester, 2011; pp 122–136.

(41) Riccardi, C. M.; Cole, K. S.; Benson, K. R.; Ward, J. R.; Bassett, K. M.; Zhang, Y.; Zore, O. V; Stromer, B.; Kasi, R. M.; Kumar, C. V. **2014**.

(42) Prajapati, S.; Bhakuni, V.; Babu, K. R.; Jain, S. K. *Eur J Biochem.* **1998**, *255*, 178–184.

(43) Takada, H.; Kokubo, K.; Matsubayashi, K.; Oshima, T. *Biosci. Biotechnol. Biochem.* **2006**, *70*, 3088–3093.

(44) Noble, R. W.; Gibson, Q. H. *J. Biol. Chem.* **1970**, *245*, 2409–2413.

(45) Berg JM, Tymoczko JL, S. L. *Biochemistry.*; W H Freeman: New York, 2002.

(46) Campbell, M.; Farrell, S. *Biochemistry*; Cengage Learning: Australia, 2007.

(47) Stenesh, J. *Biochemistry*; Springer Science & Business Media: New York, 2013.

(48) Beckman, J. S.; Minor, R. L.; White, C. W.; Repine, J. E.; Rosen, G. M.; Freeman, B. a. *J. Biol. Chem.* **1988**, *263*, 6884–6892.

(49) Ashihara, Y.; Kono, T.; Yamazaki, S.; Inada, Y. *Biochem. Biophys. Res. Commun.* **1978**, *83*, 385–391.

(50) Rittner, D.; McCabe, T. L. *Encyclopedia of Biology*; Infobase Publishing, 2014.

(51) Roberts, M.; Reiss, M. J.; Monger, G. *Advance Biology*; Nelson Thornes, 2000.

(52) Banga, A. K. *Therapeutic Peptides and Proteins: Formulation, Processing, and Delivery Systems*; CRC Press: New York, 2015; pp 37–63.

(53) Woody, R. W. *Methods Enzymol.* **1995**, *246*, 34–71.

(54) Greenfield, N. J. *Nat. Protoc.* **2006**, *1*, 2876–2890.

(55) Greenfield, N. J. *Nat. Protoc.* **2006**, *1*, 2891–2899.

(56) Haber, J.; Maslakiewicz, P.; Rodakiewicz-Nowak, J.; Walde, P. *Eur. J. Biochem* **1993**, *217*, 567–573.

(57) Prakash, K.; Prajapati, S.; Ahmad, A.; Jain, S, K.; Bhakun, V. *Protein Sci.* **2002**, *11*, 46–57.

(58) Li, D.; Ji, B.; Jin, J. *J. Lumin.* **2008**, *128*, 1399–1406.

(59) Dodero, V. I. *Front. Biosci.* **2011**, *16*, 61–73.

(60) Aubin-Tam, M.-E.; Hwang, W.; Hamad-Schifferli, K. *Proc. Natl. Acad. Sci. U. S. A.* **2009**, *106*, 4095–4100.

(61) Gaertner, H. F.; Puigserver, A. J. *Enzyme Microb. Technol.* **1992**, *14*, 150–155.

Chapter 6: Conclusion and future work

6.1 Conclusion

A possible solution for the problem of hair greying was investigated. Hair greying is attributed to the loss in colour pigments from the hair and is caused by the increase in hydrogen peroxide concentration.[1] A possible solution, through the use of polymer therapeutics, is studied in the hope of finding a viable solution of removing hydrogen peroxide from the hair follicle. The aim of the study is the conjugation of catalase used in the decomposition of hydrogen peroxide, to poly(*N*-vinylpyrrolidone) (PVP). PVP is used as stabilizer and carrier for the catalase enzyme due to its low toxicity,[2–4] biocompatibility[5,6] and water solubility.[7] The enzymatic activity of the conjugate was evaluated and compared to unconjugated catalase to ensure the PVP did not remove the catalase activity or denatures the enzyme.

In Chapter 2, a theoretical background was given into the problem of colour loss from the hair follicle. Hydrogen peroxide, found in grey and white hair, has a negative effect on the pigmentary system, enzymes capable of removing hydrogen peroxide and hair repair mechanisms.[1] Catalase, the enzyme capable of decomposing hydrogen peroxide under physiological conditions, is present on the hair. However, with time this hydrogen peroxide decomposing enzyme is impacted negatively and undesirable results, in the form of grey hair, is found. Catalase being an enzyme consists of proteins. These proteins are formed due to the different sequences formed by the 20 amino acids residues in the polypeptide chain.[8,9] The amino acid, lysine, containing a primary amine is used in bioconjugation reactions to form polymer-protein conjugates. PVP is one of the polymers used in the bioconjugations with proteins and is easily polymerized through the reversible addition–fragmentation chain transfer (RAFT) mediated polymerization process, using a suitable chain transfer agent (CTA).[10] The RAFT polymerization process is used for the polymerization of NVP due to the control achieved over the molecular weight and dispersity.

S-(2-cyano-2-propyl), *O*-ethyl xanthate CTA was successfully synthesised as described by Pound *et al*.[11] Due to NVP being a less activated monomer, an alkoxy is used as the stabilizing Z group on the CTA, forming a xanthate. On the free radical leaving R group a tertiary carbon bonded to a nitrile and two methyl groups is used. The Z and R groups are used in combination to stabilize the radical and control the polymerization. Successful bulk polymerization of PVP at 60 °C using AIBN as initiator, with controlled molecular weight and dispersity was achieved as described by Pound *et al*.[11] Four well defined molecular weight PVP polymers (10×10^3 g/mol, 18×10^3 g/mol, 26×10^3 g/mol, 37×10^3 g/mol) were synthesized. The molecular weights were confirmed with size exclusion chromatography (SEC) and proton nuclear magnetic resonance (^{1}H-NMR) spectroscopy. Low dispersities of 1.2 for the

four polymers were determined from SEC. Good control over the polymerization regarding molecular weight and dispersities was expected.[12–14]

In addition to polymerizing, CTAs can also be used in end functionalization reactions. A specific functionality can be placed on the end groups of the polymer, which can be used for post polymerization reaction. In Chapter 4 the end functionalization of the polymers, as described in Chapter 3, was successfully performed. In order to covalently conjugate the PVP to catalase, an aldehyde end group is required on the polymer. Two methods were used in the end functionalization of the xanthate ω end group to an aldehyde functional group. A one step method adapted from Ilchev *et al.*[15] and a two-step method adapted from Pound *et al.*[11] The functionalization using the one step method was not successful, due to unknown functionalities forming on some of the polymer in addition to the aldehyde functional groups. The method as described by Pound *et al.*[11] was successful in functionalizing the xanthate ω end group to an aldehyde functionalized ω end group, through a hydroxyl ω end group intermediate. After each end functionalization step, SEC analysis was performed. From SEC, the analysis demonstrated molecular weights were very close to that of the starting molecular weights. Little change in the dispersities of the polymers was found after each functionalization step. From ^{1}H-NMR the successful removal of the *ω* xanthate end group, was observed by the loss of the peaks at 4.6 ppm and between 5.5 ppm and 6 ppm, and the formation of the intermediate hydroxyl group, observed between 5 ppm and 6 ppm. After the aldehyde functionalization, of the intermediate, a new peak is observed at 9.5 ppm.

Chapter 5 describes the bioconjugation of PVP to catalase. The lysine residues in catalase were targeted for conjugation. For the covalent conjugation, reductive amination was used. The aldehyde functional *ω* end group on the PVP, as functionalized in Chapter 4, formed a Schiff base with the primary amine on the lysine residue, to form an imine. The imine bond is reduced to a secondary amine to form the covalent conjugation.

The effect of conjugating different concentrations of the same molecular weight (10×10^3 g/mol) PVP on catalase was measured. From the SDS-PAGE analysis a increase in the molecular weight of the conjugates was observed with the increase in concentration of PVP. A complete loss in unconjugated catalase is seen at ~ 64 kDa, with enough PVP in the solution. It was observed that the unconjugated catalase can still detected if the concentration of PVP is low. From the enzymatic activity, the decrease in concentration of hydrogen peroxide is measured. All of the conjugates decompose hydrogen peroxide, indicating the presence of enzymatic activity of catalase after conjugation. With the increase in PVP concentration, the enzymatic activity of catalase increases until a concentration of 5.85×10^{-6}M for PVP polymer end groups, were a maximum in enzymatic activity is reached. A decrease in the enzymatic activity is observed with further increase in PVP concentration. A point, in enzymatic activity, is reached where the enzyme activity is lower than the activity for unconjugated

catalase. It has also been shown that unconjugated PVP does not decompose hydrogen peroxide. From the circular dichroism (CD) analysis a change in the structure of catalase is seen with the increase in PVP concentration, leading to the hypothesis that PVP conjugation disrupts the structure of catalase and possible denaturing of the enzyme. With the increase in disruption of the structure with PVP, the enzymatic activity decreases as shown with UV and CD analysis.

In the second conjugation experiments, the effect of molecular weight on the enzymatic activity of catalase was measured in comparison with unconjugated catalase. The concentration of the polymer end groups was kept constant and the molecular weight of the polymer was increased. The four molecular weight polymers, as synthesized in Chapter 3 and functionalized in Chapter 4, were used for the conjugation. From the SDS-PAGE analysis an increase in the molecular weight is observed, without any unconjugated catalase observed, as expected. The enzymatic activity measured by UV, showed the decomposition of hydrogen peroxide increases when compared to unconjugated catalase. A small difference is observed, when comparing the activity of the different molecular weight polymers conjugates to each other. A trend was seen that with the increase in molecular weight, the rate of decomposition increases until the conjugate with a polymer molecular weight of 26×10^3 g/mol is reached, were after a decrease is observed. From CD, a change in the structure of the conjugated enzyme was observed, when compared to unconjugated catalase. The same change in the structure of the enzyme is seen for these different molecular weight conjugates.

The bioconjugation of PVP to catalase through reductive amination of the aldehyde functional ω end group, on the PVP, to the primary amine on catalase is shown to be successful and the enzymatic activity of catalase is still present after conjugation.

6.2 Future work

The conjugation of PVP to catalse has been carried out successfully with retention of enzymatic activity. The stabilization under various conditions and use of the conjugate in cosmetic applications requires evaluation.

The conjugates must be used on skin and hair samples to determine the effect they will have on the decomposition of hydrogen peroxide from hair and skin. Cytotoxicity evaluations of the conjugates towards humans must be determined, for the aim of human use.

If the conjugates are fit for human usage, stability under various usage conditions requires evaluation. The stability, enzymatic activity and structure of the conjugates towards elevated temperature must to be determined, especially at the temperature where it will most likely be used. The stability and enzymatic activity of the conjugates after time must also be determined, to evaluate the shelf life of the conjugates.

Other future work would also include using different CTA architectures for the polymerization of NVP. In this study a CTA with only one end functionalized group was used for the conjugations. The same study on multifunctional star CTAs (Figure 6.1), with three or four arms, must be undertaken. Multifunctional CTA's will have more functional groups to which the catalase can conjugate in the same manner as this study. The effect of this on enzymatic activity and stability must be studied, for these multifunctional conjugated catalase.

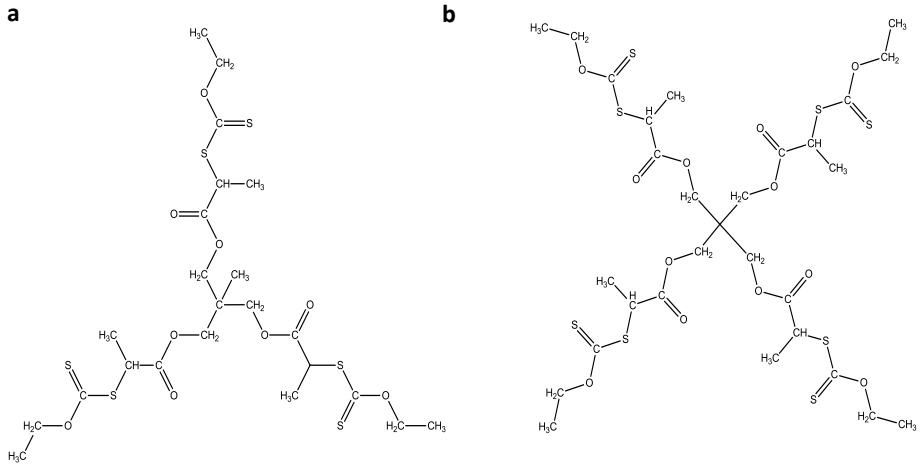

Figure 6.1: Examples of three (a) and four (b) armed star CTAs closely related to the CTA used in thesis

6.3 References

(1) Wood, J. M.; Decker, H.; Hartmann, H.; Chavan, B.; Rokos, H.; Spencer, J. D.; Hasse, S.; Thornton, M. J.; Shalbaf, M.; Paus, R.; Schallreuter, K. U. *FASEB J.* **2009**, *23*, 2065–2075.

(2) Hueper, W, C. *Cancer*. **1957**, *10*, 8–18.

(3) Hueper, W, C. *Arch. Path.* **1959**, *67*, 589–617.

(4) Hueper, W, C. *J. Natl. Cancer Inst.* **1961**, *26*, 229–237.

(5) Higa, O. Z.; Rogero, S, O.; Machado, L, D, B.; Mathor, M, B.; Lugão, A, B. *Radiat. Phys. Chem.* **1999**, *55*, 705–707.

(6) Bindu, N. *Int. J. Toxicol.* **1998**, *17*, 95–130.

(7) Kirsh, Y. E. *Water Soluble Poly-N-Vinylamides: Synthesis and Physicochemical Properties*; Wiley, Ed.: Chichester; 1998, pp 129–215.

(8) Raven, P, H.; Johnson, G, B.; Losos, J, B.; Singer, S, R. *Biology*, 7th ed.; McGraw-Hill higher education; Boston, 2011; pp 34–40.

(9) Alberts, B.; Johnson, A.; J, L.; Morgan, D.; Raff, M.; Roberts, K.; P., W. *Molecular Biology of the Cell:* Garland Science: New York, 2002.

(10) Wan, D.; Satoh, K.; Kamigaito, M.; Okamoto, Y. *Macromolecules* **2005**, *38*, 10397–10405.

(11) Pound, G. Reversible Addition Fragmentation Chain Transfer (RAFT) Mediated Polymerization of N -vinylpyrrolidone, University of Stellenbosch, 2008.

(12) Chiefari, J.; Chong, Y. K.; Ercole, F.; Krstina, J.; Jeffery, J.; Le, T. P. T.; Mayadunne, R. T. a.; Meijs, G. F.; Moad, C. L.; Moad, G.; Rizzardo, E.; Thang, S. H. *Macromolecules*, **1998**, *31*, 5559–5562.

(13) Keddie, D. J.; Moad, G.; Rizzardo, E.; Thang, S. H. *Macromolecules* **2012**, *45*, 5321–5342.

(14) Moad, G.; Rizzardo, E.; Thang, S. H. *Aust. J. Chem.* **2005**, *58*, 379–410.

(15) Ilchev, A. Amine End-Functional Poly(*N*-vinylpyrrolidone) as a Macroinitiator for L-lysine *N* -carboxyanhydride Polymerization - Towards the Preparation of pH-Responsive Micelles for Drug Delivery, University of Stellenbosch, 2014.